A STUDY ON WEATHER-INDUCED DEGRADATION OF LLDPE IN A TROPICAL CLIMATE

A Thesis Submitted

for the Degree of

DOCTOR OF PHILOSOPHY

to

The City University

By

SYED HALIM HAMID

The City University
London, England

September 1988

TABLE OF CONTENTS

LIST OF TABLES

LIST OF FIGURES

ACKNOWLEDGEMENTS

It gives me great pleasure to express my gratitude and thanks to Dr. W. H. Prichard, for his supervision, help, and encouragement, which made it possible for me to successfully complete this work. Much is owed to him for stimulating my thoughts and interest in the subject. I am grateful to him for his extra efforts during my stay in London. I would also like to thank the [redacted] for his selfless help which he provided in the early stages of my work. I owe my thanks to [redacted] for his encouragement, help and lively discussions.

My special thanks are due to [redacted] and [redacted] for their technical and administrative support during the course of this work. I also express my appreciation to [redacted], and [redacted] for their helpful discussions and constructive suggestions.

The support provided by the Research Institute, King Fahd University of Petroleum & Minerals, Dhahran is deeply acknowledged.

I am obliged to all my friends in the Petroleum and Gas Technology Division for the very useful discussions I often had with them on the subject, and particularly to [redacted] for his critical review of the work, helpful suggestions, and cooperation.

Many thanks to [redacted] for the excellent job he has done in typing this thesis. Thanks are also due to [redacted] and [redacted] for their timely assistance.

Finally, I would like to express my thanks to my family members who were always a source of inspiration and were the ones who suffered most during the course of thesis work.

DEDICATED TO MY FATHER

ABSTRACT

Linear low density polyethylene (LLDPE) samples were exposed to the unique natural environmental conditions of Dhahran, Saudi Arabia. The changes in the significant mechanical, thermal, and chemical properties were monitored using tensile testing system, Fourier transform infrared (FTIR) spectroscopy, and differential scanning calorimeter (DSC), respectively.

Exposure site (Dhahran) selected for study is considered to be a unique laboratory for evaluating the outdoor performance of polymer. Meteorological and radiation environment of test site is influenced by the nearness of the very shallow Arabian Gulf and typical desert surrounding. Resulting in monthly mean temperatures reaching close to 37^{o}C during summer, with daily maxima often approaching the 50^{o}mark. The relative humidity exhibits a large diurnal cycle on the order of 60 percent throughout the year, with daily maxima often rising over the 80 percent level during most months. The solar radiation reaching the ground surface is function of atmospheric turbidity and cloudiness, and because of very little cloud cover throughout most of the year, radiation doses are high in this region.

LLDPE is a relatively new type of polyethylene and unlike low density polyethylene (LDPE) and high density polyethylene (HDPE), which are homopolymers, LLDPE is a comonomer of ethylene and higher-alpha-olefin (e.g. 1-butene). The significant difference between them is of branching with LLDPE having evenly distributed short chains as against HDPE having few short chains, and LDPE containing both short and long chain branches. The unique branching structure of LLDPE imparts certain combination of properties which distinguishes it from conventional polyethylenes.

The weather-induced degradation behavior of LLDPE cannot be predicted from the knowledge obtained for LDPE or HDPE. The FTIR spectroscopic analysis of LLDPE samples exposed in Dhahran, Saudi Arabia, have revealed that using difference spectroscopic technique growth in functional groups (carbonyl, hydroxyl, alkene, vinyl, etc.) is detected at very early stages of degradation. Band indexing and dimensionless number techniques of presenting spectroscopic data of weathered samples have also been used and they present a steady increase in degradation products. DSC technique was used to monitor the percent crystallinity and crystalline melting temperature (T_m) of exposed specimens. Percent crystallinity as determined from heat of fusion (H_f) shows an increasing trend, whereas T_m was almost constant for most of the exposure duration implying that -CH_2 groups in the amorphous region are replaced by the degradation products. Tensile strength and percent elongation have also exhibited a linearly decreasing trend with exposure time, carbonyl groups formation, and percent crystallinity.

Mathematical modelling of degradation in significant properties as a function of weather parameters was accomplished using statistical analysis system (SAS) software package. Tensile strength, carbonyl groups, and percent crystallinity were mathematically shown to be dependent on different weather parameters with UV dose having impact on every property.

Chapter 1

INTRODUCTION

1.1 POLYMER DEGRADATION

The development of polymers as an important engineering material was inhibited at the first place by the premature failure of these versatile compounds in many applications. The deterioration of the significant properties of both natural and synthetic polymers is the results of irreversible changes in composition and structure of polymer molecule. The term polymer degradation is used to denote changes in physical properties caused by chemical reactions involving bond scission in the backbone of the macromolecule. The most appropriate way to distinguish between different modes of polymer degradation is to subdivide this broad field according to its various modes of initiation. These comprise photochemical, thermal, radiation, mechanical, chemical, and biological degradation of polymeric materials.

Light-induced polymer degradation, or photodegradation, concerns the physical and chemical changes caused by irradiation of polymers with ultraviolet (UV) or visible light. The importance of photodegradation of polymers derives from the fact that the UV portion of the sunlight spectrum can be absorbed by various polymeric materials. The resulting chemical processes may lead to severe property deterioration. Thermal degradation refers to the exposure of polymer to elevated temperature, at which it starts to undergo chemical changes without the simultaneous involvement of another compound.

High energy radiation such as electromagnetic radiation (X-rays, gamma-rays) or particle radiation (alpha-rays, fast electrons, neutrons, nuclear fission products), is not specific with respect to absorption. The existence of chromophoric groups is not prerequisite as in the case of photodegradation since all parts of the molecules are capable of interacting with the radiation. The extent and character of chemical and physical changes depend on the

Mechanically initiated degradation generally refers to macroscopic effects brought about under the influence of shear forces. Polymer fracture plays an important role in determining the application of plastics. Chemical degradation refers exclusively to processes which are induced under the influence of chemicals (e.g., acids, bases, solvents, reactive gases, etc.) brought in contact with polymers. Biologically initiated degradation also is strongly related to chemical degradation as far as microbial attack is concerned. Microorganisms produce a great variety of enzymes which are capable of reacting with polymers.

There exists a strong inter-relationship between the various modes of polymer degradation. Often circumstances prevail that permit the simultaneous occurrence of various modes of degradation. Typical example is of weather-induced degradation, which involves the simultaneous action of sunlight, oxygen, temperature, and harmful atmospheric emissions. Oxidative deterioration of thermoplastic polymers during processing is another example. This involves the simultaneous action of heat, mechanical forces and oxygen [Schnabel, 1981].

It is now generally recognized that stabilization against degradation is necessary if the useful life of polymer is to be extended sufficiently to meet design requirements for long term applications. The stabilization of the polymer is still undergoing transition from an art to a science as mechanism of degradation becomes more fully developed. A scientific approach to stabilization can only be approached when there is an understanding of the reactions that lead to degradation [Hawkins, 1984].

Almost all the polymers, including polyolefins, are subjected to degradation at nearly all stages of their life cycle, i.e., during manufacturing, storage and transportation, processing, and end-use. Plastics offer an impressive range of attractive properties and are used in many applications where they are exposed to the outdoor environment. Outdoor uses of plastic products include buildings and construction, agriculture and horticulture, automobiles, solar heating equipment, and packaging. It has been estimated that roughly half the annual tonnage of polymer is employed outdoors [Davis and Sims, 1983], where performance is often limited by weathering.

1.2 PLASTIC WEATHERING

There is always a natural concern regarding the durability of polymeric materials because if the useful lifetime of these materials can be predicted their maintenance and replacement can be planned. The deterioration of a material depends on how and to what extent it interacts with its surroundings. Degradation of plastics during outdoor exposure is influenced to varying degrees by all natural meteorological phenomena. Heat, radiation (ultraviolet and infrared), rain, humidity, atmospheric contaminants, thermal cycling, and oxygen content of air, all contribute to the degradation of plastics subjected to outdoor exposure. None of these factors are constant in any one location, and weather conditions vary widely with location. To attain maximum accuracy in predicting the useful life of an outdoor plastic, all components of the anticipated exposure environment must be considered. This is best accomplished by conducting exposure trials in that environment.

1.2.1 Solar Radiation

The sun is the primary cause of most climatic phenomena found on earth. From an examination of the angle of elevation of the sun at London, San Francisco, Innisfail, and Singapore, it is seen that the annual range of sun position is less for tropical than for temperate sites, as shown in Figure 1.1 [Davis and Sims, 1983]. For most polymeric materials the main cause of loss of properties is photooxidative attack. This implies a combined action of oxygen and sunlight on their chemical structure. The three aspects of sunlight, sunshine duration, total solar radiation, and UV radiation can be used to quantify sunlight as an agent of deterioration. Many commercial polymers are degraded outdoors, primarily because of photodegradation and efforts have been made to relate their resistance to the number of sunshine hours they can withstand before they lose their useful properties. The search of a quantitative relationship between sunshine hours and global solar radiation has been a subject of considerable interest.

Total solar radiation reaching earth's surface is only about half to two-thirds its value at the outer limits of the atmosphere. The most deleterious of the environmental factor in weathering phenomena is UV section of radiation

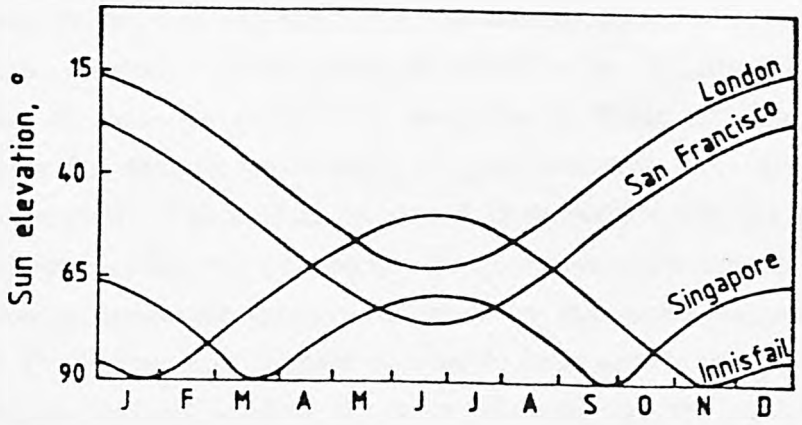

Figure 1.1. Annual variation of angle of elevation of noon sun for different locations.

Table 1.1

Type of Radiation in the Solar Spectrum

Type of Radiation	Wavelength
Cosmic Ultra Radiation	10^{-12} m
X-ray Radiation	10^{-12} - 10^{-7} m
UV Radiation	10^{-7} - 4 x 10^{-7} m (100-400 nm)
Visible Light	4 x 10^{-7} - 7.8 x 10^{-7} m (400-780 nm)
IR Radiation	7.8 x 10^{-7} - 10^{-3} m
High-Frequency Radiation	10^{-3} - 10^{6} m

which is responsible for the weather-induced degradation of plastics [Winslow, 1977a]. The sun sends a continuous spectrum of energy radiation to the earth, whereby various types of radiation are usually differentiated on the basis of their wavelengths as presented in Table 1.1. The atmosphere is permeable for certain wavelength of radiation and there are two so-called optical windows. The optical window I is permeable for the radiation from approximately 290-1400 nanometers (nm). Above 1400 nm the infrared (IR) radiation is almost completely absorbed by the water vapors in the atmosphere. The atmosphere is again permeable from approximately 1 cm to 100 m wavelength (optical window II, radio window) and the radiation of higher wavelength is again absorbed completely [Henderson, 1970]. The physical nature of these radiations are the same and they vary only in wavelength and, therefore, their photon energy. The wavelength has an inverse relationship with quantum energy as shown in Figure 1.2 [Ranby and Rabek, 1975]. The extra terrestrial radiation of the sun is largely constant in its spectral composition. Its intensity depends on the angle of incidence. This changes as a result of the tilt of the earth's axis and the rotation of the earth in a daily and annual cycle and is linked with the geographical latitude of the place of measurement [Coulson, 1975].

The solar spectrum is modified by the atmosphere unevenly over the spectral range. The effect is more pronounced in the IR and UV regions than it is in the visible range. The radiation wavelength ranges reaching the earth surface is from about 290-1400 nm. The percentage of longwave radiation in IR region (800-1400 nm) is about 53, the visible region (400-800 nm) provides about 43%, and the UV-region (290-400 nm) only about 4-6% of the total global radiation [Davis and Sims, 1983]. The portion of sun's spectrum between 290 and 400 nm shown in Figure 1.3 is a small fraction of the total spectrum but is important to polymer because it includes the highest energy region and is the only portion which can cause direct harm to unmodified polymers [Klemchuk, 1986]. The visible region of the solar spectrum, 400-800 nm, does not usually cause direct harm to polymers but can do so by interaction with sensitizing substances in the polymers. The IR portion, >800 nm, is generally considered harmless in a photochemical sense but may have a role in the thermal oxidative degradation of some polymers.

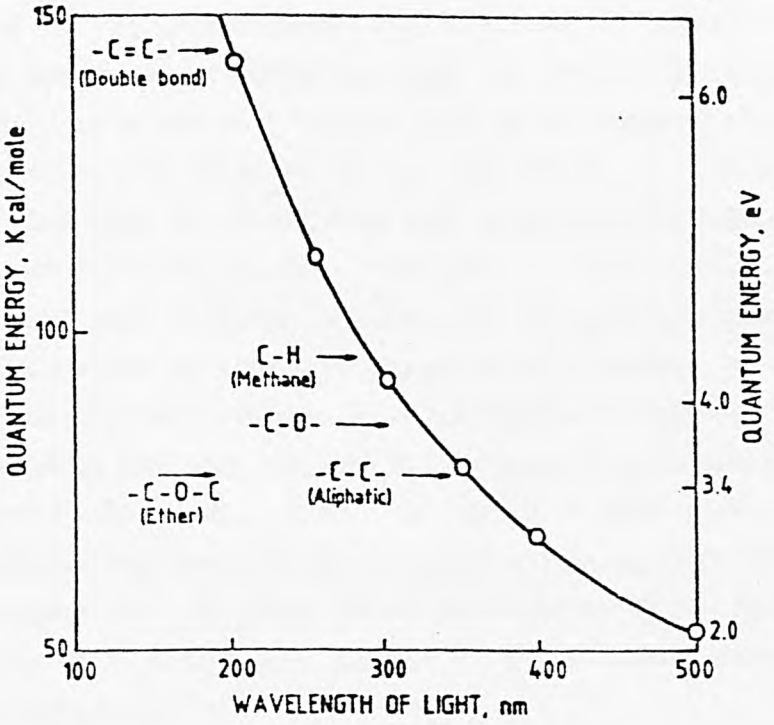

Figure 1.2. Energy of the light quantum as a function of the wavelength

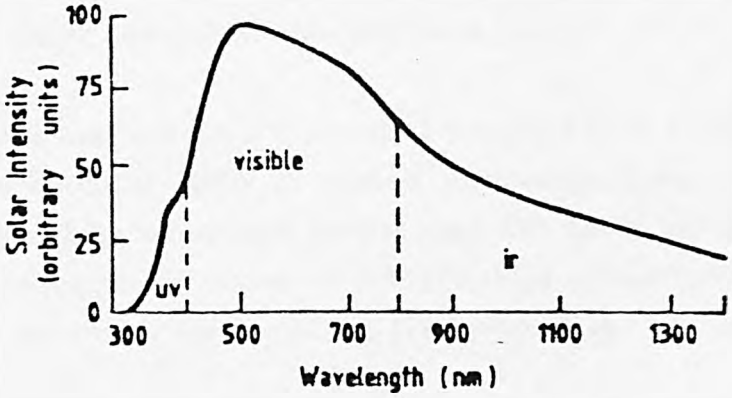

Figure 1.3. Typical midday solar spectrum.

The UV portion of the radiation is mainly responsible for the degradation of polymers, because the energy at visible and high wavelengths is too low to damage the chemical structure of a polymer. Due to its chemical structure every polymer is susceptible to photochemical degradation at a particular wavelength. The absorption of UV radiation and its concomitant degradative effects vary for each individual polymer. Stability is strongly dependent on the specific chemical and molecular structure of the polymer. Since the molecular structure governs the absorption ranges of each polymer, variations in structure leads to differences in the absorption ranges of individual polymers. Table 1.2 shows a few polymers with the corresponding wavelengths of maximum sensitivity [Stretansky, 1986]. In theory a pure hydrocarbon molecule, e.g., polyethylene, does not contain functional groups that would be capable of absorbing UV radiation [Pross and Black, 1950]. However, polyolefins are known to absorb, and degrade by UV radiation. Sources of UV absorbing chromophores are:

- Polymer structure
- Feedstock or process impurities
- Residual catalyst
- Thermal processing degradation products
- Antioxidants and transformation products
- Colorants
- Fillers
- Other additives (flame retardants, etc.)

Table 1.3 shows that enough UV energy is available from sunlight to break many of the chemical bonds in organic compounds. Since most polymer should not absorb at wavelength greater than 300 nm it has been assumed that the above mentioned sources of UV absorbing chromophores present in polymers are responsible for weathering [Trozzolo, 1972].

1.2.2 Atmospheric Oxygen

Residual double bonds in some molecules such as polyethylene are specially susceptible to attack by atmospheric oxygen although most polymers react very slowly with oxygen. However oxidation is greatly promoted by elevated temperatures and UV radiation, and the reactions of polymers with oxygen

Table 1.2

Summary of Wavelength Sensitivity of Polymers

Polymer	Activation Spectra (Maxima in Nanometers)
Nylon	290-315
Polymethyl Methacrylate (PMMA)	290-315
Styrene-Acrylonitrile	290,310-330
Polycarbonate	280-310
Polystyrene	310-325
Polyethylene	300-310,340
Polypropylene	290-300,330,370
Polyester (Aromatic)	325
Acrylonitrile-Butadiene-Styrene (ABS)	300-310,370-385
Poly(Vinyl Chloride) Homopolymer	320
Poly(Vinyl Chloride) Copolymer	330,370
Polyarylate	350
Polyamides (Aromatic)	360-370,415
Polyurethanes (Aromatic)	350-415

Table 1.3

UV Light Energy *versus* Chemical Bond Strength

Chemical Bonds	Bond Dissociation Energy (kcal/mol)	Wavelength (nm)	Photon Energy (kcal/mol)
C-H (primary)	99	280	102.3
C-H (tertiary)	85	300	95.5
C-H (allylic)	77	300	95.5
C-C	83	340	89.5
C=C	145	360	79.6
C=C	191	380	75.4
C-Cl	78	400	71.6
C-N	82		
C=N	153		
C-O	93		
C=O	186		
C-Si	78		
Si-H	76		
N-O	37		
-O-O-	66		

under these conditions can be very complex. Oxygen is not usually regarded as an experimental variable in the study of polymer weatherability since the oxygen concentration in the environment is substantially constant. Moreover, most weathering phenomena occur at the surface of the plastic which is in equilibrium with air.

1.2.3 Ambient Temperature

Under extreme outdoor exposure conditions, a plastic sample may reach 170°F (about 77°C). The temperature of an object in sunlight is usually significantly higher than that of the surrounding air. The difference between the air and surface temperature depends on factors such as radiation intensity, wind speed, object shape, and the nature of the material, in particular its surface finish, color, heat capacity and thermal conductivity. Weathering process depends on temperature along with other factors and the maximum temperature attained by the polymers is not sufficient to promote bond cleavage of any structures likely to be found in commercial plastics. The principal of heat in the outdoor degradation of plastics is in accelerating processes otherwise induced, such as hydrolysis, secondary photochemical reactions, or the oxidation of trace contaminants. It is a well experienced fact that deterioration rates of polymers in the tropics far exceed those in frigid zones. Simulated weathering experiments have shown that the oxidation rates of polyethylene exposed to 300 nm radiation increases fourfold from 10° to 50°C [Winslow et al., 1972].

1.2.4 Humidity

The significant role of water in weather-induced degradation of plastics lies in the combination of its unique physical properties with its chemical reactivity. Water can have at least three kinds of effects which are important for the degradation of polymers. One is chemical: hydrolysis of labile bonds such as those of polyesters or polyamides; a second is physical, destroying the bond between a polymer and a filler like glass fiber or pigment and resulting in chalking or fiber bloom. Rain can wash away water- soluble degradation products from the exposed surface and moisture swells, softens, and plasticizes selected plastics; and a third is photochemical, involving the generation

of hydroxyl radicals or other reactive species which can promote a host of free radical reactions [Kamal and Saxon, 1967].

1.2.5 Weathering Trials

Weathering trials are always an important means of evaluating plastics, but they are of particular importance in hotter regions such as Dhahran, Saudi Arabia. Almost invariably, the high levels of temperature humidity, and solar radiation found in such regions proves more aggressive to plastic materials than those of temperate zones such as England. Thus, as well as being of intrinsic interest, exposure trials in hotter climate are a means of obtaining advanced information on the resistance of a particular plastic material in temperate climatic conditions.

A new polymeric material is generally put on the market with a comprehensive account of its physical and mechanical properties. However, there is seldom sufficient information available to asses the length of time the material will fulfill its function satisfactorily outdoor before it needs repair or replacement. This is difficult to determine particularly if an attempt is being made to predict the service life of a polymer which is only subjected to limited period of outdoor exposure. It is imperative to determine basic experimental data on the weatherability of a material so that the designers, formulators and researchers have enough information for correctly formulating a polymer product for outdoor exposure. Basic weathering data provide enough technical basis for selection an appropriate UV stabilizer and its concentration for particular outdoor application. These data may be based on the results of actual outdoor exposure or artificial exposure in a weatherometer.

Artificial weathering can be regarded as exposure of test samples to one or two arbitrary combinations of radiant energy, thermal energy, and moisture. It is generally recognized by now as having very limited value in precisely predicting outdoor performance of plastics [Kamal, 1970]. The deficiencies in artificial weathering which lead to poor or inconsistent correlation between such tests and outdoor exposures are due to the fact that the simulation of dynamic factors of natural weather is not possible in an artificial devises.

The best utilization of artificial devices is in the indication of the tendency of degradation parameters qualitatively.

1.3 LINEAR LOW DENSITY POLYETHYLENE (LLDPE)

1.3.1 Introduction

Polyethylene was first commercialized in the 1940s and was considered a single class of commercial plastic. The situation in the mid 1980s is much more complex with a wide variety of polyethylenes ranging in density from 0.910 to 0.960 g/cm^3 [Flesher, 1980]. The basic property differences between high density polyethylene (HDPE) and low density polyethylene (LDPE) were a result of the linearity of the polymer chain and lack of side-chain branches in HDPE in contrast to the highly branched structure of LDPE. The short branches disrupt the crystal structure to give the material its low density, while the fewer long branches affect the properties such as melt strength and drawdown. Both the polymers though well established in the market have different types of application. LDPE is known for its flexibility and transparency thus finding wide applications in films, flexible tubing, etc. On the other hand HDPE is more rigid polymer lacking in transparency and established in products manufactured by injection molding, blow molding, etc.

It has always been felt imperative to find a suitable polyethylene which might combine the application areas of both the types described above. The polymer scientists have realized earlier that the density of polyethylene can be altered by purposely copolymerizing ethylene with alpha-olefins. However, the copolymer was not commercialized earlier because of the good economic situation of the plastic sector in early 1960s. With the advent of the general economic decline, LLDPE was successfully promoted by manufacturers in the mid 1970s because of its cost effectiveness. This opened a new field of resins spanning the entire density range associated with high pressure LDPE to completely linear HDPE resins. Therefore, the term linear low density polyethylene (LLDPE) was introduced for any ethylene-alpha-olefin copolymer prepared by a low pressure process and ranging in density from 0.910 - 0.940 g/cm^3 s [Short, 1981]. LLDPEs as against LDPE and HDPE, are

comonomers of ethylene and alpha-olefin (propene, 1-butene, 1-hexene, 1-octene, and/or 4-methyl-1-pentene). One distinguishes among the lower crystalline LDPE, where crystallinity is disrupted by occurrence of branching during polymerization, and LLDPE where crystallinity is disrupted by copolymerization with small amount of a second monomer (alpha-olefins). Branching in LLDPE is affected by the type and amount of comonomer present and by processing factors. Figure 1.4 shows the branching structure of LDPE, HDPE, and LLDPE molecule. It shows that LDPE molecule contain short-chain as well as long chain branches, whereas, HDPE has few short branches and no long chain branches and therefore the molecule of the polymer is linear. LLDPE molecules consist of long sequences of methylene units with periodic uniform short side chains.

A large portion of the range of LLDPE's now commercially available are ethylene/butene-1 copolymer, and so contain ethyl branches. Hexyl branched material, as well as a limited number of methyl, butyl, and isobutyl branched copolymers have also been produced. [France et al, 1987]. Although butene grades have achieved greater market volumes than other forms of LLDPE, long carbon chain comonomers yield a better overall balance of resin toughness properties than do the short carbon chain comonomer. Also, comonomer choice is not the only determinant of resin properties, equally important are the choice of catalyst and manufacturing process used to produce LLDPE [Leaversuch, 1986].

The developments in the field of LLDPE are reviewed in this section. The production processes will be discussed alongwith the properties, application, and the role of LLDPE and LDPE/HDPE blends. Degradation and stability of LLDPE will also be discussed so as to give an idea of the extent of work done in this field and the need of additional work in studying the weathering effects on LLDPE.

1.3.2 Production processes

LLDPE is made by copolymerizing ethylene with selected alpha-olefins, resulting in many short branches along the polymer chains. Crystallization of the resin is affected by molecular weight and molecular weight distribution, as well as by the type, numbers, and arrangements of the branches. The size

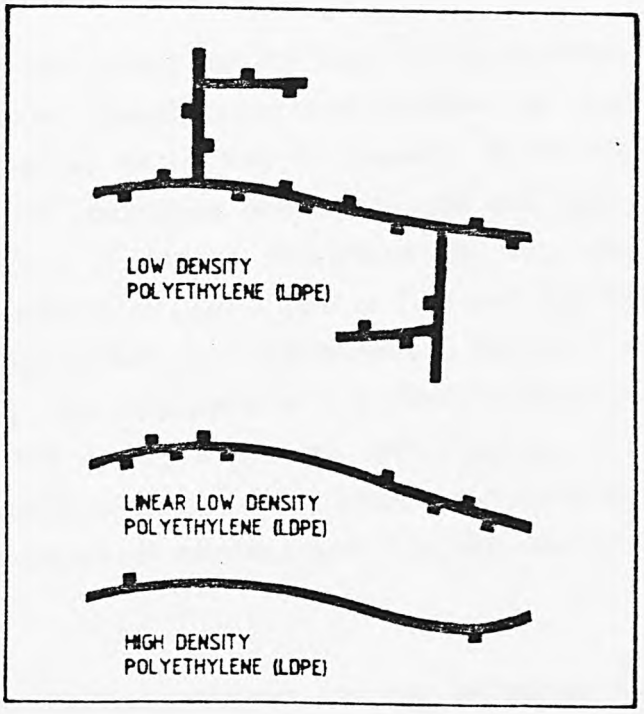

Figure 1.4. Branching structure of LLDPE, HDPE, and LLDPE molecule.

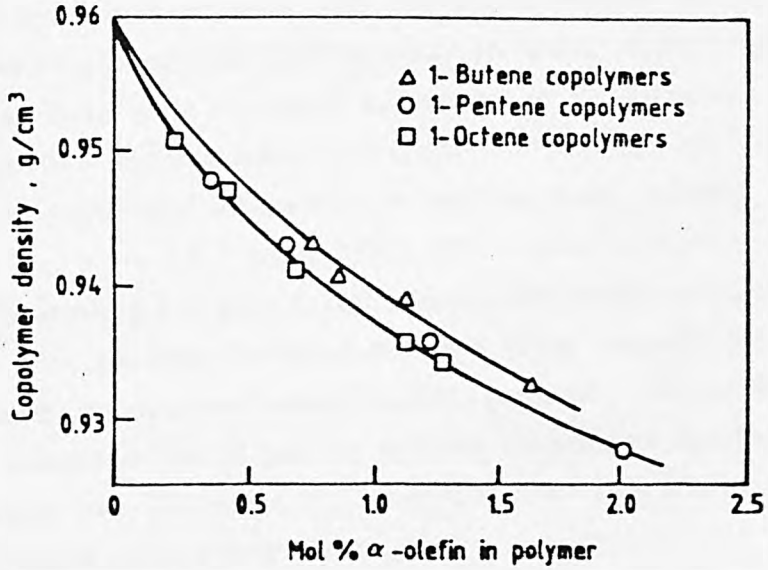

Figure 1.5. Effect of branching type and concentration on density of ethylene-α olefin-copolymer.

of the comonomer used determines the length of the branches; the amount of comonomer used determines the number of branches; the catalyst and process employed determine the distribution of branches in the polymer. Although the opportunities for controlling comonomer type and number are straightforward, the control of branch distribution is more elusive. Branching uniformity is considered to play a role in film strength and is seen to be related to the nature of different comonomers as well as to processing conditions [Cady, 1987]. The magnitude of this effect is illustrated in Figure 1.5, which compares the density at various concentrations of comonomers for polyethylenes containing methyl, ethyl, propyl, and hexyl side chains, corresponding to copolymers of ethylene and 1-butene, 1-pentene, and 1-octene [Short, 1981].

In the years since Phillips petroleum company introduced LLDPE, a number of other process technologies have been developed. Four basic processes have become established for the manufacture of LLDPE, whereby the reaction as yet can only be started with Ziegler-Natta catalysts.

The gas phase Unipol process was developed by Union Carbide Corporation (UCC). UCC is the leading company promoting gas-phase polyethylene technology. Initial emphasis with the Unipol process was placed on developing general purpose (GP-LLDPE) products based on butene-1 as comonomer. These products were developed to compete in large volumes commodity film and injection molding markets. Compared to conventional LDPE, GP-LLDPE provided substantial advantages in melting point, strength, and modulus as shown in Figure 1.6 [James, 1987]. Other major companies involved in gas phase processing are Exxon, Gulf, Mobil, and Amoco. British Petroleum (BP) works with its own fluidized bed gas phase process that uses butene as comonomer to produce valued LLDPE granules. The advantage of the gas phase process is that it gets by without solvent and ensuing distillation and equipment cost. Therefore, the process is more cost effective as compared to conventional polyethylene plants.

The emulsion process (slurry) is developed by Phillips company and it works in a loop reactor with hexene-1 as the comonomer in iso-butane. The density of the LLDPE produced is more in the medium range (0.93 to 0.94 g/cm^3) and mechanical values of the product are better than those of butene copolymer.

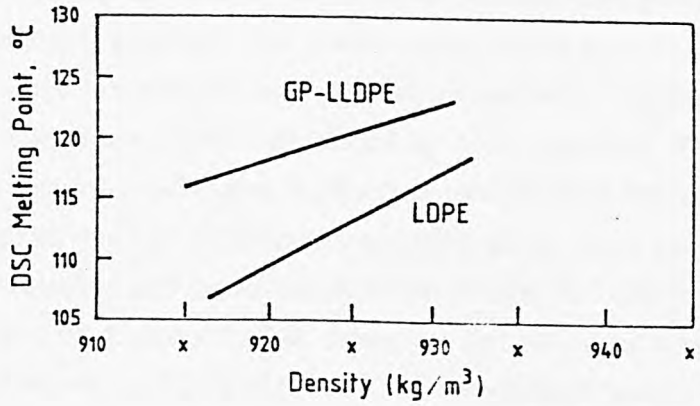

(a)

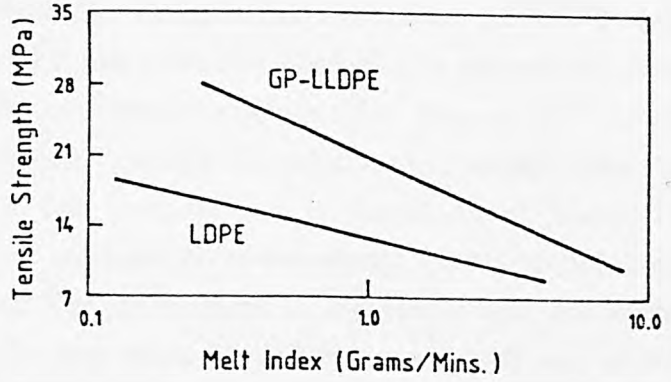

(b)

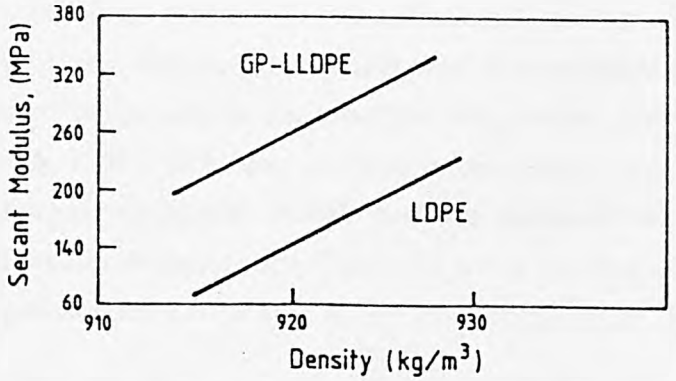

(c)

Figure 1.6. Comparison of GP-LLDPE versus LDPE, (a) melting point, (b) tensile strength, and (c) secant modulus.

The solution process is used by Dow, DSM (Stamicarbon process) and DuPont Canada (Sclairtech process). The process uses octene as a comonomer and the products of solution process are reputed to be more readily processed and better in quality than LLDPE produced by other methods. The high pressure process is licensed by CDF and is the cheapest solution for the production of LLDPE to retrofit an already existing LDPE plant. Both autoclave and tube reactors are suitable and pressure of between 800 to 1200 bars are employed for autoclave and slightly higher pressures for the tube reactor. A Ziegler-Natta system serves as the catalyst and the comonomer is butene [Bork, 1984].

1.3.3 Properties and Applications

The linear structure of LLDPE does indeed produce relatively pronounced deviations from the property configuration of LDPE with its long chain branches. LLDPE has increased markedly in commercial importance in recent years because of distinct reasons. The first is the development of more versatile catalysts, making it possible to copolymerize alpha-olefins with ethylene in a low pressure gas or liquid phase process. Secondly, LLDPE shows superior qualities to conventional LDPE, particularly the mechanical characteristics. The differences in the nature and the amount of short-chain and long-chain branching of LLDPE and LDPE also affect melt properties and melt rheology. The advantage of LLDPE over LDPE is because of its property of down guaging to 5 microns, higher toughness and tensile strength for same density, higher tenacity (puncture resistance, dart-drop, tensile impact strength) even at lower temperature, operational reliability during processing, splitting tendency, advantageous sealing properties, higher environmental stress cracking resistance, and less warpage [Ghani, 1987]. The disadvantageous properties in conjunction with poorer processing behavior as compared with LDPE are low shrinkage properties, limpness of the film despite the frequently higher secant modulus measured, excessive elongation capacity and lesser transparency. Table 1.4 gives an idea of the properties of LLDPE compared with LDPE and HDPE [Mukherjee et al, 1985]

The present wide applications of LLDPE worldwide are mainly due to their superior properties which are toughness, stiffness, stress-crack resistance, and electrical properties. Polyethylene resins used in pipe applications are true engineering plastics designed for useful life upto 50 years. LLDPE is

Table 1.4

Properties of LLDPE,Relative to LDPE and HDPE

Property	LDPE	HDPE	Relative to LDPE	Relative to HDPE
Tensile Strength (MN/m^2)	6.9-15.9	21.4-38	Higher	Lower
Elongation (%)	90-650	50-800	Higher	Higher
Impact Strength (/12.7 mm)	No break	1.02-8.15	Better	Similar
Environmental Stress-cracking Resistance	--	--	Better	Similar
Heat Distortion Temp.	40-50	60-82	15^oC Higher	Lower
Stiffness (4.5 MN/m^2)	1.18-2.42 Mode of elasticity	5.53-10.4 Mode of elasticity	Less	Can be same
Warpage processibility	Excellent	Good	More difficult	Easier
Haze (%)	40	--	Worse	Better
Gloss (45^o in %)	83	--	Worse	Better
Clarity	Near transparent to opaque	Translucent to opaque	Worse	Better
Melt Strength	--	--	Lower	Lower
Softening point range (^oC)	85-87	120-130	Narrower	Narrower
Permeability (ml cm^{-2} g^{-1} ml^{-1} cm Hg^{-1} at 25^oC x 10^{-3}				
(a) H_2O vap	420	55	Better	Worse
(b) CO_2	60	13	Better	Worse

gradually replacing polyethylenes as pipe resins which are frequently subjected to harsh environmental conditions and high stresses.

The films market is expected to become a very large outlet for LLDPE resins because of down-gauging property. This implies that the greater strength and toughness of LLDPE makes it possible to produce significantly thinner film with strength and impact properties equal to or better than a thicker LDPE film. This leads to a 20 - 25 % saving on resin consumption [Turley, 1979]. The usage of LLDPE in adhesive lamination film or for heat sealing layer in multilayer co-extrusion has increased rapidly over the past few years. The biggest performance application for LLDPE is pallet stretch film which has shown enormous growth in the last few years [Turtle, 1986].

LLDPE has been used as a blend with other polymers to gain performance advantage in many applications [Speed, 1982]. Some of the applications are blends with LDPE, HDPE, and ethylene vinyl acetate (EVA), to improve heat sealing and hot tack in packaging films, sacks, etc. Blends were also used in shrink films to improve burn-through resistance. There are many film applications that are moving from low level LLDPE blending to LLDPE-rich blends. They include liner bags, refuse sacks, produce bags, carrier bags, shrink film, pallet shrink hoods, etc . LLDPE is now being increasingly used to improve film specifications by its use in blends and co-extrusions. Application of LLDPE in the field of agriculture and other outdoor uses is greatly limited because of the doubts about the weathering stability of this polymer. The potential of LLDPE in some major agricultural film application is in greenhouse, ensilage, and mulch films.

1.3.4. Blends of LLDPE and LDPE/HDPE

In recent years blends of various polyolefins have received more and more attention because of two main reasons. The first being that the polyolefins form most of plastic waste and their recycling leads to mixture without separation. The second is that the blends lead to new materials with tailored properties for specific purposes. Extensive studies on compatibility of blends of amorphous-amorphous and amorphous-crystalline systems have been conducted by a variety of approaches [Hu et al, 1987]. Studies of crystallizable

polymers have been more difficult because of their complex morphology [Kyu et al., 1987].

Blending of polyethylenes of different degrees of branching has long been employed to adjust the properties such as modulus and toughness of the material, or to improve the melt properties for processing. The compatibility of such systems is hence of interest, compatibility being defined as the ability to form an isomorphic system. In the case of semi-crystalline polymers, an isomorphic system can be taken to comprise one amorphous phase and one crystalline phase [Edward, 1986]. The compatibility of conventional LDPE and HDPE have been observed to be either incompatible or semi-compatible [La Mantia and Acierno, 1985].

The introduction of a new class of polyethylene, viz. LLDPE having some of the advantages of both previous polyethylenes, gives the possibility of obtaining a new class of blends (LDPE/LLDPE). The possibility of obtaining a new class of blends which are easily processable and which have good mechanical properties has been successfully investigated [Acierno et al, 1984]. The elastic modulus, tensile strength and elongation at break of these blends, which show semi-compatible behavior in the solid state, increase with the LLDPE content [La Mantia and Acierno, 1985].

Hu et al have studied a blend of LLDPE (ethylene butene-1 copolymer) with HDPE using differential scannining calorimeter (DSC), wide angle x-ray diffraction(WAXD), small angle x-ray scattering (SAXS), Raman longitudinal acoustic mode spectroscopy (LAM), and light scattering (LS) [Hu et al, 1987]. Examination of the melting and crystallization behavior of the blends indicate that crystallization has taken place between the components. In dynamic birefringes studies, the blend manifests optical and mechanical relaxation behavior intermediate between that of the components for all regions, which is reminiscent of the characteristics of the compatible blends.

Melting and crystallization phenomena in blends of LDPE and LLDPE were explored, with emphasis on composition, by DSC and LS [Ree et al, 1987]. The polymers were found to form co-crystalline phase under a variety of conditions, and can thus be regarded as compatible [Edward, 1986].

1.3.5 Degradation and Stability

LLDPE is considered as an important engineering material and there are a large, and still increasing number, of studies published in this relatively new type of polyethylene. The majority of these publications deal with the rheological properties and technological problems of processing and applications [Acierno et al., 1985, Huang and Campbell, 1986, Minoshima and White, 1986, and White and Yamane, 1987]. Another field of great practical significance is the degradation and stability which is almost entirely dealt with patent literature except for some comprehensive studies.

The degradability of ethylene-alpha-olefin copolymer depends very much on chain branching which in turn depends on the comonomer content. Polymethylene, which has no side branches or any imperfection in the linear chain, proves to be more stable against oxidation while the degradability of the copolymers increases with increasing comonomer content. This phenomenon is ascribed to the enhanced reactivity of tertiary C-H bonds . Moreover, in a solid polymer the oxidizability depends on the degree of crystallinity. Short chain branching decreases the crystallinity in LLDPE, so it is possible that the observed phenomena is caused mainly by the increase in the amorphous content [Willbourn, 1959].

The oxidative stability of LLDPE was studied under static and dynamic conditions. The induction period was found to be inversely proportional to the vinyl content of the polymer while the oxygen uptake was proportional to the amount of chain branching. Dynamic degradation was found to involve chain scission (and oxygen uptake) [Iring et al, 1986]. Commercially available stabilizers were studied for the outdoor usefulness of LLDPE in the natural environment of Florida. The change in mechanical properties were determined as a criterion for determining the weathering degradation rate on different formulations used. It was concluded that the use of selective stabilizers can increase the life of polymer in outdoor environment upto 33 months compared to 4 to 5 months for unprotected LLDPE [Pouncy, 1985]

The photo-oxidation of the blend of LLDPE and LDPE and of pure polymers were studied. The loss in mechanical properties were greater for LLDPE than

for LDPE. On the contrary, infrared results show an almost complete dependence of composition [La Mantia, 1985].

The review on various aspects of LLDPE have revealed that there have not yet been any published broad-based experimental investigation on the effect of harsh climate on the significant properties of LLDPE. However, an extensive literature on processing, and rheological properties of LLDPE exist.

1.4 CHARACTERIZATION OF WEATHERED PLASTICS

The weathering of plastics can be followed by many different analytical techniques. Their validity depends on the nature of the material and the mode of deterioration. If a technique is relevant to the characterization of a polymer then it is often an appropriate means of assessing the degraded material [Davis and Sims, 1983]. Since most of the degradation result from irreversible chemical reactions of polymers molecules, changes in molecular composition provide a logical method for measuring the course of polymer degradation. As hydrocarbon polymers degrade, many different changes in polymer composition occur. In this work Fourier transform infrared spectroscopy (FTIR) is used to study the changes in the functional groups (carbonyl, vinyl, vinylidene, alkene, and hydroxyl) of plastic as a function of exposure to the natural weather. Thermal properties of plastics plays an important role in the useful lifetime of a particular plastic. Differential scanning calorimetric technique is used to study the changes in plastic thermal properties (crystalline melting temperature (T_m)), heat of fusion (H_f), and percent crystallinity with exposure time. The effects of degradation on polymer performance, e.g. loss of mechanical strength, should be determined by measurement of that specific property which will cause eventual failure once specified limits are exceeded. Mechanical properties do not change at the same rate as chemical reactions take place in a polymer [Hawkins, 1984]. It is important therefore to determine how a polymer will fail in service and to follow changes in that property which is critical to failure. In this work mechanical properties (tensile strength and percent elongation) are considered critical performance properties and are studied as a function of plastic exposure to natural weather.

1.5 FOURIER TRANSFORM INFRARED (FTIR) SPECTROSCOPY

1.5.1 Introduction

IR spectroscopy has long been recognized as a powerful tool for polymers characterization. The uses of dispersive infrared spectroscopy for polymer studies have been clearly documented in the review by Krimm [Krimm, 1960]. With the advent of Fourier transform infrared (FTIR) spectroscopy numerous problems in the field of polymer physics and polymer analysis have become more readily accessible to spectroscopic investigation than with conventional dispersive instrumentation [Siesler, 1979]. The increased speed and higher signal-to-noise ratio of FTIR as compared to dispersive IR has lead to a substantially greater number of applications of IR in polymer research. The availability of the dedicated computer, which is required for the FTIR instrumentation, has allowed the digitized spectra to be treated by powerful data processing techniques. This has increased the utility of the IR spectra for qualitative and quantitative analysis.

Application of IR spectroscopy to polymers involve identification of chemical composition or state of order or both. Both qualitative and quantitative information can be obtained on the chemical composition of polymers, copolymers, polymer blends, composites, and the various additives used in these materials. The IR spectral frequencies and intensities may also be sensitive to chemical order, that is, tacticity, branching, end groups, and degradation products. IR spectra of solid polymers provide information on the type and amount of crystalline forms, the degree of crystallinity, orientation, trans-gauche ratios, characterization of noncrystalline material, and the nature of both intermolecular and intramolecular branching [Fanconi, 1984].

This section will briefly outline the FTIR method and the comparison of FTIR with dispersive IR spectroscopy. A complete review of the involvement of IR spectroscopy in studying the weathering degradation of polyethylene will be presented.

1.5.2 The FTIR Method

The historical development of FTIR spectroscopy goes back to the time when light was first dispersed so that it can be more easily analyzed. At first the dispersion element was a prism, then later, a grating and after a time, resolution was there for greater dispersion that may discern fine feature. In 1881 Michelson developed the two beam moving mirror device which were called interferometer and were found better than prism and grating in studying fine band structures. By 1911, the technology had advanced sufficiently and it was possible to record the first true interferogram. Figure 1.7 shows the historical development in FTIR spectroscopy. The British astrophysicist, Peter Fellgett, used an interferometer for astronomical spectroscopy, where the multiplex advantage was critically important. He was also the first to transform an interferogram into a spectrum by means of Fourier analysis. Due to the complexity of the Fourier transform and state of the computer art during the 1950's and early 1960's, interferometric spectroscopy was a high cost research tool. It is the combination of software techniques (principally the Fast Fourier transform algorithm) and the development of low cost mini- and microcomputers that FTIR spectrometer has become a practical tool for the analytical laboratory.

The basis of the IR spectroscopy is the absorption of radiation in the IR frequency range due to the molecular vibrations of the functional groups contained in the polymer chain. A plot of some function of radiation intensity versus frequency is obtained. The manner in which this is accomplished in FTIR is quite different from what is done in dispersive system. Dispersive instrument utilize prism or grating to geometrically disperse the infrared radiation as shown in the optical diagram of the IR dispersive spectrometer (Figure 1.8). Using a scanning mechanism, the dispersed radiation was passed over a slit system which isolated the frequency range falling on the detector. In this manner, the spectrum, that is, the energy transmitted through a sample as a function of frequency was obtained. This IR method is highly limited in sensitivity because most of the available energy does not fall on the open slits. Hence to improve the sensitivity Michelson interferometer was used as an optical device which allows the examination of all of the transmitted energy all the times. The heart of a FTIR system is the Michelson interferometer which consists of a beam splitter, a fixed mirror, and a constant-velocity

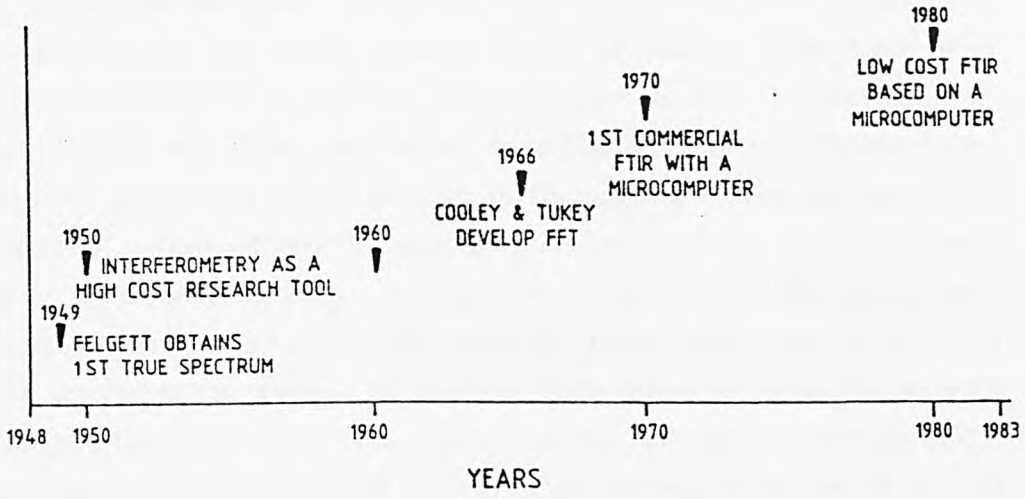

Figure 1.7. Historical development of FTIR spectrometer.

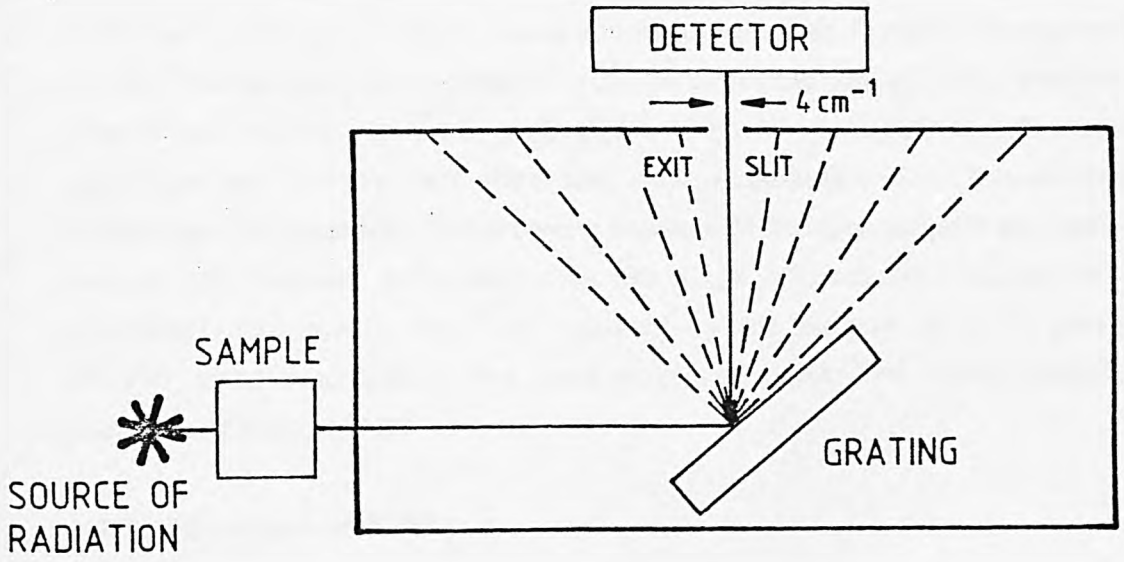

Figure 1.8. Optical diagram of IR dispersive spectrometer

moving mirror, as illustrated in Figure 1.9. The incident beam is split into two components at the beam splitter which is usually KBr plate with germanium coating. Half of the light is transmitted through the beam splitter, and half is reflected. These two beams, on reflection, are recombined at the beam splitter. Depending on the position of the moving mirror, the two beams will interfere constructively or destructively to produce an interference pattern or interferogram (light intensity as a function of the optical-path separation of the moving and fixed mirrors). These interferogram data are typically converted to normal IR spectra (light intensity as a function of frequency) which are useful for characterizing and identifying molecular species. This conversion is carried out by the mathematical process of Fourier transformation which involves an integration similar to the following expression [Griffiths, 1975]:

$$B(\bar{\nu}) = \int_{-\infty}^{+\infty} I(\delta) \cos 2\pi \bar{\nu}\delta \cdot d\delta, \qquad (1)$$

where $B(\bar{\nu})$ represents the intensity of the source at frequency $\bar{\nu}$, in cm^{-1}, as modified by instrumental characteristics and $I(\delta)$ represent the intensity as a function of mirror separation, . In practice it is necessary to place finite limits on the integral with a truncation or apodization function. Computation of the Fourier transform integral requires manipulation of large number of data points and is extremely impractical without a combination of software technique and the low cost mini- and micro-computers. Fast Fourier transform algorithm provided the software support. Hardware support was possible because of immense development in the field of dedicated computers for analytical instruments. The time required by the modern FTIR to perform Fourier transformation is less than a second with fast array processors [Coates and Setti, 1983].

1.5.3 Advantages of FTIR

The advantages of FTIR over dispersive IR spectroscopy have contributed to its widespread use. In conventional spectroscopy the light is dispersed and each wavelength is examined separately. FTIR multiplexes the signal so that each point on the interferogram contains information about all the wavelengths present. Therefore, multiplex or Fellgett advantage makes it possible that all frequencies are observed simultaneously and a complete spectrum can

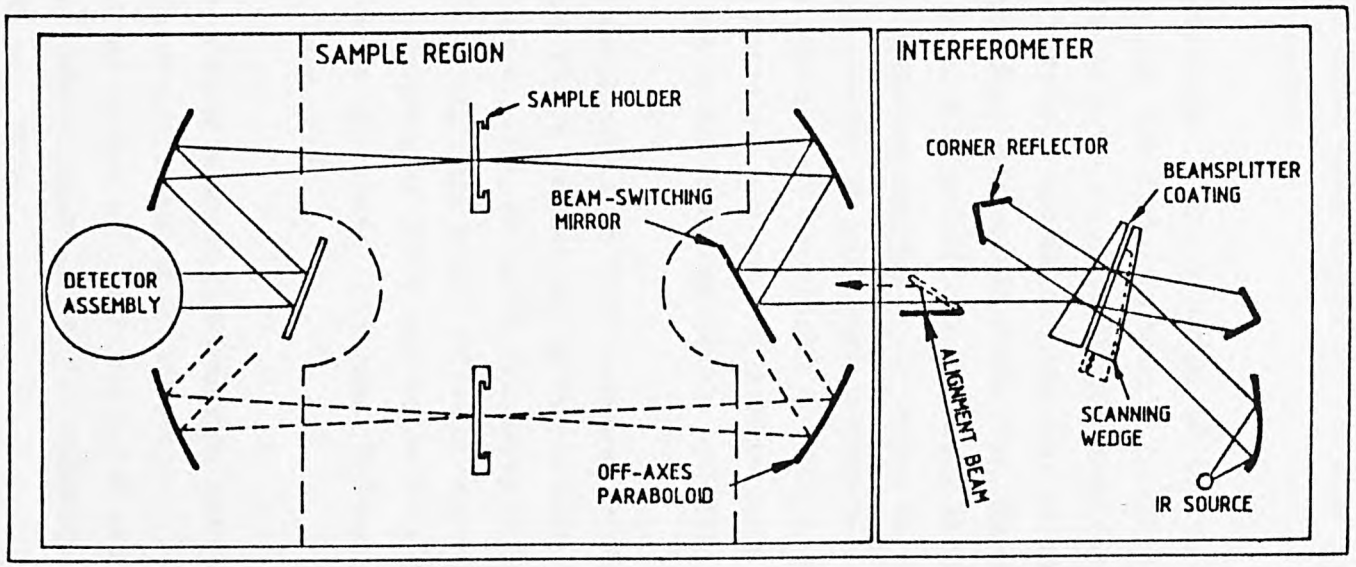

Figure 1.9. Optical diagram of FTIR spectrometer.

be obtained very rapidly. The second main advantage is the throughput or Jacquinot advantage. Since there are no slits or other obstructions in the optical path greater throughput is achieved. Therefore, for a given resolution the energy throughput in an interferometer can be greater than in a dispersive instrument. In combination with the multiplex advantage this leads to shorter measurement times to achieve the same signal to noise ratio as a dispersive instrument.

The third advantage is the precision of the wavelength measurement or Connes advantage. The frequency scale of an interferometer is derived from a laser which serves as an internal reference. The frequency accuracy and long term repeatability are much better than in dispersive instrument. Stray light specifications are better than for dispersive instruments. Each wavelength appears as a different frequency in the interferogram and the separation is mathematical, not being subject to the mechanical implicit in the physical separation of wavelength in dispersive system. The advantage of constant resolution at all wavelengths in FTIR is a cause of very high noise level at the end of the spectrum. As there are no gratings or filter changes in FTIR there are no discontinuities [Siesler and Holland-Moritz, 1980].

The overall simplicity of an FTIR compared to dispersive instrument is also an advantage. This is exemplified by the versatility of the single instrument to study the near, mid, or far-IR frequency region whereas the dispersive method will require three totally different instruments. It is also convenient to improve resolution of FTIR instrument by slightly modifying the basic design while in dispersive instrument different optical components are required [Koenig, 1975]

FTIR has also some inherent disadvantages and the predominant is that the raw data, an interferogram, is for all practical purposes unintelligible. This implies that the contact with real data is lost and a computer is required to interpret the interferogram and so the technique approaches the black box syndrome [Koenig, 1984].

1.5.4 Weathering Degradation Studies of Polyethylene

IR spectra arise from the molecular transitions between quantum states of differing internal energies [Cernia et al., 1963]. The frequency of the emitted or absorbed radiation is related to energy differences and is associated with molecular vibrations and rotations characteristic of chemical groups, e.g., alkyl, hydroxyl, carbonyl [Silverstein et al., 1981]. In the case of oxidation, the carbonyl groups associated with the products of degradation are detected by the absorption bands between 1850-1700 cm^{-1}. These bands comprise the carbonyl compounds of carboxylic acids, aldehydes, esters, and ketones [Stivala et al., 1983]. Until recently, such measurements have invariably been made with conventional prism spectroscopes which have limited sensitivity. Sensitivity is a major factor in the early stages of degradation. The commercial appearance of FTIR spectroscopy has brought about a revival in infrared spectroscopy [D'Esposito and Koenig, 1978]. FTIR measurements were particularly useful in providing information on initial product formation, which had previously eluded detection [Webb, 1984]. Weathering effects on polymers, particularly those resulting from photooxidation, are generally concentrated in the surface layers. Reflection FTIR spectroscopy has been used to study the surface of degraded polymers [Webb et al., 1983].

Infrared spectroscopy has been used since 1950 in the study of photooxidative degradation [Pross and Black, 1950] of polyethylene. One of the studies concluded that carbonyl groups are formed during photooxidation of polyethylene which are well distributed among the aldehyde, acid, and ketone forms. [Rugg et al., 1954]. Since the effects of weathering are initially concentrated on the surface of the sample, one approach is to use internal reflection spectroscopy in the infrared region. It was noticed that after weathering during the summer, a considerable amount of carbonyl is formed on the sample surface [Chan and Hawkins, 1968].

In another study, it was found that temperature, film thickness, ozone, and moisture play significant roles in polyethylene degradation. The key role, however, is played by UV radiation and polyethylene structure and morphology were considered to be dominant [Winslow et al., 1966; Adams, 1970; Weiner, 1971]. It was concluded that carbonyl absorbance is directly

proportional to oxygen consumption up to at least 20 ml per gram of polymer [Winslow et al., 1972].

A number of studies have been reported from around the world using IR spectroscopy to monitor degradation of polyethylene. The effect of natural weathering on the chemical structure of low density polyethylene (LDPE) was studied in Ankara, Turkey by Akay et al. [1980b]. Formation of carbonyl and vinyl groups was investigated by IR spectroscopic measurements. The most important spectral changes occurred in the carbonyl region and the changes in the unsaturation region corresponding to vinyl groups were considered to be of secondary importance [Akay et al., 1980]. Moreover, a study has been made of the effect of orientation on the oxidative degradation of LDPE and HDPE under UV radiation. The drawing effect decreases the rates of oxidative degradation of LDPE and High Density Polyethylene (HDPE) in terms of the carbonyl index as shown in Figure 1.10 [Akay et al., 1980a; Akay and Tincer, 1981]. The effect of drawing temperature and the presence of various types of additives on UV-induced oxidative degradation of HDPE were also interesting to consider. The IR spectroscopy revealed that for a given draw ratio, the oxidative degradation is retarded with an increase in drawing temperature, irrespective of additive combination in the polymer [Tincer et al., 1986].

The photodegradation of polyethylene, brought about by exposure to the natural environment of Kuwait, was studied by Rasoul and Hameed [1980]. The IR spectra of polyethylene changed dramatically during the summer exposure period and new absorption peaks appeared at 1700-1800 cm^{-1} and 3400-3500 cm^{-1}. Furthermore, these peaks grew with increased exposure time. Moreover, outdoor weathering of colored polyethylene films was conducted, and the results revealed that films containing yellow and pink degraded faster than films containing blue, green, and black pigments (Figure 1.11). After 35 days of exposure, the IR spectra of all the polyethylene films except the black one showed formation of carbonyl groups between 1710-1720 cm^{-1}. At the same time, all the films showed evidence of the formation of hydroperoxides in the region of 3410-3600 cm^{-1} [Hameed et al., 1980]. Mlinac and coworkers [Mlinac et al, 1976] have also reported that the extent of deterioration of colored polyethylene film, during weathering, depends on the nature of the pigment utilized.

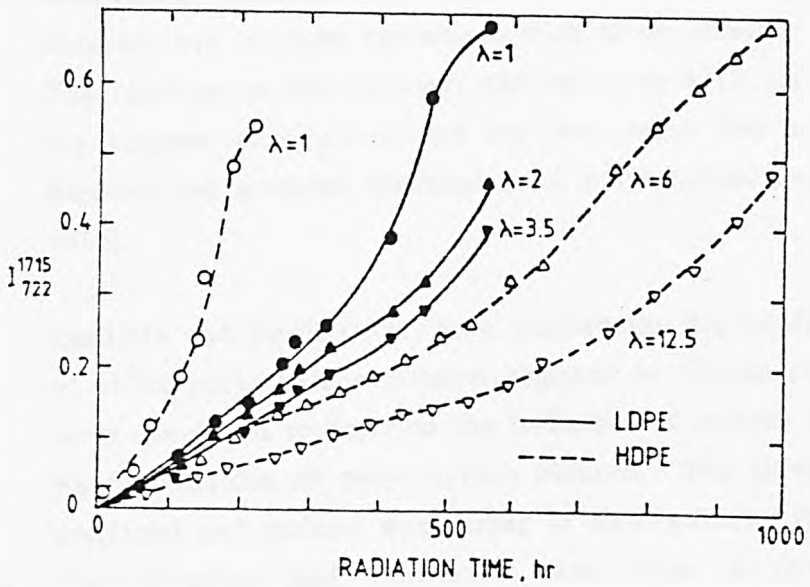

Figure 1.10. Variation of the carbonyl index for various ratios (λ) of polyethylene

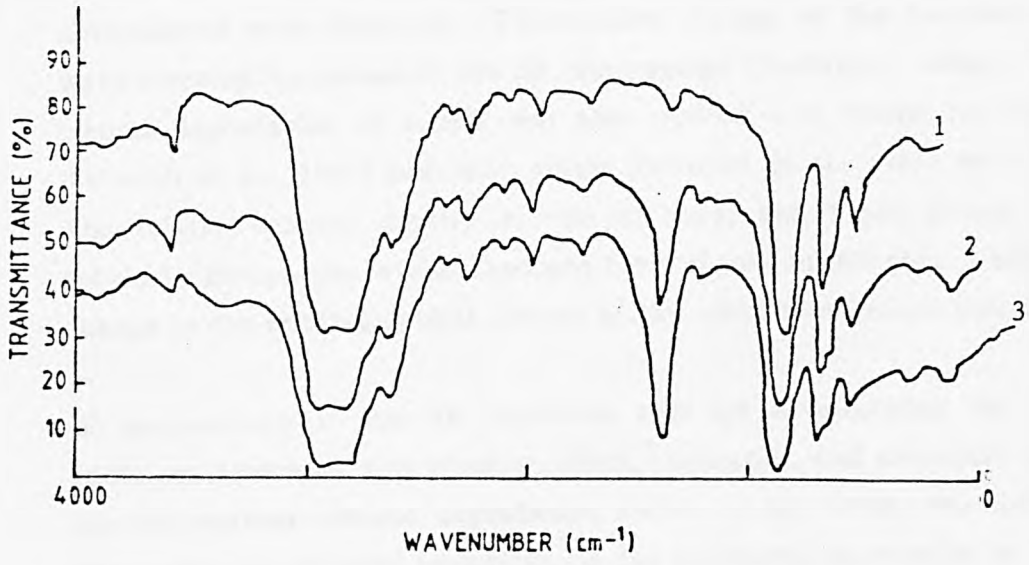

Figure 1.11. IR spectra of unexposed and exposed green polyethylene.
(1) zero day, (2) 35 days, and (3) 66 days
Natural exposure at Safat, Kuwait

Weathering and degradation of polyethylene sheets for agricultural applications were also studied in Kuwait using IR spectroscopy [Mobasher and Bahr, 1981]. In addition, photoacoustic spectroscopy (PAS) was used to study natural weathering of polyethylene film exposed in Safat, Kuwait. The results obtained are in close agreement with those obtained using IR spectroscopy. The increase in the carbonyl absorption at 1715 cm^{-1} was dramatic during the summer exposure period but was much less so during winter. PAS supports the accepted mechanism of polyethylene degradation [Anani et al., 1984].

Cunliffe and Davis [1982] have studied the degradation in rough weathering of thick polyethylene samples exposed at Cloncurry, Australia. Equations were developed to describe the influence of oxygen diffusion on the rate of photo-oxidation of polyethylene plaques. The theory was applied to both artificial and natural weathering of unstabilized LDPE samples, 3mm thick. The observed and calculated rates show a relatively weak distance-dependence to a depth of about 1 mm, beyond which they are diffusion-controlled [Furneaux et al., 1981].

Structural changes occurring in LDPE exposed to natural weather at Palermo, Italy, have also been reported [LaMantia, 1984a]. The influence of a light stabilizer was also considered and possible mechanisms of photooxidation and antioxidants were discussed. The relative changes of the functional groups were revealed by means of the IR spectroscopy [LaMantia, 1984a]. Environmental degradation of LDPE was also studied and results for the initial [Severini et al., 1986] and later stages [Severini et al., 1987] were reported. The relative optical density of the carbonyl and vinyl groups increases regularly during the whole exposure time of the initial step, while a small change in the relative optical density of the vinylidene groups was observed.

IR spectroscopy is also an important tool for investigating the effect of additives [Mätreyek and Winslow, 1975], impurities, and structural irregularities on weather-induced degradation [Amin et al., 1975]. The influence of unsaturation and metal impurities on the oxidative degradation of polyethylene has been studied using IR spectroscopy. The results show that the degree of unsaturation is important for both thermal and photochemical oxidation, in the solid and in solution. It was concluded that unsaturation content is

more important than metal impurities when determining oxidation rate for the HDPE samples [Chirinos-Padron et al., 1987a]. The effect of several commercial antioxidants, used in the synergistic formulation of two grades of HDPE, has also been examined using IR spectroscopy. The results show that as expected, synergism is generally obtained between specific antioxidants in HDPE films during UV irradiation conditions [Chirinos-Padron et al., 1987b].

The lifetime of polyolefins in the presence of UV light is markedly dependent on the degree of oxidation that occurred during the prior processing operation. This is strongly influenced by the presence of prooxidants and antioxidants, and their effect on subsequent UV life can be rationalized on the basis of their functions during processing. The effect of metal dithiocarbamates on the carbonyl content of polyethylene during processing and accelerated UV exposure showed an increasing trend [Mellor et al., 1973].

The effects of photosensitizers have been studied by considering several important classes of UV activators. The oxidation progress was followed by measuring carbonyl formation in polyethylene films (carbonyl index). Three different kinds of UV oxidative behavior were observed: the first, typical of the efficient triplet activators such as benzephenone and its derivatives; the second, typical of transition metal ions; and the third, characteristic of sulphur-containing metal complexes. It was shown that, in each class, UV behavior is an extension of the function of the additive in the polymer melt during processing [Amin and Scott, 1974].

The effect of prior irradiation in an inert atmosphere and the subsequent photooxidative stability of LDPE has been examined using IR spectroscopy. Prior prolonged irradiation in an inert atmosphere of nitrogen was found to have no significant effect on the subsequent rates of photooxidation of the polymer films [Allen, 1980].

The number of reprocessing cycles of LDPE have been reported to considerably affect its short and long term performance [Sadrmohagheh and Scott, 1980] when subjected to UV radiation. The recycling of the waste polymer must be approached cautiously particularly where it might have been subjected to previous reprocessing operations [Sadrmohagheh and Scott, 1980].

The IR spectroscopic studies for naturally or artificially weathered LLDPE are rarely reported in literature. In one of the studies films of blends of LLDPE and LDPE and of pure polymer were photooxidized for different time in an artificial weathering device. The growth in functional groups shows dependence on composition during the early stages of degradation [La Mantia, 1985]. Allen et al. [1985] studied the photostabilization action of a light stabilizer in LLDPE. Rates of photooxidation were measured by monitoring the buildup in concentration of the nonvolatile carbonylic oxidation products. Carlsson et al. [1985], using FTIR, has identified a series of reactive gases for the rapid quantification of many of the products from the photooxidation of LLDPE.

The review on the application of IR studies on studying the weather-induced degradation of polyethylene indicate that substantial amount of work is done on LDPE and HDPE. However, FTIR studies of the LLDPE samples exposed in the natural environment are not available in the literature.

1.6 THERMAL ANALYSIS

1.6.1 Introduction

The term "thermal analysis" applies to a family of techniques which monitor primarily physical properties as a function of temperature or time at fixed temperature. Whenever a material undergoes a change in physical state, such as melting or transition from one crystalline form to another, or whenever it reacts chemically, heat is either absorbed or liberated. Many of such processes can be initiated simply by raising the temperature of the material. The field of thermal analysis of polymers has expanded exponentially since the introduction of simple, low cost instruments for several types of thermal measurements just over 20 years ago. In addition to the traditional calorimetric and differential thermal analysis, the field now includes equipments for thermogravimetric analysis, thermomechanical analysis, electrical thermal analysis, and effluent gas analysis. The wide range of instruments facilitate the study of the enthalpy changes associated with heating, annealing, crystallizing, or otherwise thermally treating polymers. In addition, one can now

study a wide variety of responses of the system to temperature, including polymerization, degradation, or other chemical changes [Billmeyer, 1984].

The desirability of obtaining calorimetric data on polymer systems is obvious and has been the subject of considerable research using various classical techniques. Much of this work is characterized by very precise results and the methods usually are very time consuming which prohibit their widespread use. This is especially true for polymer characterization where frequently many samples must be compared. Watson et al. [1966] described a differential scanning calorimeter and analyzed its performance. This instrument became commercially available (Perkin-Elmer Corporation) and has been widely used because of its design.

Differential scanning calorimeters (DSC) are designed to determine the enthalpies of the processes by measuring the differential heat flow required to maintain a sample and an inert reference at the same temperature. This temperature is usually programmed to scan a temperature range by increasing linearly at a predetermined rate. This is separated from differential thermal analysis (DTA) where the temperature difference between a sample and reference is measured as a function of time or temperature. In presently available DSC equipments the heat flow is measured by keeping the sample and reference thermally balanced by changing a current passing through the heaters under the two chambers.

This section will concern primarily with applications of differential scanning calorimetry, a brief description of instrumentation, and its role in studying the weathering of polyethylene.

1.6.2 Instrumentation

DSC is a technique of non-equilibrium calorimetry in which heat flow into or out of a sample and reference is measured as a function of time or temperature, thereby, providing a convenient technique to study heat of transition. A block diagram of a typical system is shown in Figure 1.12 [Barrall.II and Johnson, 1970]. Two symmetrically located sample holders are fixed inside a metal block and the temperature sensing devices and heating units are built into the holders to allow individual heating of the sample and reference

materials. In DSC the requirement is to maintain equivalence of sample and reference temperature at all times. The energy difference between sample and reference heaters as the sample and reference experience a linear temperature or time change is measured. Prior to transition, the energy difference is effectively constant. As a sample undergoes transition, the sample heaters must supply additional energy to the material in order to keep the sample and reference temperature the same. As differential energy is recorded as a function of temperature or time, one detects a deflection from the baseline. At the conclusion of the transition, the energy supplied to the sample to maintain temperature equivalence drops back to its pretransition level.

A major benefit which is claimed to be derived from the operating principle of these instruments is that they directly measure the differential power absorbed or evolved by the sample, and, therefore, peak areas are directly convertible to energy units. Moreover, this conversion is claimed to be independent of variables such as sample geometry, sample placement or thermal resistances in the instrument system, which are well known to have a major influence on peak areas produced by instruments of other types [Brennan and Gray, 1973].

1.6.3 Applications

The main quantities that are determined from a DSC curve are the temperature of the beginning and end of the thermal event, the temperature of the peak maximum, the amount of the material involved in the transition or the heat of transformation [Runt and Harrison, 1980]. Within these general headings fall the measurement of glass transition temperature, crystallinity, purity, rate of reaction, rate of crystallization, and rate of decomposition, and the analysis of active material. It has been found that the results of DSC are affected by factors connected with the type of apparatus, physical and chemical nature of the sample, and also the technique employed.

The most frequent application of DSC has been to the measurement of transition heats and temperatures. There has been a variety of theoretical treatments of DSC curves but one feature common to all is that the area under an exotherm or endotherm can be related to the heat of reaction. Specific heats and thermal emissivity can be measured with a DSC rapidly

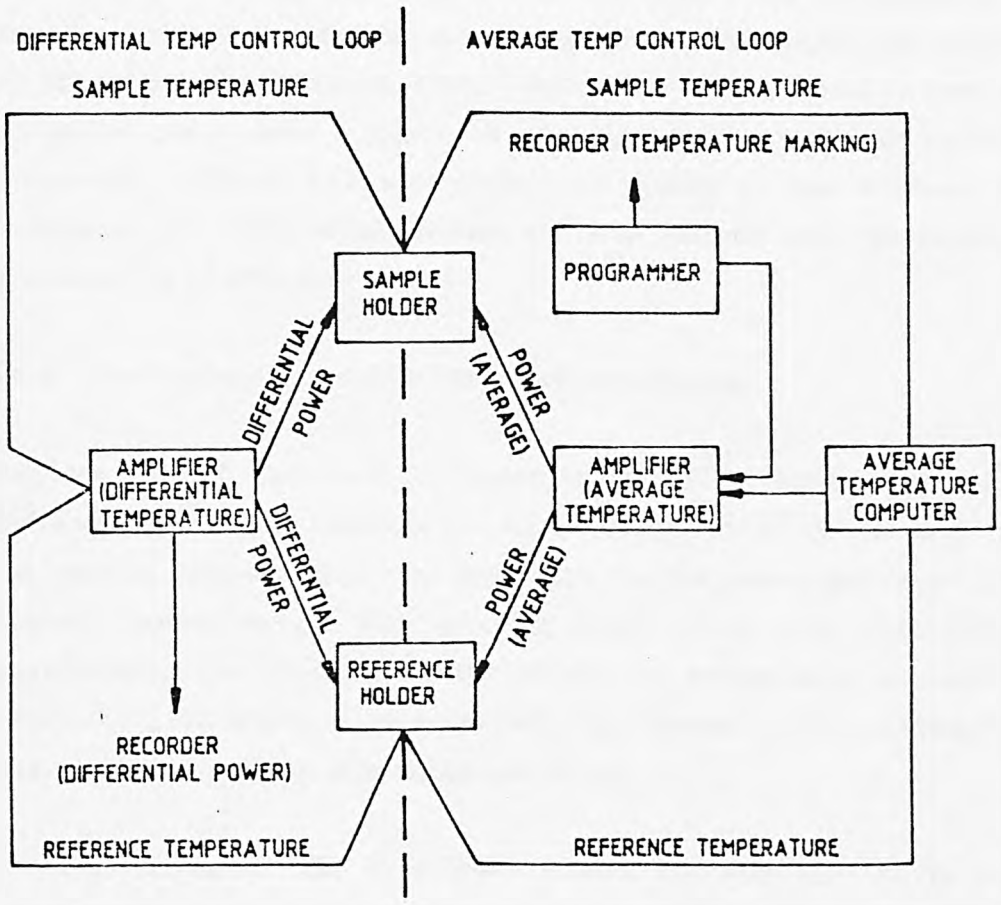

Figure 1.12. A schematic of a typical differential scanning calorimetry system.

and with good accuracy over the temperature range of -100 to 600^{o}C [Barrall II and Johnson, 1970]. Reaction rates and energy of activation can be studied by DSC not only in the isothermal mode but also in the program mode at different scanning rates. Other applications of DSC is in studying the kinetic parameters, rates of crystallization, and purity determination. Blends of LLDPE and HDPE are also examined by DSC and X-ray techniques in order to characterize the crystalline morphology and to investigate the compatibility of the polymers [Edward, 1986]. The polymers were found to form a CO-crystalline phase under a variety of conditions, and can thus be regarded as compatible. Figure 1.13 shows that the results of two methods (X-ray techniques and DSC) which differs and also indicate that the crystallinity decreases for LLDPE rich blends.

1.6.4 Weathering Degradation studies of polyethylene

Polymer research and characterization is one of the major applications of Differential Scanning Calorimetry. As a consequence of the research carried out, routine methods have been developed for the determination of thermodynamic properties, for distinguishing folded chain from extended chain morphologies, for determining the effects of comonomers, additives, for determining the degree of cure, crystallinity, thermal stability, crystallization rate, and other polymer processing operations.

The application of DSC to polymer studies has generally led to a much greater appreciation and understanding of the effects of thermal history on polymer properties. Fundamental studies in the area of polymer morphology almost universally employ DSC.

Thermal analysis have also played a significant role in the degradation studies of a semicrystalline polymers. For a variety of practical reasons, it is customary to think of the solid state of a "semicrystalline" polymer as being composed of x weight fraction crystalline material and (1-x) weight fraction amorphous material. Assuming that the two phase model is a fair representation of a polymer's morphology, the value of x should be a fair representative of its crystallinity [Gray, 1970]. Early studies of cellulose degradation revealed for the first time that hydrolytic agents selectively attacked the amorphous fraction of the polymer, breaking and reordering

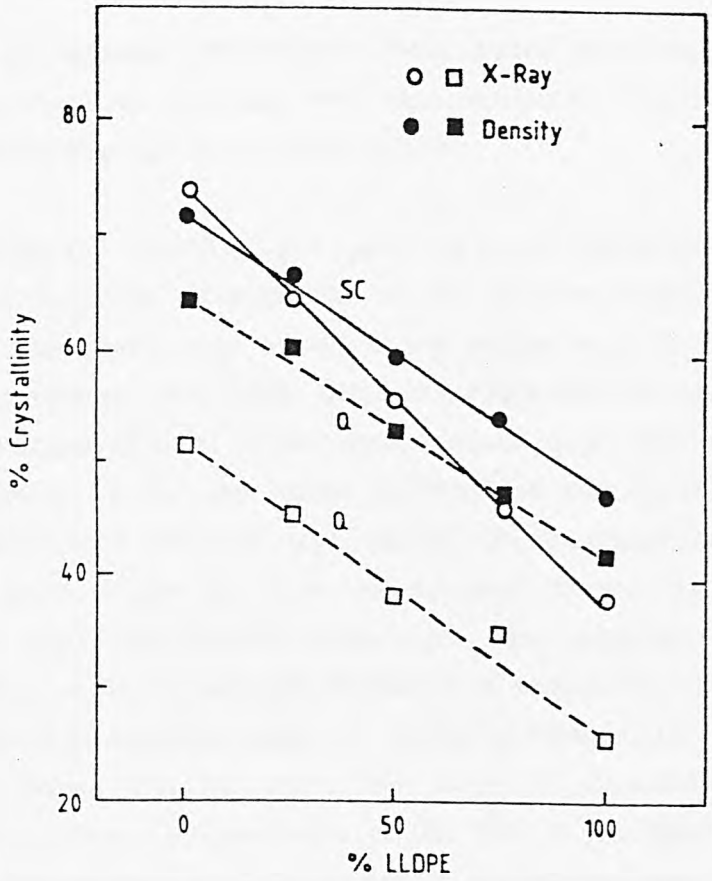

Figure 1.13. Crystallinity of blends of LLDPE and HDPE, circles are for slow cooled specimens and squares for quenched.

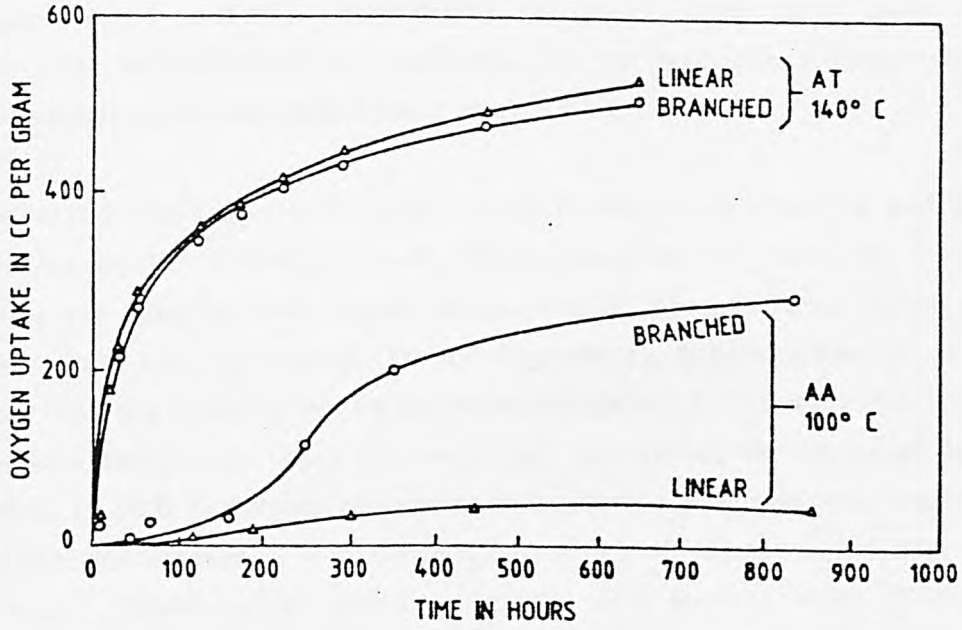

Figure 1.14. Oxidation of polyethylene above and below melting point.

accessible chain segments [Nickerson, 1941]. Later work on polyethylene confirmed that localized reactions were characteristics of all polymers with impervious crystalline regions [Winslow, 1977b]

It is reported that the rate of oxygen uptake in polyethylene during oxidative degradation is inversely proportional to the percent crystallinity in the polymers. It was shown that at 100^{o}C the oxidation rates of linear and branched polyethylene are quite different [Hawkins et. al., 1959]. The oxidation rate appeared to be roughly proportional to the amorphous fraction which was almost 5% for the linear polyethylene and about 40% for the branched polyethylene [Winslow et.al., 1963a]. The oxidation rates at 140^{o}C, however, are quite similar for these two polymers, because at that temperature, which is above the melting temperature, both polymers are completely disordered. This result suggests that oxidation of semicrystalline polyethylene is restricted to the amorphous region as shown in Figure 1.14. In an another study it was shown that the crystalline phase of polyethylene does not absorb gas molecule to any detectable extent. This implies that in crystalline phase oxygen is not consumed for oxidative degradation reactions [Michaels and Bixler, 1961]. In contrary, Meltzer and Morgano, studying the accelerated weathering of polyethylene samples, found no increase in crystallinity [Meltzer and Morgano, 1961]. Although there is some doubt about the detailed consequences of oxidative degradation of polyethylene there seems little doubts that autooxidation is confirmed to the amorphous phase of the semicrystalline polymers [Billingham et al., 1976].

DSC analysis was also used to study the influence of unsaturation and metal impurities on the degradation of polyethylene. It was observed that the polyethylene samples with lower unsatauration contents have higher crystallinity and are less susceptible to degradation [Chirinos-Padron et. al., 1987a]. Drawing ratios effect on the crystallinity of LLDPE were also studied by Seguela and Rietch. They have reported that during the course of tensile drawing, LLDPE undergoes structural changes that has improved crystalline organization (increase in crystallinity, narrowing of crystal size distribution, and slight thickening of crystals) [Seguela and Rietch, 1986]. Blends of LLDPE and HDPE are examined by DSC in order to characterize the crystalline morphology and to investigate the compatibility of the polymers [Edward, 1986]. It was concluded that blends of LLDPE and HDPE are

compatible and crystalline distribution is dominated by the HDPE, probably due to higher mobility rate, but LLDPE molecules form co-crystals with HDPE.

The experiments so far described were all performed under accelerated weathering conditions, often at temperature lying well within the melting range of typical polyethylene samples. However, natural weathering studies were conducted by exposing stabilized LLDPE samples in Messina, Italy [Severini, et. al., 1986]. The increase in crystallinity was determined by DSC method and an insignificant increase was observed after an exposure of 13 x 10^3 hours (18 months) of natural environment [Severini et. al., 1987]. It was concluded that the slight increase in crystallinity cannot be attributed to the formation of cross-linking structures because of complete solubility of the sample. Ram et al [1980] have observed that the crystallinity of LDPE increases with time of exposure to photooxidation and the permeability to gas decreases consequently. It was concluded that the samples with highest branching frequency verifies also the increase in crystallinity [Winslow et. al., 1963b]. The structural and morphological characteristics of branched polyethylene were studied during the atmospheric and accelerated weathering [Rybniker, 1976]. It was indicated that the degradation process taking place during extrusion of branched polyethylene leads to structural changes. These changes influence the number and size of lamellar morphology [Rybniker, 1978].

The review presented in this section indicates that the thermal analysis studies for LLDPE samples exposed to natural environment are not reported in literature. The need for such a study is imperative for a long useful lifetime of LLDPE product utilized for outdoor purposes.

1.7 MECHANICAL BEHAVIOR STUDIES

1.7.1 Introduction

The prime consideration in determining the general utility of a polymeric material is its mechanical behavior. The mechanical properties of a polymer are the facets of behavior that are evident when polymer is subjected in some

form to a mechanical stress. It is from the mechanical properties that the end uses become apparent and limitations recognized.

Polymers differ from ordinary low molecular weight compounds in the nature of their physical state or morphology. Most polymers simultaneously show the characteristics of both crystalline solids and highly viscous liquids [Sharples, 1972]. The term crystalline and amorphous are usually used to indicate the ordered and unordered polymer region, respectively. The term semicrystalline is used to refer to polymers that show crystalline behavior, since no polymer is completely crystalline, and polyethylene is an example [Odian, 1981]. Within any type of polyolefin the most important structural parameter is the crystallinity. This is dependent on the composition of the polymer and the crystallization conditions and it effects all the thermodynamic and mechanical properties.

The properties of polymer depend upon the flexibility of the chains themselves and on the way they are arranged in the structure. The toughness and strength of polyolefin is largely due to their semicrystalline structure consisting of alternating thin lamellar crystals and amorphous regions. In general, mechanical properties of the olefins depend on crystallinity or density, molecular weight, molecular weight distribution, presence of branches, and cross-linking effects.

This section will review the parameters effecting the mechanical properties of polyethylene during degradation with emphasis on natural or artificial weathering.

1.7.2 Determination of Mechanical properties

The precise determination of mechanical properties requires that samples used be free of defects or flaws, such as voids, cracks, nicks, and other abnormalities that could act, for example, as stress concentrators. Because these factors are hard to eliminate under the best of circumstances, a number of samples are usually tested and averaged, the number depending on the kind of sample, the test involved, and the confidence level required.

Descriptive statistical analysis of the results will identify the sources of variability and a reliable estimate of its magnitude. From this information reliability of the results and hence their significance can be judged. The sources of variability are numerous. In testing a sheet of plastic for mechanical properties it is necessary to take into account the intrinsic variability due to the testing procedure, including test piece preparation, machine accuracy, and operator error.

1.7.3 Weathering Degradation studies of Polyethylene

During the lifetime of polymers they undergo deterioration in physical and mechanical properties. Specially when exposed to a combined prolonged effect of UV radiation, temperature, humidity, air pollutants, mechanical stresses, oxygen, and thermal cycling. Practically, the most vulnerable material are organic polymers under the oxidative effect of oxygen in air. Two basic changes that occur are destruction and structurization of materials. These processes of irreversible change in materials are very significant under the enhancing detrimental influence of UV and temperature [Kovacevic, 1986]. Among physical test methods commonly used for evaluating the oxidative stability of polymers are tensile strength and elongation, and impact strength. Elongation is more useful measure of oxidative degradation than tensile strength. Tensile strength may not be markedly affected by sample embrittlement, whereas elongation is much more sensitive and can provide evidence of degradation more readily [Klemchuk, 1985].

The characteristic that determine the ultimate usefulness of a plastic are its retention of mechanical properties and therefore, measurement of these properties are used to assess the effect of weather and exposure [Gray and Cadoff, 1967]. The effects of weathering on mechanical properties are of major importance in most applications. Tensile properties have long been used for quality control purposes in plastic material specifications. Elongation at break can indicate the transition from a ductile to a brittle material [Kay et al., 1976].

The ultimate problem associated with degradation of polyolefins is failure of product to meet its specification, usually by virtue of mechanical breakdown. The aim of all studies of polymer degradation may be to understand the

mechanism of the reactions in enough detail to be able to develop suitable stabilizing systems. But for many practical purposes it is much more important to be able to predict the lifetime of the production accurately under conditions of use. The best practical assessment of the extent of degradation is to look in the loss of mechanical properties. The effects of degradation on polymer performance, e.g., loss of mechanical strength, should be determined by measurement of that specific property which will cause eventual failure once specified limits are exceeded. Unfortunately, mechanical properties do not change at the same rate as chemical reaction takes place in the polymer. For example, a polymer which undergoes chain scission as the predominant degradation reaction will show a rapid decrease in modulus and in ultimate strength. Polymers which tends to cross-link will undergo a decrease in tensile strength and elongation. It is important therefore to determine how a polymer will fail in service and to follow changes in that property which is critical to failure.

Tensile strength and ultimate elongation are sensitive mechanical properties and their measurements are widely used in the evaluation of degradative effects of the polyolefins. Polyethylene and other plastics show a comparatively small initial elongation up to quite high stresses and then elongate steadily without further increase in stress. The results of these measurements, monitored as a function of time under given atmospheric conditions are dependent on size, shape, and preparation of specimens.

Changes in the mechanical properties of a high polymer does not depend so much on the overall oxidation as on important side reactions. Polymer derive their advantageous mechanical properties from their high molecular weights, and loss of mechanical strength is due in many cases to a lowering of the molecular weight by chain breaking. It seems that the most important reactions in which molecular chains are severed is the decomposition of $R_1R_2CHO\cdot$ radicals which themselves result from hydroperoxide decomposition. The absorption of UV radiation by groups in the main polymer chain also tend to break the polymer chain directly. The absorbing groups may be part of the repeating unit or the result of the previous decomposition such as ketonic groups in polyethylene. In general the ultimate tensile strength and elongation, brittle temperature, and softening point will be effected adversely by a decrease in molecular weight. The relative magnitude of the effect will

depend on the initial molecular weight. This is because most properties become independent of molecular weight when the degree of polymerization is greater than 700-800. The influence of chain scission reaction is retarded by other reaction leading to molecular aggregation or cross-linking. In general, chain scission will cause a fall in ultimate tensile strength and elongation, while cross-linking will cause an initial hardening and rise in tensile strength. Cross-linking is a precursor to chain scission [Burgess, 1952].

The significant dependence of mechanical strength on the density of tie chains connecting crystalline lamellae is well established. When tie chains break they relax into a more compact brittle structure by a chemicrystallization process that accounts for most of the initial rise in polymer densities. Oxidative changes in polyolefins precede macroscopic changes in their physical and mechanical properties. Photolysis of hydroperoxides leading to backbone cleavage occurs predominantly in the amorphous phase because of oxygen accessibility. Surface crazes and cracks initiation, which lead ultimately to the failure of polymer artifacts, are a manifestation of the prolonged exposure to an oxidative environment. Over prolonged periods this can take the form of chemicrystallization as a result of rearrangement of the shortened polymer chains.

It is generally believed that chain scission and crosslinking reactions occurring during oxidation are the direct cause of mechanical failure. The chemicrystallization process results from oxidative chain scission reactions. As chains break in amorphous regions, the freed fragments relax into a more compact arrangement. The relaxation process is inhibited by branching or crosslinking, and is therefore a function of polymer structure and reaction conditions [Winslow and Hawkins, 1967].

Bobalek et al. [1959] noted a dramatic drop in the ultimate elongation of Alathon 34 polyethylene and branched polyethylene DYNH-3 following oxidation in air at 100^{o}C. The percent elongation of Alathon 34 dropped from 500 to 100% in 3 days, thereafter decreasing linearly to near 0% in about 11 days. The branched polyethylene increased slightly from about 650% in 2 days then fell sharply to about 150% in 6 days.

The effects of natural weathering on the mechanical properties of LDPE have been studied in Ankara, Turkey. It was observed that there is an initial increase in strain at break due to crosslinking followed by a steady decrease until the sample become very brittle.. However, it was noticed that there is a recovery period during the winter months. In this duration there is no observable increase in carbonyl or vinyl peaks but both strain at break and the stress at break increase while the modulus of elasticity appears to decrease. This recovery is probably due to the predominance of the cross-linking reactions over chain scission [Akay et al., 1980b].

The tensile strength and elongation at break of the polyethylene samples, exposed in the natural weather of Palermo, Italy, were studied by LaMantia [1984b] and Sevirini et al [1986]. Qualitative property/structure correlations are proposed by LaMantia, taking into account previous structural results for the same samples. Whereas Severini et al. concluded that during the weathering macromolecules of polyethylene undergo, simultaneously, processes of photooxidation and chain breaking which cause the decay of the mechanical properties.

It has been observed that photochemical degradation of polyethylene does not occur uniformly across the thickness of the material and a gradient of degraded material seem to exist. The damage is localized within a few microns of the surface and quickly decreases with depth [Raab et al., 1982]. Such a gradient give rise to internal stresses. In addition the spherulitic boundaries characterized by high concentration of surface irregularities (including chromophores) result in the weak center formation. These defects eventually lead to stress concentration and micro cracks [Blaga and Yamasaki, 1976]. Figure 1.15 shows a schematic representation of the phenomenon.

An increase in ultimate tensile strength and elongation is observed during early stages of exposure in polyethylene as shown in Figures 1.16 and 1.17 [Severini et al. 1987]. Both of these properties steadily decrease till the completion of the test or failure of the sample. An increase in elongation and tensile strength during early stages of exposure is usually attributed to predominance of chain scission and increase in crystallinity [Gilroy, 1979].

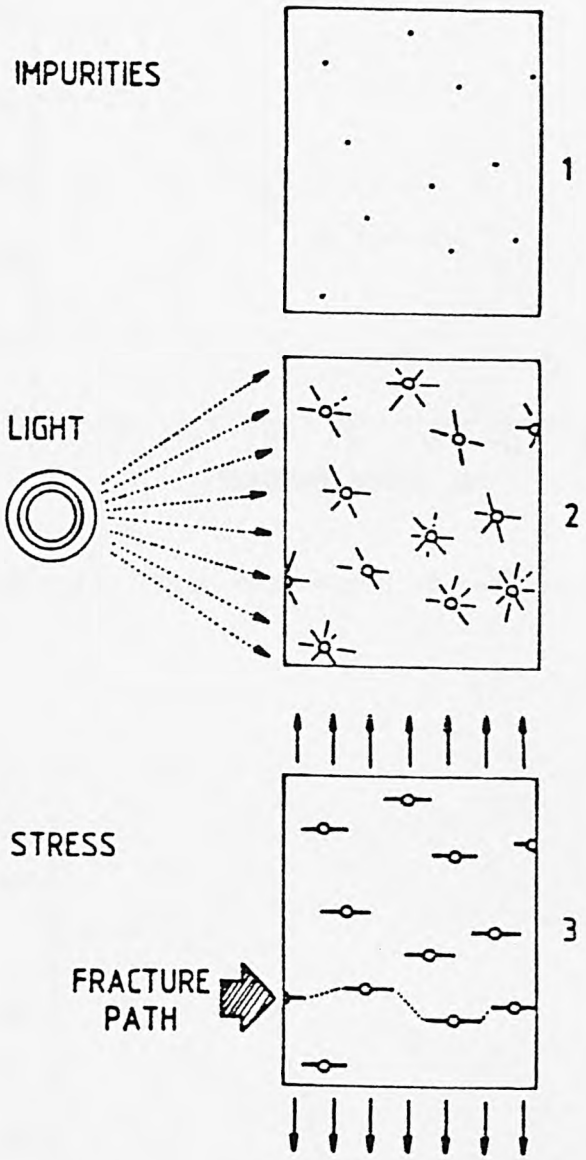

Figure 1.15. Schematic diagrams illustrating the subsequent effects of UV radiation and mechanical stress on the formation of weak centers.

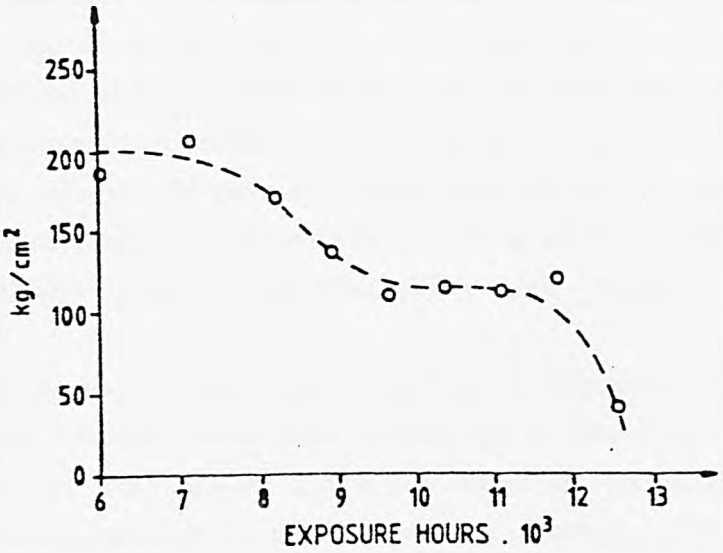

Figure 1.16. Time dependence of tensile strength.

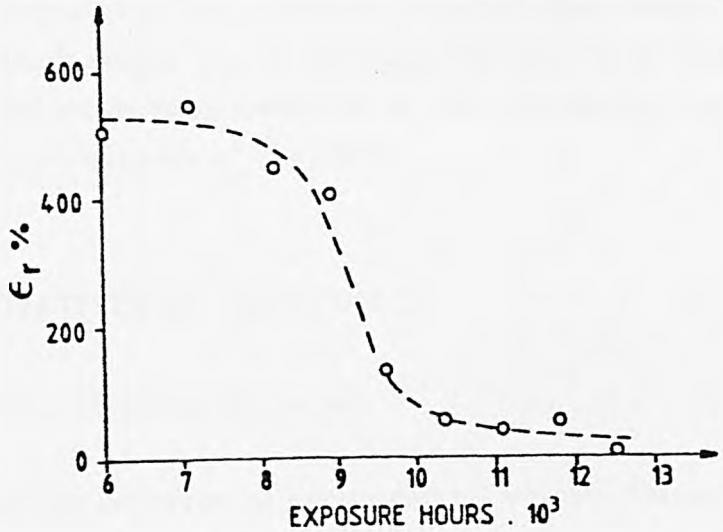

Figure 1.17. Time dependence of elongation at break.

It is generally believed that the physical property degradation is caused by chain scission and crosslinking which occur simultaneously but at different rates. A number of attempts have been made to correlate different test methods with that of mechanical properties. The tensile strength of polymer has been shown to decrease with a decrease in its molecular weight as expected [Severini et al., 1986]. It has however been shown that the ageing of flexed specimens and tensile strength compare very closely [Martinovich and Hill, 1967]. Similar attempts have been made to correlate carbonyl absorption with retained elongation [Ram et al.], but it is difficult to have a meaningful generalization of such a relationship [Akay et al., 1980b].

A number of studies regarding the mechanical behavior of LDPE and HDPE exposed to weather have been published in literature. However a few attempts have been made to study changes of mechanical properties of LLDPE when exposed to natural weather [Pouncy, 1985 and Meyer and Pedrazzetti, 1986]. Artificially weathered LLDPE samples were studied for changes in mechanicals properties by LaMantia [1985] and Geetha et al. [1987]. It was observed in both the studies that the loss of mechanical properties in LLDPE is more than both, LDPE and HDPE.

Measurement of mechanical properties of weathered LLDPE is not covered in literature extensively. The published literature have limited information on effect of harsh climate on the mechanical properties of LLDPE. Additional work on the mechanical properties of this engineering material will help researcher and designers of this field.

1.8 OBJECTIVES OF THE PROJECT

The objectives of this project were:

i) To study the effect of severe natural weather (temperature, humidity, rain, UV, and total solar radiation) of Dhahran, Saudi Arabia on the performance of linear low density polyethylene (LLDPE).

ii) To develop the weatherability data in terms of:

Changes in functional groups (carbonyl, vinyl, hydroxyl, alkene, and vinylidene groups) as a function of exposure to severe natural weather using Fourier Transform Infrared (FTIR) spectroscopy.

Changes in mechanical properties (tensile strength and percent elongation) as a function of exposure to severe natural weather using Material Testing System (MTS).

Changes in thermal properties (crystalline melting temperature (T_m) and Heat of fusion (H_f), and percent crystallinity) as a function of exposure to severe natural weather using Differential Scanning Calorimeter (DSC).

iii) To develop the mathematical correlation model for predicting the degradation of significant properties of LLDPE as a function of radiation and meteorological variables.

The weathering data obtained will be used to identify the appropriate UV stabilizers and its optimum concentration that will extend the useful lifetime of LLDPE products meant for outdoor applications.

Chapter 2

EXPERIMENTAL EXPOSURE STUDIES

2.1 INTRODUCTION

Degradation of plastics during outdoor exposure is influenced to varying degrees by all natural climatic phenomena. Heat, radiation (UV and IR), rain, humidity, and atmospheric contaminants all contribute to the degradation of plastics subjected to outdoor exposure. None of these phenomena are constant in one location and weather conditions vary widely with location. To attain maximum accuracy in predicting the useful life of an outdoor plastic, all aspects of the anticipated environment to which it will be exposed should be considered. This is best accomplished by conducting actual outdoor exposure trials [Meyer, 1983].

Saudi Arabia is now producing petrochemicals in huge quantities [Maadhah et al., 1985] and the production slate includes LLDPE, HDPE, PVC, and PS. Table 2.1 shows the Kingdom's production capacities for these polymers. LLDPE is a relatively new type of polyethylene and is a copolymer of higher-alpha-olefin and ethylene. It was discussed in Chapter 1.3 that the outdoor utilization of LLDPE is limited because of doubts about its stability when exposed to natural environment [Turtle, 1986; Iring et al., 1986; and LaMantia et al., 1986]. In this work LLDPE was selected for studying the effects of severe natural weather of Dhahran, Saudi Arabia on its significant properties.

Weathering trials in hot climatic regions (such as Saudi Arabia) are of particular importance. Almost invariably, the high levels of temperature, humidity, and solar radiation found in such regions prove more aggressive to plastic materials than the conditions in cold regions (such as England). Thus as well as being of intrinsic interest, tropical and subtropical exposure trials are a means of providing accelerated exposure sites as compared to colder regions like England.

Table 2.1

Production Capacities of Polymers in Saudi Arabia

Polymer	Annual Capacity (1000 ton)	Start up
LLDPE	605	1984
HDPE	91	1985
PVC	200	1986
PS	100	1988

In order to assess the durability of polymer, it is mandatory to expose it to natural weather, or to simulated conditions of UV radiation, temperature, rain and humidity. Excellent reviews of the techniques employed for natural and artificial weathering of polymers are available in literature [Kamal, 1970 and Ranby and Rabek, 1975]. A number of methods have been or still are being employed as criterion to monitor the degradation of polymers resulting from natural or artificial weathering exposures. Some of the methods include tensile properties, carbonyl absorption, flex tests, brittleness temperature, flexural strength, dielectric constant, solution viscosity, melt index, surface crazing, decrease in molecular weight, and photoacoustic spectroscopy. In order to estimate the weathering performance of a plastic, it is required to expose it to natural weather for longer periods of time during which degradation process affects almost all properties of the plastic.

It is unlikely that any one meteorological element is the sole contributor to the degradation of plastics exposed to outdoor conditions. The complete phenomenon of weathering involves the combined effects of photo and thermally initiated oxidation and ozonolysis, associated with the purely physical effects of wind, temperature variation and humidity variation. These work together in the breakdown of the material.

A comparison of the levels of total solar radiation received in various parts of world revealed that Saudi Arabia receives a high dose of total solar radiation (Table 2.2) [Meyer, 1983]. It is obvious from the table that the total solar radiation received in Saudi Arabia is almost three times more than a European country (Switzerland). It is already discussed in Section 1.2 that the main cause of polymer degradation when exposed to outdoor environment is the UV portion of solar radiation.

The average total and UV radiation received in Dhahran, Saudi Arabia is shown in Figure 2.1. This indicates that the Langleys (cal/cm^2) received during summer is more than double of winter season. This implies that the degradation rates during summer should be more than in other seasons. The average monthly temperature and relative humidity of Dhahran is shown in Figure 2.2 which demonstrate the seasonal variation similar to that observed for total and UV radiation. The heavy dose of solar radiation and temperature reaching upto $50^{o}C$ in summer, and severe thermal cycling

Table 2.2

Total Solar Radiation Received
by Different Parts of World

Location	Total Solar Radiation (KLy/year)*
Florida, USA	130-140
Arizona, USA	190-200
Dhahran, Saudi Arabia	180-220
Basel, Switzerland	70-80
Palermo, Italy	130-140

*Kilo Langleys per year.

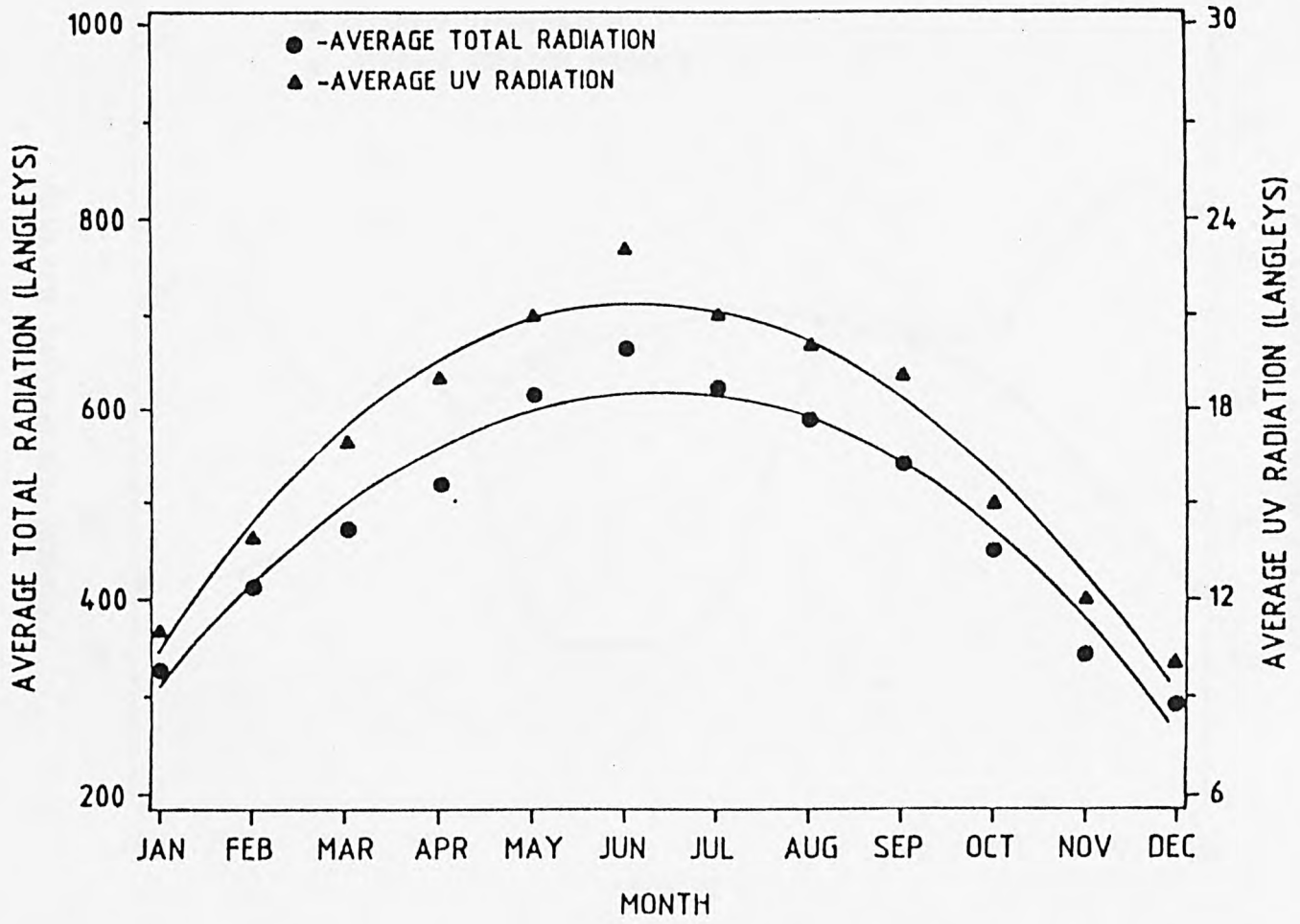

Figure 2.1. Monthly average temperature and relative humidity for Dhahran, Saudi Arabia.

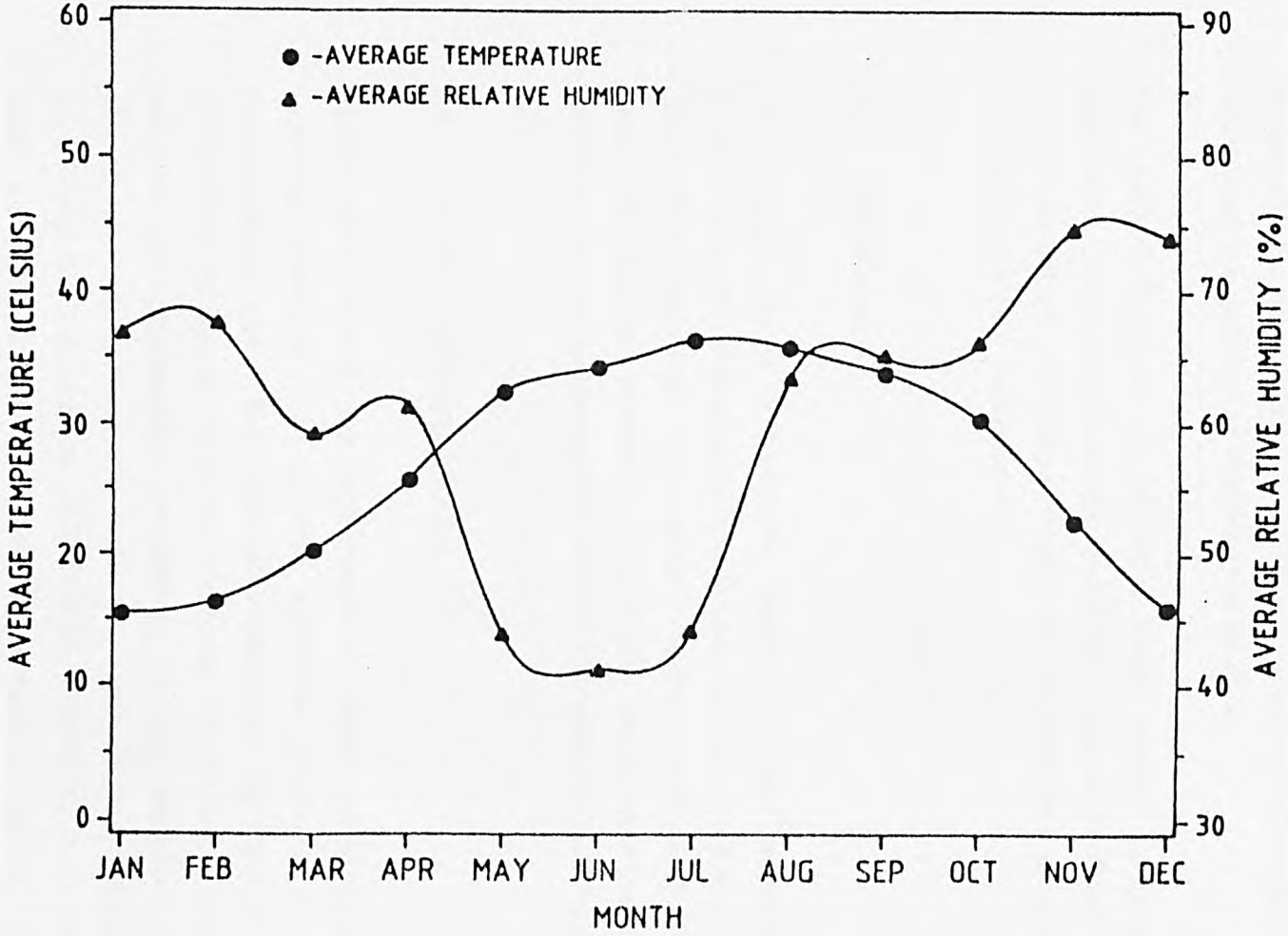

Figure 2.2. Monthly average temperature and relative humidity for Dhahran, Saudi Arabia.

would result in extreme thermal stresses in the specimen. Such a combination of very high UV dose, temperature extremes, and thermal cycling proves to be extremely aggressive to the plastic and results in much faster rate of degradation of plastic than is observed in other parts of the world. Dhahran's weather could be considered as a naturally accelerated laboratory to evaluate the weathering resistance of plastics.

The study dealing with the effect of Saudi Arabian harsh weather on the significant properties of polymer (LLDPE) produced in Saudi Arabia is not carried out before. The state-of-the-art of this work is a new polymer studied in a unique outdoor environment.

2.2 MATERIALS

The polymer used in the study was linear low density polyethylene (LLDPE) in pellet form containing no UV stabilizer and identified as Ladene FH10018 (Saudi Basic Industries Corporation - SABIC). The physical properties of Ladene FH10018 are tabulated in Table 2.3. The polymer grade used is a slip, antiblock, and antioxidant-modified LLDPE resin [SABIC Marketing, 1984].

2.3 SAMPLE PREPARATION

Specimens of LLDPE can be prepared by either compression moulding or injecting moulding. In general, injection moulding is attractive for thermoplastics, but it does raise questions about the state of the specimens, particularly the degree of moulded-in stress. In the case of a semi-crystalline polymer, like polyethylene, morphology is also important as this can be altered in time-temperature scale of many exposure trials. This can complicate the interpretation of data if weathering is to be distinguished from ageing. Compression moulded specimens can be expected to be practically free from residual stress and may accordingly be preferred, but the morphology of the sample can still be important [Kay et al., 1976].

In this study, test specimens were prepared by compression moulding LLDPE pellets in the form of films and plaques. The principal stages followed in the

Table 2.3

Physical Properties of LADENE FH10018 (LLDPE)

Physical Property	Test Method	Value	Units
Melt Index	ASTM D-1238	1.0	g/10 min.
Density	ASTM D-1505	0.918	g/cm^3
Secand Modulus at 1% Elongation	ASTM D-638	2460 35000	kg/cm^2 psi
Film Properties			
Tensile Strength (MD)	ASTM D-882	405 5800	kg/cm^2 psi
Elongation (MD)	ASTM D-882	600	%
Coefficient of Friction	ASTM D-1203	Typel	-
Dart Drop Impact, F50	ASTM D-1790A	110	g
Puncture Resistance	SABIC Method	53	j/mm

compression moulding process were as follows [British Standard 2782, 1977].

(a) raising the temperature of the material to a level where application of pressure can cause sufficient flow without thermal decomposition;

(b) application of pressure to the material, causing it to flow and assume the shape of the mould in which it is contained; and

(c) cooling the material to a temperature at which the moulding can be removed from the mould without distortion taking place.

2.3.1 Apparatus

The test sheets were compression moulded using a Carver laboratory press for films and Wabash 75 tons press for plaques in accordance with American Society for Testing Standard Material (ASTM) standard [ASTM Standards D-1928, 1980]. The press is provided with platens that can be heated to 200^{o}C using electrical resistance heaters. It is designed so as to provide maximum heat without the occurrence of "hot spots" and maintains the rigidity of the plates. Cooling was accomplished by passing water through channels provided for this purpose. The chases used were single-cavity picture frame moulds with dimensions appropriate to the production of test sheets, 140 micron 6in x 6in films and 1/16in x 16in x 16in plaques. Flat backing plates flat for the chases were strong enough to resist warping or distortion by moulding. Stainless steel plates of the same length and width as the outside chase dimension were employed. Aluminum foil 0.05 mm thick was used as a parting agent in the moulding operation.

2.3.2 Procedure

Compression moulding was performed using parting sheets of aluminum foil. The foil was cleaned by wiping with acetone and then dried with clean, absorbent cloth. Any wrinkles in the foil were smoothed out before use. LLDPE plastic was placed in the chase between cleaned aluminum foil parting sheets backed by smooth backing plates. The mass of the mould charge was sufficiently greater than that of the finished moulding to

compensate for any flash loss. The assemble was inserted between the platens which were maintained at 160 ± 5°C. The platens were then closed and the material maintained under slight pressure for a period of five minutes which was sufficient to ensure that the material reached a relatively free-flowing state. After the preheating period, pressure was increased for a further period of five minutes. Cooling was then provided by water passing through the channels. After the moulding had formed, the assembly was removed from the press. The backing plates were removed very carefully without disturbing the aluminum foil, which was adhering tightly to the chase and LLDPE specimen. Finally, the aluminum foil was stripped off the and test sheet taken out of the chase.

Test specimens were prepared from the test sheets using blanking die but without disturbing the thermal history introduced during sheet preparation, which provided specimens of an acceptable quality, as judged by visual examination.

2.4 METEOROLOGICAL AND RADIATION ENVIRONMENT OF TEST SITE

Dhahran (26.32°N, 50.13°E) is situated just north of the Tropic of Cancer on the eastern coastal plain of Saudi Arabia and is closed to 10 Km inland from the Arabian Gulf (Figure 2.3). Despite its nearness to the coast, Dhahran is located in very much a desert environment. The environment of the site plus the limited human activities and population means that the radiation characteristics of the atmosphere are not significantly altered by man made pollution sources.

Four distinct seasons cannot be identified in the classical mid-latitude sense. Rather, the year may be divided into a very hot period and a cooler period. For the Dhahran region, this division may be set at the maximum change between monthly mean temperature, giving the separation into the two six month intervals May to October (hot) and November to April (cooler).

Annual precipitation totals are very low, typically around 80 mm in Dhahran and somewhat less inland; 60 percent falls in December/January and there is no rain at all from June to October during most of the years. Wind speed

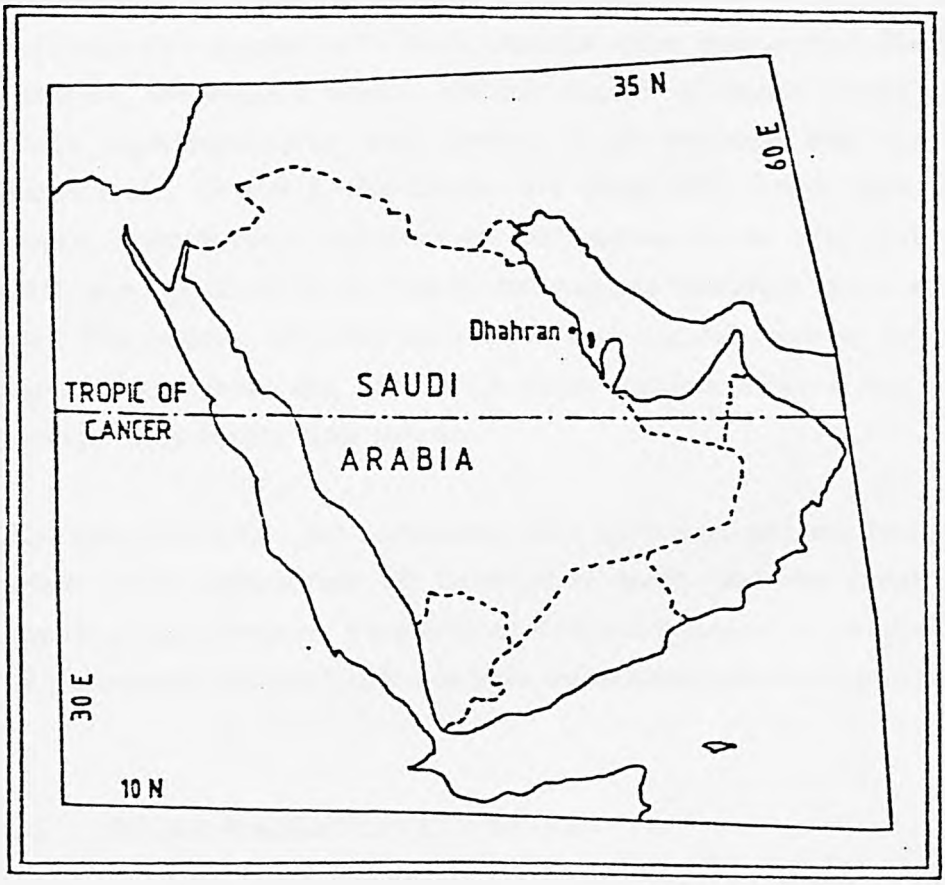

Figure 2.3. Map of the location.

show a clear diurnal variability within the typical range from near zero to 10 m/s; there is no regular diurnal march. The synoptic wind direction exhibits long period of more or less constant direction between north and northwest, though this synoptic flow is overlaid with a sea/land breeze. An additional feature with some longevity is the tendency for the wind to swing to the east, in particular the quadrant between east and south.

The parameter of most general interest in Saudi Arabia is always the temperature. At Dhahran, monthly mean temperatures reach close to 37^{o}C for both July and August, with daily maxima often approaching the 50^{o}C mark. However, the eastern coastal climatic region of Saudi Arabia is a region where significant year end cooling is in evidence and monthly mean temperatures in the cooler season are some 20^{o}C lower than the hottest months. Despite the desert location, the nearness of the very shallow Arabian Gulf (average depth 30 m) means that relative humidity values are relatively high. The relative humidity exhibits a large diurnal cycle on the order of 60 percent throughout the year, with daily maxima often rising over the 80 percent level during most months.

The desert location, the prevailing wind direction, and the relatively strong winds often experienced all combine to mean that the lower atmosphere almost always possesses a significant dust/sand content. A detailed assessment of the atmospheric turbidity has been undertaken [Abdelrehman et al, 1988].

2.5 SOLAR RADIATION CONDITIONS

2.5.1 Radiation Monitoring at Dhahran

The KFUPM solar radiation and meteorology station was established by Research Institute personnel in July of 1979 with the deployment of Eppley global and tracking direct normal instruments [Nimmo and Said, 1981]. The station underwent a major upgrade in 1984 with the installation of a computer-driven data acquisition system and a considerably enhanced array of radiation and meteorological instruments [Bahel et al., 1986]. Finally, a number of additional sensors were installed and a complete overhaul at all levels was carried out during 1987. The sensors are located on the roof of

the 7-storey Research Institute building from which site the horizon is unobstructed; the station is 92.5 m above sea level.

2.5.2 Quality Control

The quality of the radiation data is maintained *via* a range of factors and activities, including: the use for the measurement of all major parameters of World Meteorological Organization (WMO) [WMO, 1983]. First class instruments (e.g., Eppley PSP, NIP, etc.); daily inspection and cleaning of all sensors; real-time and post-processing data verification using the three techniques of range checking, sensor intercomparison, and model-produced to measured-value comparison; regular calibration of all sensors against transferable reference sensors; and the regular calibration of the reference sensors themselves.

2.5.3 Radiation Environment

The clearness index (K_T), which is the ratio of the horizontal-surface global radiation reaching ground level to the equivalent extraterrestrial quantity, is a measure of the combined effects of atmospheric turbidity and cloudiness on reducing the radiation reaching the ground surface.

The meteorological conditions in the Gulf region are such that there is very little cloud cover throughout much of the year. This factor tends to increase clearness index values as shown in Figure 2.4. However, the high humidity and atmospheric dust content conditions of the lower atmosphere work in the opposite direction. The radiation environment of the Gulf region during a given year is characterized by a high percentage of cloud free days and the clearness index variability from year to year is quite small.

2.6 NATURAL EXPOSURE

The outdoor weathering of plastics can be used to evaluate the stability of plastic materials that are exposed to varied meteorological influences. It is indicated in Figures 2.1 and 2.2 that the climatological and radiation data varies with the season. Therefore it is necessary to obtain a detailed weather

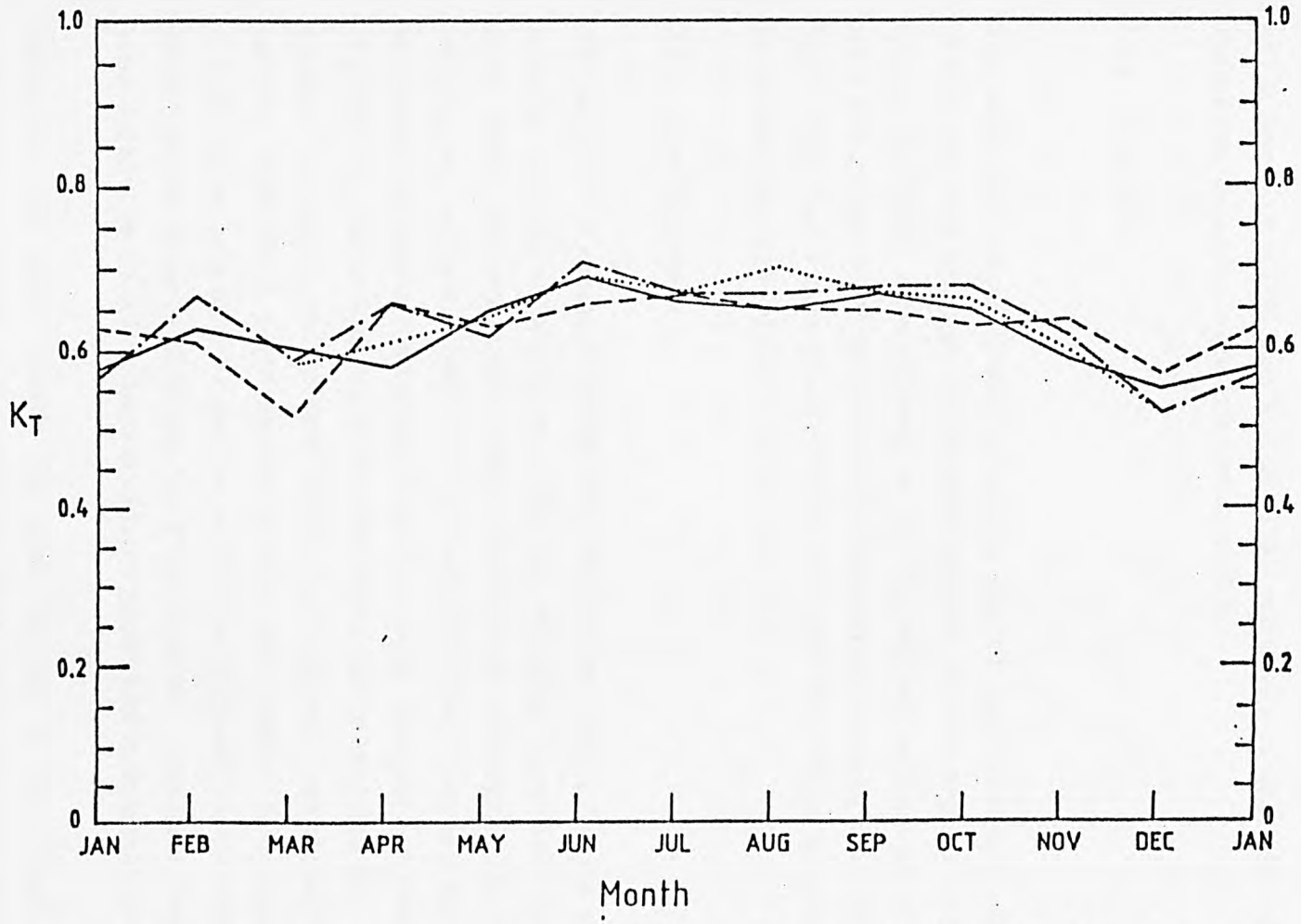

Figure 2.4. Monthly mean measured clearness indices at Dhahran for the four years 1984 to 1987 (dotted, dash-dotted, solid, dashed, respectively).

data of the exposure duration for a meaningful analysis of weathering effects on a given polymer.

In this study, the outdoor weathering of LLDPE was carried out according to ASTM Standard [1979]. and British [1981] standards on exposure to natural weathering were also taken into consideration.

2.6.1 Apparatus

The racks were placed in such a location that no shadow from a neighboring obstruction with an angle of elevation greater than 20 degrees fell on any sample. The racks were adjusted so that the exposed surfaces of the samples were at an angle of 45 degrees to the horizontal and facing south [Davis and Sims, 1983]. Racks were constructed of untreated wood which is recommended for desert areas [ASTM Standard D-1435, 1979].

2.6.2 Test Specimens

The samples for exposure testing were mounted on holders and the evaluation samples were cut in such a way that the mounting edges were removed in cases where the test results might otherwise be affected. The effect of backing was considered important in these weathering trials and the rack was so designed to expose the samples from both sides. Backing contributes to the degradation process with regard to reflectance, heat absorption etc. The total number of samples was 60 and withdrawal frequency was maintained on a monthly basis for a total exposure of one year (1986). Five samples were withdrawn at each interval and one sample was exposed for the complete 12-month except when withdrawn for FTIR analysis. Similarly five samples were withdrawn each for thermal analysis (DSC) and mechanical testing.

Since one can study exactly the same portion of the sample, spectral subtractions are made on a one-to-one basis during the early stages of the reaction. The resultant difference in spectra can be magnified to bring out small spectral features. The control samples were retained for determination of original and final control values. The control and withdrawn samples were retained at standard conditions of $23\pm1^{o}C$ and $50\pm2\%$ relative humidity.

They were covered with inert wrapping to prevent light exposure during the ageing period.

2.6.3 Test Site

Weathering racksare located in a cleared area at Dhahran, Saudi Arabia. The selected site is representative of a hot and humid location in a subtropical region.

2.6.4 Procedure

The samples for exposure were labelled with identifying alphanumeric characters. The marking was such that there was no interference with the exposure or subsequent testing. The FTIR spectrum of the control sample was recorded and the- samples were then mounted on holders and a diagram of the layout recorded. The date of installation and length of exposure was also recorded and specimen holders were mounted on the racks for the prescribed times. Exposure racks were inspected on a bi-weekly basis and the exposed samples drawn every month.

Chapter 3

INFRARED SPECTROSCOPIC STUDIES

3.1 INTRODUCTION

When elucidating the degradation through weathering of polyolefins, it is important to assess the nature of the degradation products. The products formed during the degradation of polyethylene and other polyolefins have been determined using the IR spectroscopic technique [Wiles and Carlsson, 1985]. Degradation by weathering is an oxidative-type reaction, and as it proceeds, competing reactions of chain scission and crosslinking take place [Wood and Kollman, 1972]. At the same time, natural weathering leads to: uptake of oxygen; the formation of carbonyl, hydroxyl, and vinyl groups; the evolution of acetones, acetaldehyde, water, and oxides of carbon; an increase in brittleness, the formation of crosslinks; and the physical failure of the sample [Winslow et al., 1969].

IR spectra arise from the molecular transitions between quantum states of differing internal energies [Cernia et al., 1963]. The frequency of the emitted or absorbed radiation is related to energy differences and is associated with molecular vibrations and rotations characteristic of chemical groups, e.g., alkyl, hydroxyl, carbonyl [Silverstein et al., 1981]. In the case of oxidation, the carbonyl groups associated with the products of degradation are detected by the absorption bands between 1850-1700 cm^{-1}. These bands comprise the carbonyl compounds of carboxylic acids, aldehydes, esters, and ketones [Stivala et al., 1983]. Until recently, such measurements have invariably been made with conventional prism spectroscopes which have limited sensitivity. Sensitivity is a major factor in the early stages of degradation. The commercial appearance of Fourier Transform Infrared Spectroscopy (FTIR) has brought about a revival in infrared spectroscopy [Koenig, 1984]. FTIR measurements were particularly useful in providing information on initial product formation, which had previously eluded detection [Webb, 1984].

3.2 EXPERIMENTAL

The IR spectra were recorded using a Perkin-Elmer Model 1500 Fourier Transform Infrared (FTIR) spectrometer linked with Model 3600 Data Station. A block diagram of the system is shown in Figure 3.1. The system consists of the Central Processor, Optical Module, Interconnecting cables, the three Data Station Modules, the Recorder, system software, and an optional printer.

The optical unit incorporates a refractively scanned interferometer where the optical path difference (OPD) is generated by the movement of a wedge of potassium bromide (or a similar infrared transparent material) - as shown in Figure 3.2. This particular design is ideal for a "work-horse" type instrument because it is very rugged and much less susceptible to misalignment problems than conventional moving mirror interferometers. The optical layout (see Fig. 1.9) shows the location of the wedge interferometer and also highlights the dual beam design of the instrument. This feature is not trivial since it provides a convenient mechanism for the application of sampling accessories that usually require time-consuming alignment. Another useful features is the ability to temporarily divert the main He-Ne laser beam into the sample area, co-axial to either infrared beam. This feature aids the initial alignment of optical accessories because it allows to trace the path of the infrared beam - a task which is otherwise tedious since the infrared beam does not contain a visible component.

The normal detector for the 1500 Series is a room temperature, deuterated triglycine sulphate (DTGS) detector. This detector is ideal for routine sample analysis since it requires no external access and it is capable of producing respectable data even from a single scan of the interferometer - a task that takes only about two seconds for data acquisition. The noise level across the spectrum is clearly acceptable for a survey scan and is therefore ideally suited for the rapid evaluation and screening of samples.

The instrument processor, or Central Processing Unit (CPU), performs several important functions as part of its role for primary data collection and instrument control. An important part of this system is a dedicated, fast Fourier transform processor that performs an on-the-fly transformation,

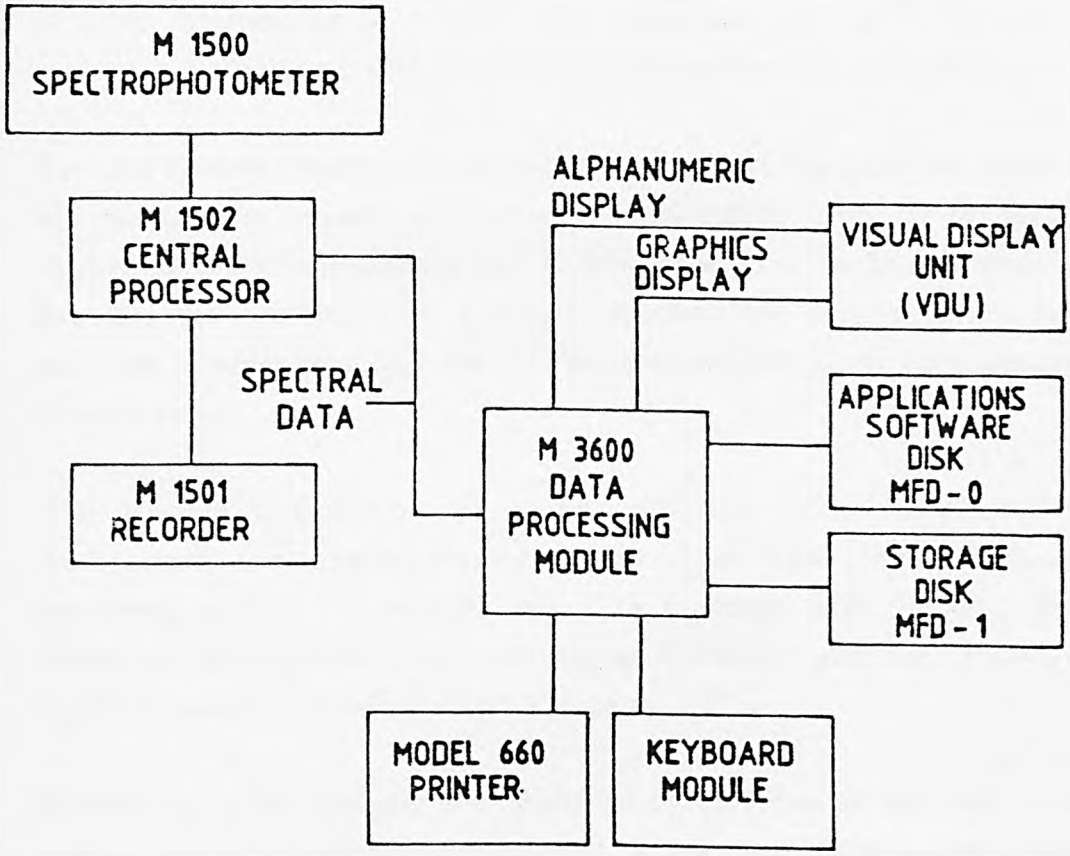

Figure 3.1. Block diagram of Perkin Elmer FTIR Model 1500.

within 0.2 seconds, on the incoming interferometric data. Co-addition is performed on the transformed complex spectrum and the magnitude spectrum from this averaged data is ratioed against a stored background spectrum to produce the familiar format of a "double beam" spectrum. This spectral data and the stored background are contained in assigned memory space within the instrument processor. During normal operation the working spectral file is fully interpolated to 1 cm^{-1} data resolution (0.5 cm^{-1} for the high resolution mode) and transferred to the Infrared Data System (3600).

The fast Fourier transform processor is a very important practical feature for the user because spectral information is made rapidly available for graphical display on the Visual Display Unit (VDU) monitor of the Data System. This provides the operator with a nearly instantaneous display of the sample spectrum - rather than just the interferogram, which is not very meaningful to most users.

The infrared software on the model 3600 data station provides a fully interpolated, fast, graphic display on the screen with good resolution (720 horizontal points) for spectral data. In practical terms, spectral data is displayed on the screen as a continuous trace, not just data points, with minimal spectral degradation in 1.3 seconds.

High signal-to-noise spectra were obtained by collection of 100 scans for each sample, using dry air as the background environment. The resultant digitized spectra were stored for further data processing. The absorbance subtraction method previously reported [Siesler, 1979; Pattacini and Anacreon, 1980; Bartick, 1979] was employed in this study. The LLDPE film showed total absorbance in the CH stretching region (2600-3100 cm^{-1}), the CH_2 deformation region (1430-1490 cm^{-1}), and the CH_2 rocking region (710-740 cm^{-1}), as shown in Figure 3.3. Consequently, absorbance subtraction of two spectra could not be done for these regions.

3.3 RESULTS AND DISCUSSION

IR measurements of LLDPE film samples were carried out periodically during 12 months of natural weathering. The IR spectra of unweathered and

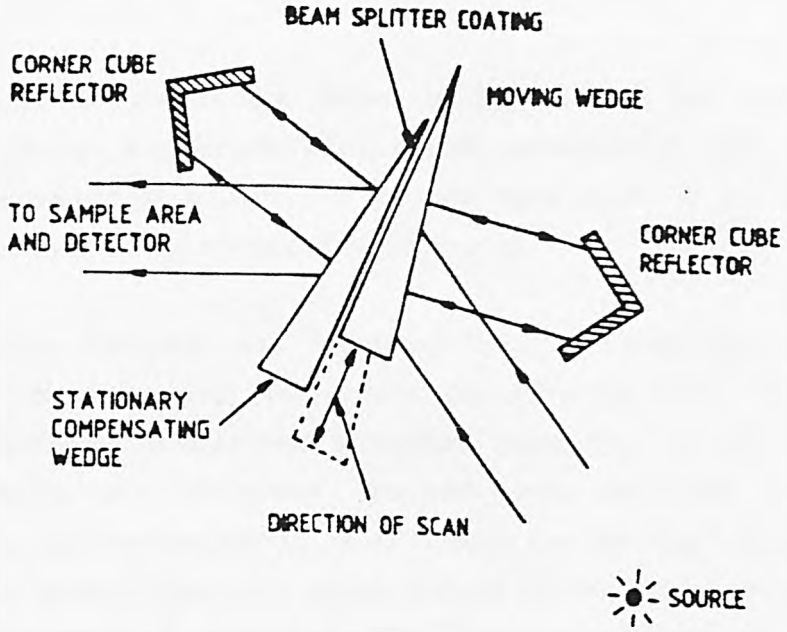

Figure 3.2. The refractively scanned interferometer.

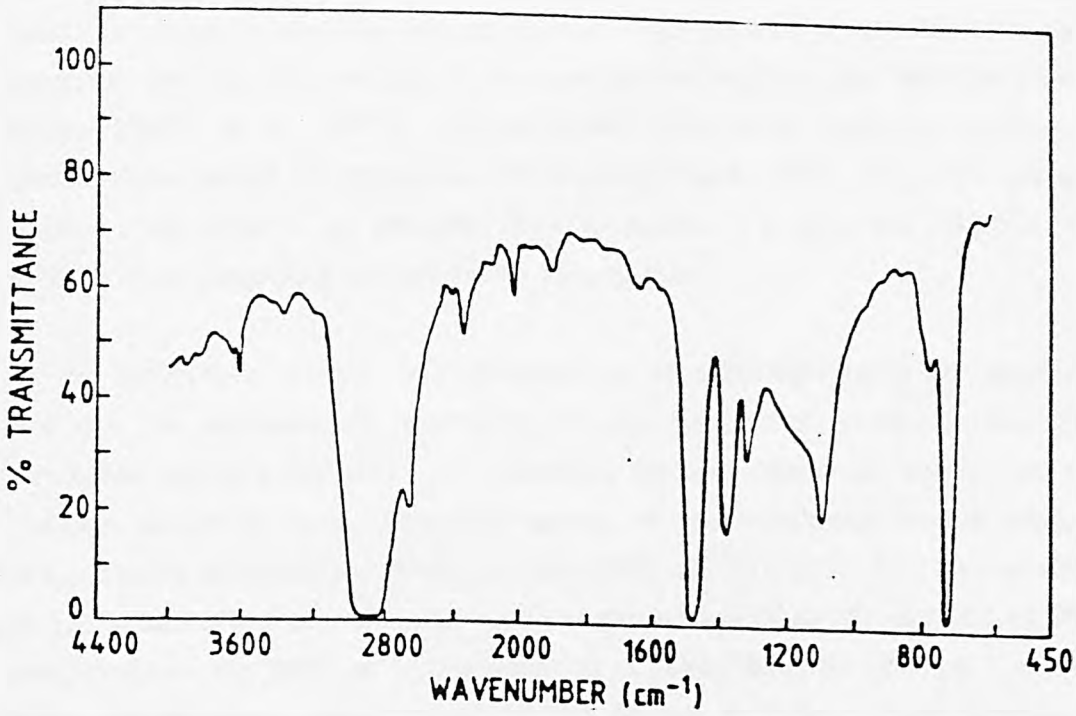

Figure 3.3. FTIR spectra of unexposed LLDPE film sample.

weathered LLDPE samples are shown in Figures 3.4, 3.5, and 3.6 for hydroxyl, carbonyl, and unsaturation region, respectively. The effect of weathering exposure on LLDPE can be seen more easily in the difference spectrum presented at the bottom of these figures.

The difference spectrum was computed by first converting both the spectrums to absorbance unit from percent transmittance. Later, the spectrum of the unweathered sample was subtracted from that of the weathered sample. Finally, the difference spectrum was converted to percent transmittance and then presented. In difference spectroscopy it is imperative to establish a reliable basis upon which to scale the individual spectra before the actual subtraction is performed. This is necessary in order to normalize for differences in thickness of the samples. An ideal case would be the elimination of an internal standard absorbance band. The most appropriate absorbance band for this study would be one that is not only a direct measure of the amount of absorbing material but one that is also unaffected by weathering. These requirements are not met by any of the absorbance bands in polyethylene. In this study, the criterion employed for difference spectrum was the elimination of the absorbance bands in the 1800-2400 cm^{-1} region [Tabb et al., 1975]. These bands have been assigned mainly to combination modes of crystalline vibration [Krimm, 1960]. Since an internal standard was used as the criterion for subtraction, it is expected that minimal error will be generated by employing this method.

In the difference spectra, any increases in absorbances above the baselines are due to increases in absorbing species (oxidation product), and any decreases are due to losses of absorbing species (point of attack on the polymer chain) [Koenig, 1980]. The spectra of the weathered sample indicate the presence of hydroxyl structure near 3400 cm^{-1} (Figure 3.4). The profiles of the samples indicate that the -OH containing group in the exposed LLDPE sample shows the 3420 cm^{-1} component as stronger than the 3360 cm^{-1} component, which implies that exposed LLDPE sample contains a large number of acid groups. The difference spectra detected this feature in the very early stages of exposure (3 months), as shown in Figure 3.4. This is consistent with the infrared and carbon NMR results of oxidized LLDPE [Jelinski et al., 1984]. The -OOH absorption at 3555 cm^{-1} is extremely weak or absent in the LLDPE samples indicating lower amounts of secondary hydroperoxide that

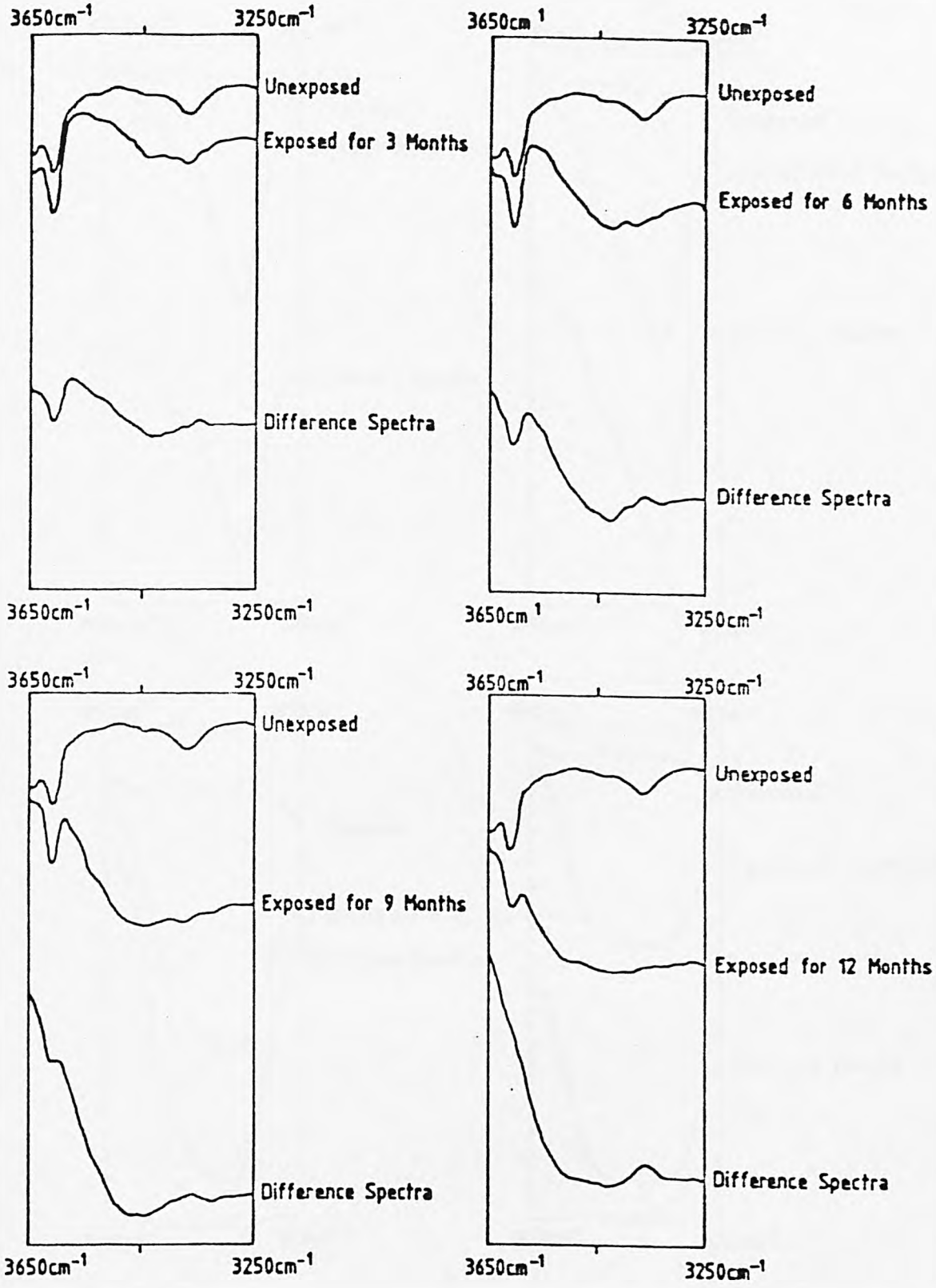

Figure 3.4. Difference spectra of hydroxyl region.

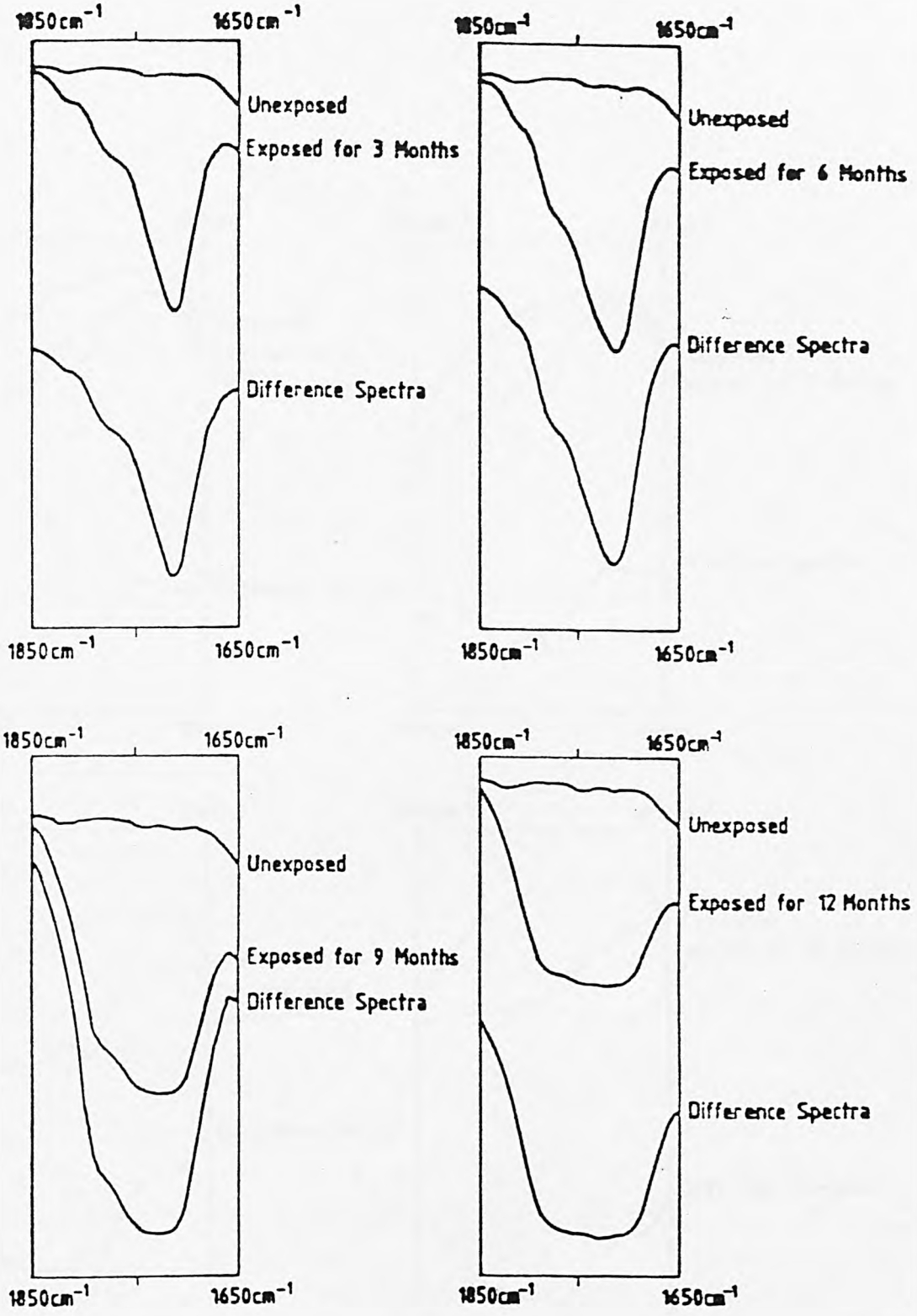

Figure 3.5. Difference spectra of carbonyl region.

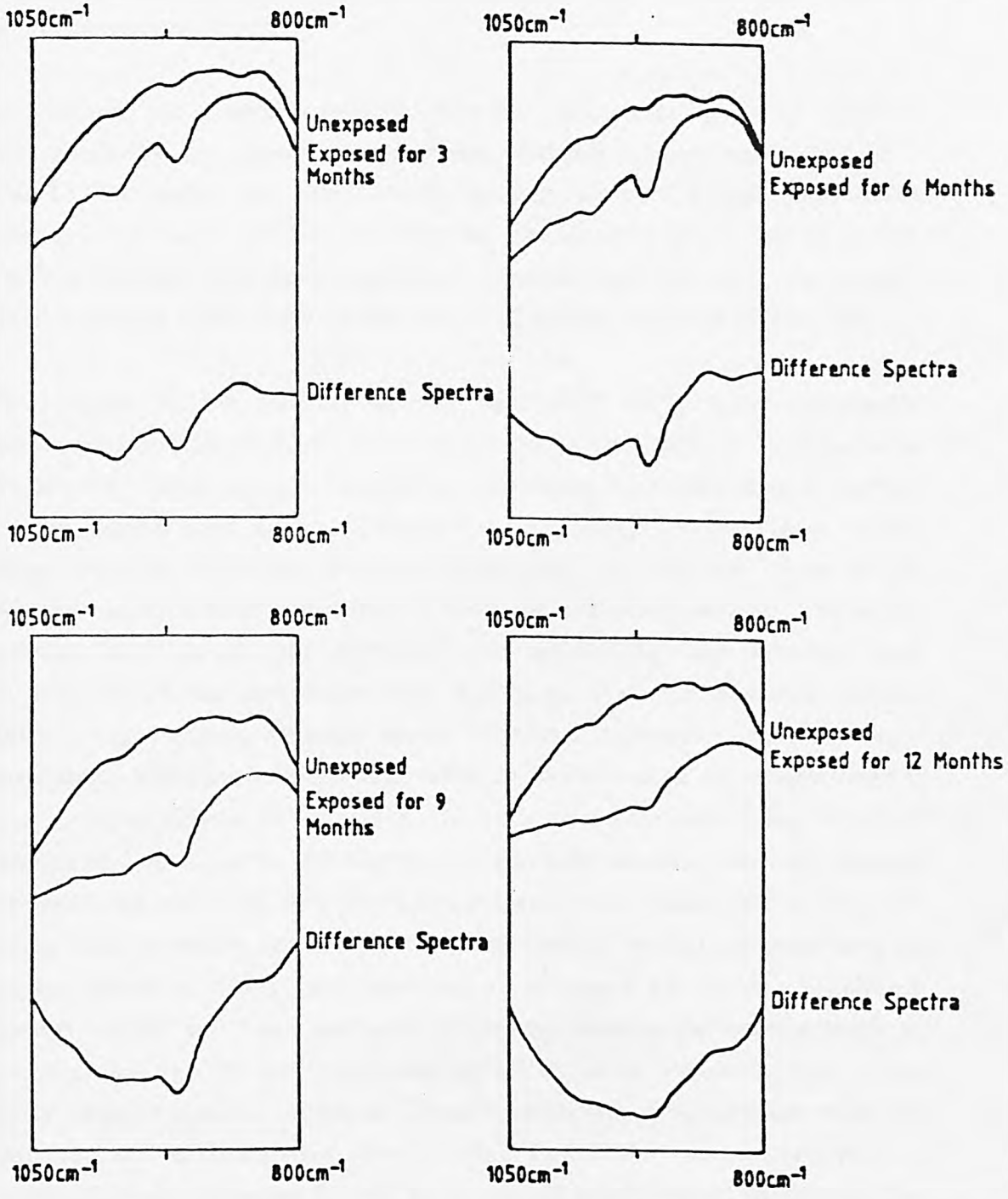

Figure 3.6. Difference spectra of unsaturation region.

may have decomposed to secondary alcohols. It is reported that the density of the hydroxyl groups in polyethylene is higher than that of the carbonyl groups present [Sato and Yashiro, 1978]. This suggests that the hydroxyl groups in polyethylenes may be mainly caused by a very small amount of impurities such as water and oxygen gas, in the ethylene gas used in polymerization methods.

In addition, the structural modifications due to weathering can be noted in the sample by the appearance of strong absorption bands near 1700 cm^{-1}. The LLDPE sample has the strongest carbonyl absorption band (maxima at 1718 cm^{-1}) owing to ketonic C=O moieties. The increase in absorbance at 1718 cm^{-1} is obvious after three months of exposure and this keeps on growing until it attains a bell shape by the end of 12 months exposure (Figure 3.5).

In addition to the spectral changes near 1700 cm^{-1}, there are readily discernable alterations in the unsaturation region (800-1050 cm^{-1}) as shown in Figure 3.6. These spectral features are associated with vibrations of carbon-carbon double bond groups [Vakhlueva et al., 1968]. Polyethylenes exhibit both vinyl and vinylidene absorption at 909 cm^{-1} and 887 cm^{-1}, even before weathering, as indicated in Figure 3.3 for the unexposed sample. The unsaturation may be of the terminal type $RCH=CH_2$, the internal type, RCH=CHR, or the side chain type, $R_2C=CH_2$. The most probable site for initial oxygen attack, when the sample is exposed to weather, would be the -methylenic hydrogen atom, though addition at one end of the double bond is also possible [Stivala et al., 1983]. In addition to the sensitizing effect of unsaturated moieties to weathering, the ethylenic unsaturation may promote cross-linking reactions, thus [Tsuji and Nagata, 1977]. Chain scission may also occur simultaneously but the rate of cross-linking to chain scission may be higher [Hawkins, 1964]. It is apparent from Figure 3.6 that the vinylidene groups (at 887 cm^{-1}) are gradually consumed, whereas the concentration of vinyl groups (at 909 cm^{-1}) increases at all stages of exposure, even at the early stage (3 months exposure). These findings are in accordance with the data reported earlier [Amin et al., 1974]. This is the expected sequence of events if vinyl groups are formed by Norrish II breakdown of carbonyl. The formation of aldehyde and carboxylic acids is almost certainly a consequence of Norrish I photolysis of carbonyl.

These results support the previous conclusion [Hutson and Scott, 1972] that once significant amounts of carbonyl are present in the polymer, either as a result of processing or by storage, they are involved in the weathering process.

The growth in functional groups as a function of weathering time is exhibited in Figure 3.7. The growth in carbonyl groups is noticeably more than that in the other functional groups.

The unexposed samples contained a measurable amount of carbonyl groups which can be seen in Figure 3.3. Moreover, in order to correct for variations in sample thickness, it is usual to measure the intensity of the particular band relative to some other band whose intensity does not vary with weathering. The resulting ratio defines an "index" [Akay et al., 1980b; Akay and Tincer, 1981; Tincer et al., 1986; Mellor et al., 1973]. In our study the reference band was taken at 1375 cm^{-1}. The initial concentration of carbonyl groups is denoted in terms of the initial carbonyl index by I_o^{1718} (ratio of absorbance at 1718 cm^{-1} and 1375 cm^{-1}). The change in the carbonyl index is defined as:

$$\Delta I^{1718} = I^{1718} - I_o^{1718}$$

Similarly, the changes in vinyl, hydroxyl, and alkene indexes are defined as:

$\Delta I^{909} = I^{909} - I_o^{909}$ for change in vinyl index,

$\Delta I^{1640} = I^{1640} - I_o^{1640}$ for change in alkene index, and

$\Delta I^{3360} = I^{3360} - I_o^{3360}$ for change in hydroxyl index.

The changes in the carbonyl, vinyl, alkene and hydroxyl indices are plotted as a function of exposure time in Figure 3.8. The variation of the carbonyl index with the vinyl index is plotted in Figure 3.9. It is obvious from the plot that a linear relationship exists between the growths of the carbonyl and vinyl groups. This relationship is also true for LDPE [Akay et al., 1980b]. This is the expected sequence of events if vinyl is formed by Norrish II breakdown of carbonyl. It is also reported [LaMantia, 1985] that during UV

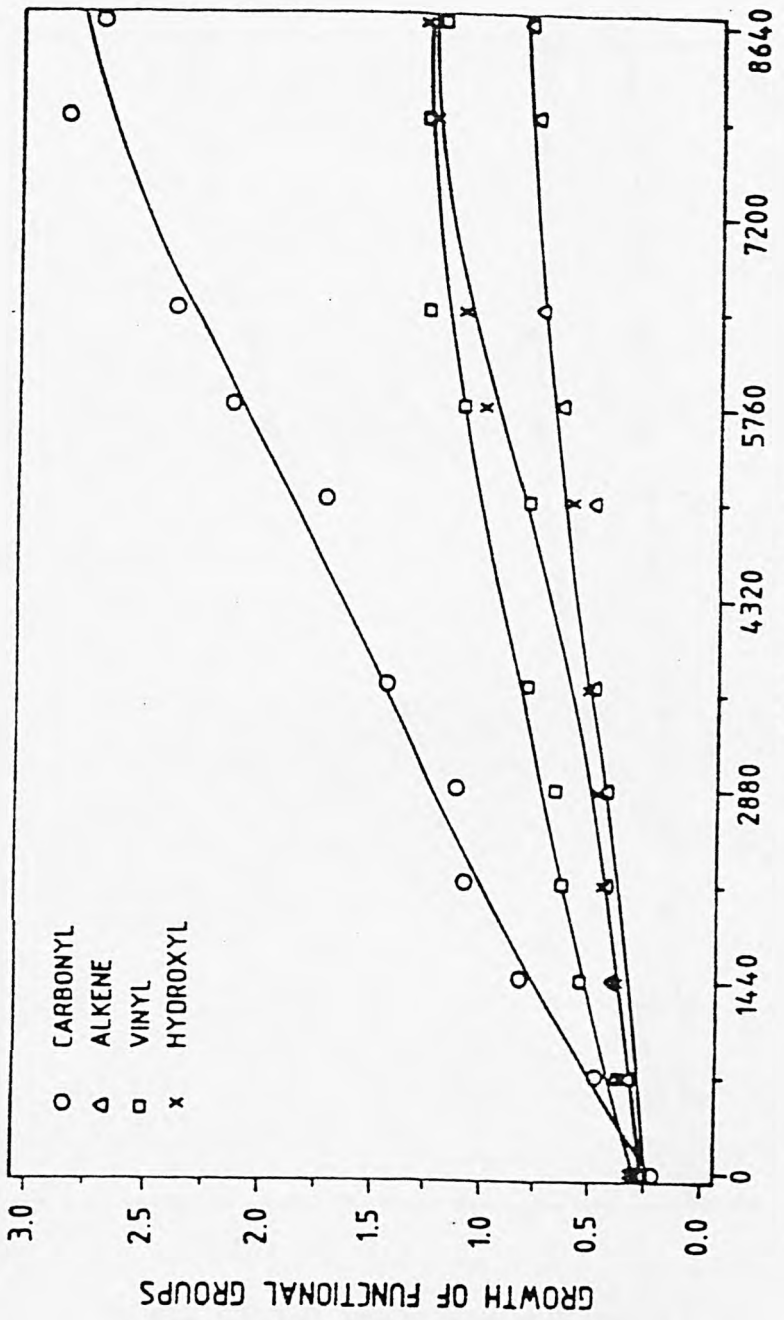

Figure 3.7. Changes in the functional groups as a function of exposure time.

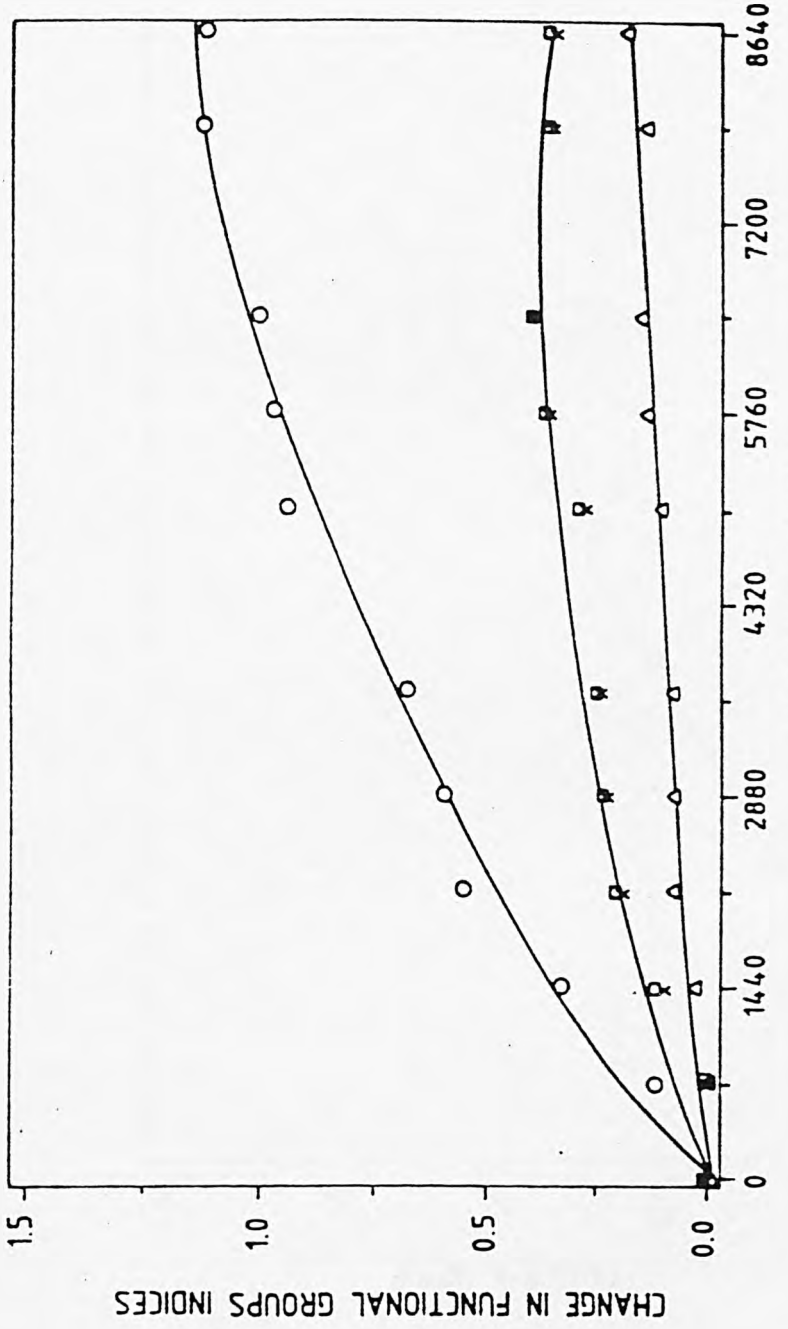

Figure 3.8. Changes in functional groups indices as a function of exposure time.

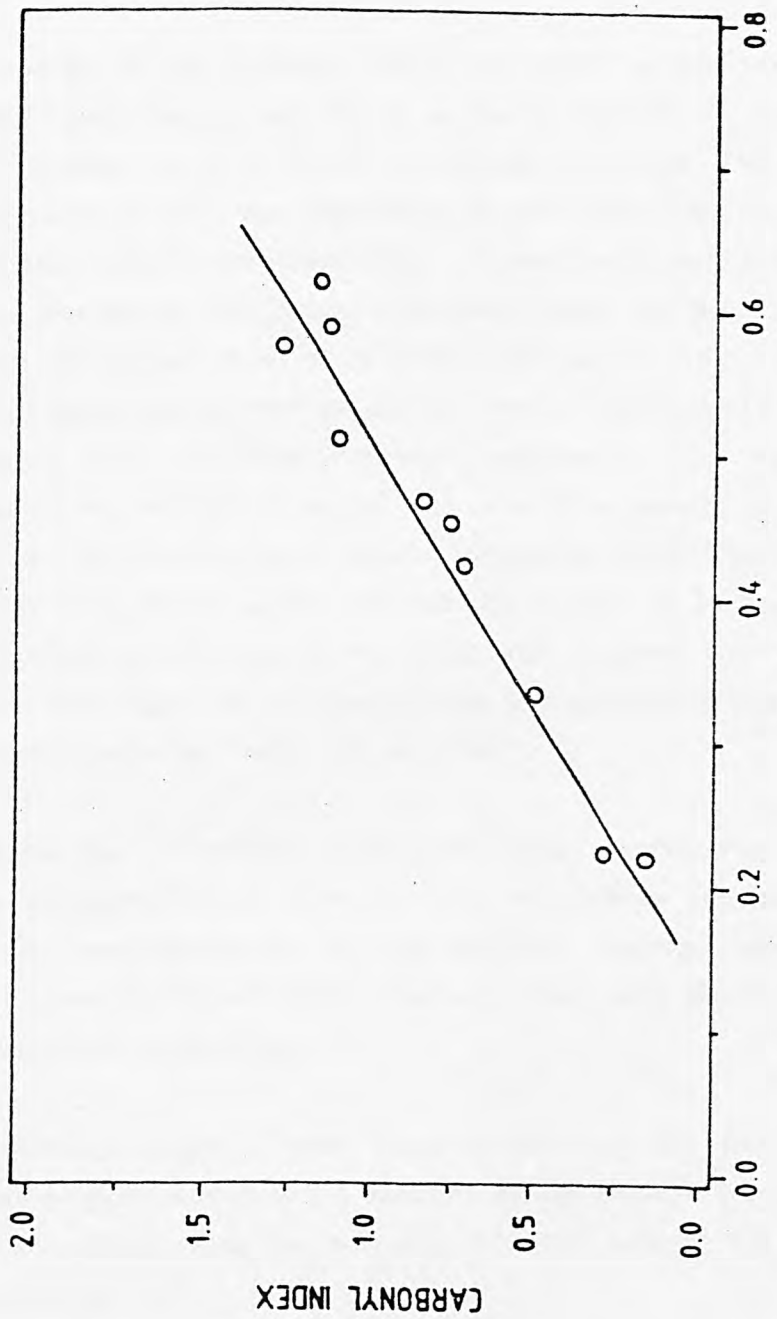

Figure 3.9. Plot of carbonyl index versus vinyl index.

irradiation of LLDPE, chain branching reactions occur. The alkyl macroradicals formed during the irradiation induce both chain scission and chain branching with branching predominant in the LDPE. On increasing the number of long chain branches, the structure of LLDPE becomes very similar to that of LDPE.

The relative changes of the carbonyl, vinyl, and alkene groups revealed by means of FTIR spectroscopy, are shown in Figure 3.10 in the form of a dimensionless number as a function of weathering time. The ordinate represents the ratio between the absorbance at each exposure time and the absorbance of the control (unexposed) film. As mentioned earlier, the major points are the increase of the groups with C=O bonds, the decrease of the vinylidene and the formation of a significant amount of vinyl. The broad absorption C=O band can be resolved into six overlapping peaks [Kato et al., 1969] associated with different carbonyl compounds. The number of vinylidene groups was reduced to almost zero after three months of exposure, whereas carbonyl and vinyl groups showed increasing trend. The formation of vinyl groups seems to be associated with the increase of carbonyls. The hydroxyl and alkene groups change very little with exposure time, as shown in Figure 3.10. The slight rise of these groups is somewhat in contradiction with the results obtained by Heacock et al. [1968].

The results show that the samples exposed to tropical weather for 12 months contain high concentration of carbonyl, vinyl and alkene groups. During weathering the macromolecules of polyethylene undergo simultaneous processes of photooxidation and chain-breaking which cause the decay of the significant properties of the film.

The photooxidation process is most likely initiated by the ketone groups present in the polymer undergoing a reaction of the Norrish I type; it then proceeds in accordance with the generally accepted scheme for oxidation reactions [Ranby and Rabek, 1975]:

PH	--->	$P^{\cdot}+H^{\cdot}$
$P^{\cdot}+O_2$	--->	$POO^{\cdot}$
$POO^{\cdot}+PH$	--->	$POOH+P^{\cdot}$
POOH	--->	$P^{\cdot}+{}^{\cdot}OOH$
POOH	--->	$PO^{\cdot}+{}^{\cdot}OH$

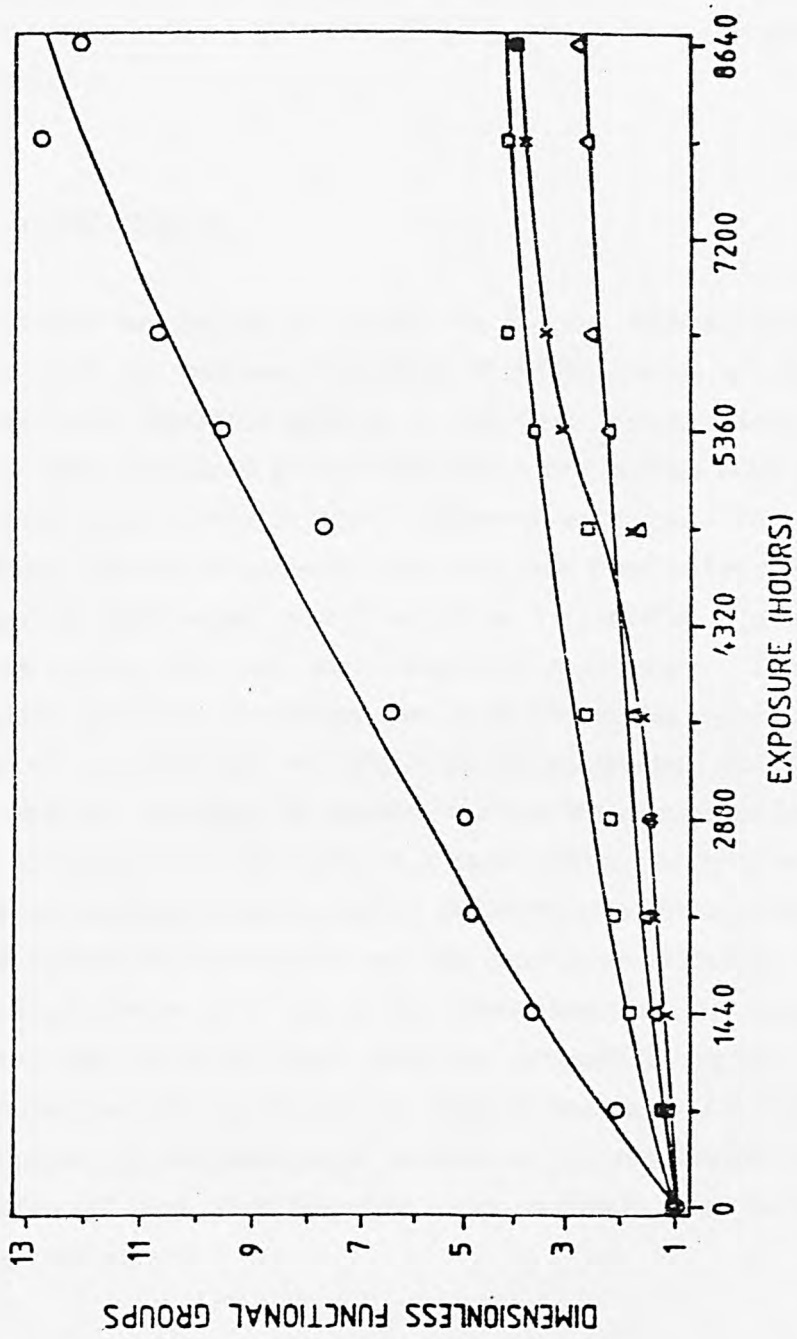

Figure 3.10. Changes in dimensionless functional groups as a function of exposure time.

The formation of polymer radicals (P·) from the polymer (PH) is necessary for rapid polymer oxidation. Macroradicals (P·) formed during initiation can easily react with oxygen molecules producing peroxy polymer radicals (POO·). The peroxy radical can abstract hydrogen from another polymer molecule to form polymer hydroxy peroxide (POOH), which later decompose under light irradiation.

3.4 CONCLUSION

The natural weathering of LLDPE in the hot climate of Dhahran, Saudi Arabia, and the periodic recording of FTIR spectra of degraded LLDPE samples have indicated growth in carbonyl, vinyl, alkene, and hydroxyl groups. The vinylidene groups were found to diminish with exposure time. A literature review reveals three different techniques for elucidating the structural changes in polyethylene that has been subjected to weathering. Difference spectroscopy was found to be very useful in detecting structural changes during the very early stages of weathering. The band indexing technique plays an important role once the initial presence of functional groups is considerable and needs to be subtracted out. In addition, the variations in thickness of samples can also be eliminated by presenting the IR spectra results in the form of a band index. The relative changes of the functional groups are presented in the form of a dimensionless number. The slight change in crystallinity and the growth of carbonyl, vinyl, and other functional groups have led to the conclusion that the amorphous areas of polymer are affected more than the crystalline regions. It is further concluded that the apparent higher degradation rates of LLDPE samples are a consequence of two concurrent phenomena: the photooxidation itself and the formation of long chain branches which radically alter the structure of this new polyethylene.

Chapter 4

THERMAL ANALYSIS (DSC)

4.1 INTRODUCTION

Studies of polymer degradation over the past decade have increasingly been carried out using thermoanalytical methods. These methods involve the measurement of a convenient variable during a gradual, linear increase in temperature. The most widely used of these techniques are thermogravimetry (TG), differential thermal analysis (DTA), and differential scanning calorimetry (DSC) [Runt and Harrison, 1980]. The morphology of a polymer sample, i.e., the crystallinity, the shape and size of the crystals, the structure of the surface of crystals and the strain of amorphous regions, influence the heat content and its dependence on temperature. The latter can be well investigated by calorimetric measurement in a differential scanning calorimeter [McNaughton and Mortimer, 1975].

The chemical structure and morphology can be related to the useful properties in order to be able to manipulate the structure to improve properties and to understand how degradation detracts from them. Crystallinity is considered to be the most important structural parameter. This is dependent on the composition of the polymer and the crystallization conditions and its effects on all the thermodynamic and mechanical properties. A wholly crystalline material would be brittle due to the weakness of crystal-to-crystal boundaries, whereas a wholly amorphous structure would be either rubbery or glassy depending on the glass transition temperature [Billingham and Calvert, 1983].

The polyolefins are considered to be very tough because at high stresses the chain slips through the crystalline region giving a very large scale deformation. They become brittle at low temperature where the amorphous region become glassy. Accordingly, oxidation tends to break bonds within the amorphous regions so that the cracks can propagate before the high stresses needed to cause chain slip within the crystal are reached.

In this section, the changes in thermal characteristics, viz., crystallinity, heat of fusion, and crystalline melting temperature, will be studied for LLDPE samples exposed to harsh natural weather.

4.2 EXPERIMENTAL

4.2.1 Differential Scanning Calorimeter

The thermal properties of the samples were determined by applying the standard techniques to the relevant thermogram obtained from a Perkin-Elmer differential scanning calorimeter, Model DSC-4 attached to a System 4 microcomputer controller. This thermal analyzer has high sensitivity, resolution, and speed. A thermal analysis data station (TADS) is connected to the DSC-4 for data handling, storage, and calculations. The procedures used in this work are consistent with conventional practice in the presentation of calorimetric data. That is, endothermic transitions (Figure 4.1) and increases in heat capacity are represented by upscale departures from the ordinate baseline [Instructions, Model DSC-4, 1983]. Exothermic reactions are represented by downscale departures from the baseline. Ordinate calibration is in millicalories per second and the abscissa is normally calibrated in degrees centigrade. When the programmed temperature of the sample holders increases, recorded temperature increases from left to right . To conform to these conventions, the left-hand sample holder is always used for sample materials and the right-hand sample holder is for reference materials, only.

4.2.1.1 Temperature (Abscissa) Calibration

Temperature calibration of DSC-4 was carried out according to ASTM standard [ASTM Standard E-967-83, 1983a] and the recommendations made by the manufacturer using one point calibration procedure. This procedure was possible due to the advanced electronics built into the Model DSC-4 and System 4 microcomputer controller, which linearizes the calibration using a single transition point. The standard which was used for temperature calibration was Indium, having melting point 156.60^{o}C, transition energy 6.80 cal/gram, and Atomic weight 114.82 [Instructions Model DSC-4, 1983]. During the course of experimentation, temperature calibration was checked when

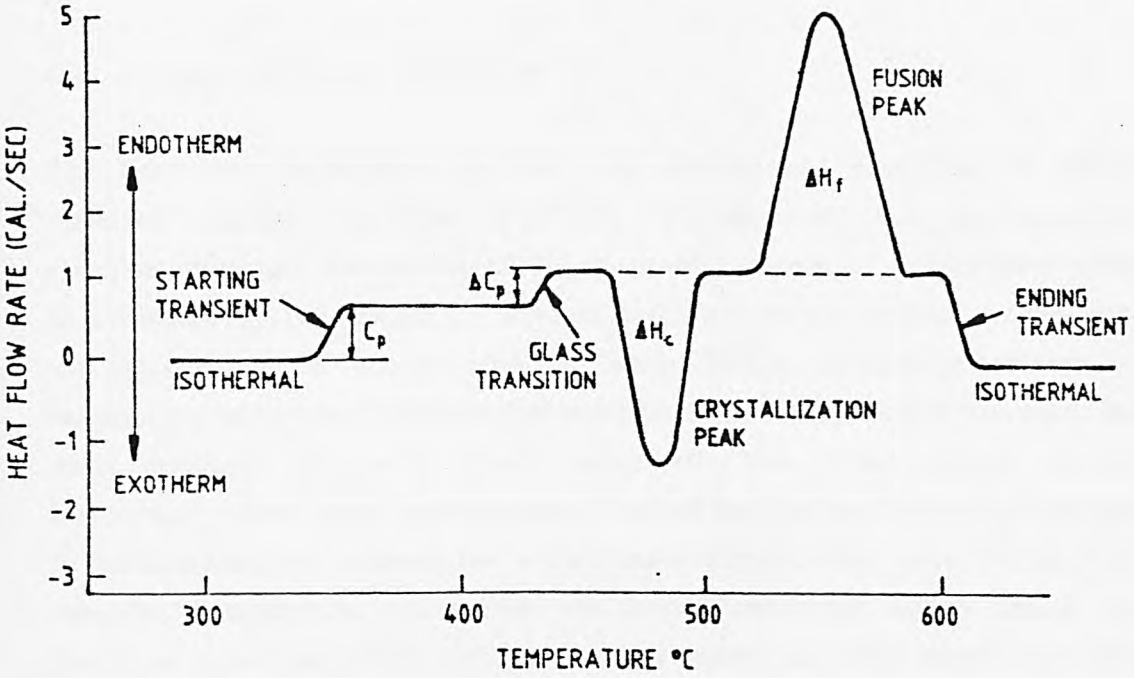

Figure 4.1. Conventions for presentation of thermal analysis data.

baseline optimization procedure was carried out. For best temperature repeatability standard was flattened, placed in the center of the aluminum pan, encapsulated, and set in the center of the sample holder. Optimum temperature calibration was obtained by observing the transition temperature for the standard and adjusting the T CAL set screw of System 4 microcomputer controller. Temperature calibration was carried out regularly every month during the course of experimentation and particularly when operating conditions were changed.

4.2.1.2 Energy (Ordinate) Calibration

The heat flow calibration of DSC was carried out according to ASTM standard [ASTM Standard E-968-83, 1983b] and the manufacturer recommendations. The Model DSC-4 measures the rate of energy absorption or evolution by the sample in units of millicalories per second. In practice, the measurement of energy with the Model DSC-4 necessarily involves an instrument calibration constant, the recorder chart speed, sensitivity used, the units employed for area measurement, etc. The range switch on the instrument control panel gives nominal values for the rate of energy change, in millicalories per second, for a full scale displacement on a 10 millivolt recorder. Temperature calibration was carried out every month during the course of experimentation and particularly when operating conditions were changed.

4.2.2 Procedure

The samples were prepared by No. 3 cork borer producing samples which fit nicely into the standard aluminum DSC samples pans (Perkin-Elmer Alum. Kit. No. 219-0041), covering nearly the entire bottom of the pan. Optimum sample weights were generally of the order of 5 to 20mg $\pm$ 0.2mg, placed into clean specimen holder. Although quantitative accuracy will remain the same regardless of the sample shape, the quantitative appearance of a run will be effected by the sample configuration [Brennan, 1978]. Therefore, for maximum peak sharpness and resolution, a configuration which maximizes the contact surface between the pan and sample was used. A standard crimper press (Perkin-Elmer) was used to crimp a aluminum cover onto the sample pan as recommended by the manufacturer. The assembly was placed in the

sample holder and the chamber was continuously perged with Argon gas. A scan rate of $10^{o}C$/min was used to heat the specimen in the temperature range of 50 to $150^{o}C$.

The crystalline melting temperature (T_m) was determined from the DSC thermogram according to ASTM Standard [ASTM Standard E-794-81, 1981]. The melting point is considered to be the peak of the melting thermogram where melting is complete. The heat of fusion (H_f) was determined according to ASTM standard [ASTM Standard E-793-81, 1981]. The area under the melting peak is considered to be the heat of fusion and is determined in units of cal/gm.

The DSC method for determining the percent crystallinity of a semicrystalline polymer is based upon the measurement of the heat of fusion and the reasonable assumption that this quantity is proportional to the percent crystallinity [Gray, 1970]. For polyethylene the heat of fusion (H_f^*) of a hypothetical 100% crystalline sample is determined through a process of extrapolation, estimation and analogy with a model compound and is determined to be 68.4 cal/gm [Wunderlich and Cromier, 1967]. The percent crystallinity may be calculated from [Brennan, 1977]:

$$\%\text{Crystallinity} = (H_f/H_f^*) \times 100$$

where $H_f^* = 68.4$ cal/gm

H_f = Heat of fusion of the sample.

4.3 RESULTS AND DISCUSSION

DSC measurements of LLDPE samples were carried out periodically during 12 months of exposure to the natural weather of Dhahran, Saudi Arabia. A minimum of five replicates of each sample were used for DSC measurement. DSC thermogram of unexposed and exposed LLDPE samples is shown in Figure 4.2. It is obvious from the thermogram that the area of the melting peak is more for exposed sample than for unexposed sample. Moreover, they exhibit relatively small effects of morphology in the temperature range sufficiently below the melting point. This can be attributed to the concept that below the melting point, the specific heats of amorphous and crystalline

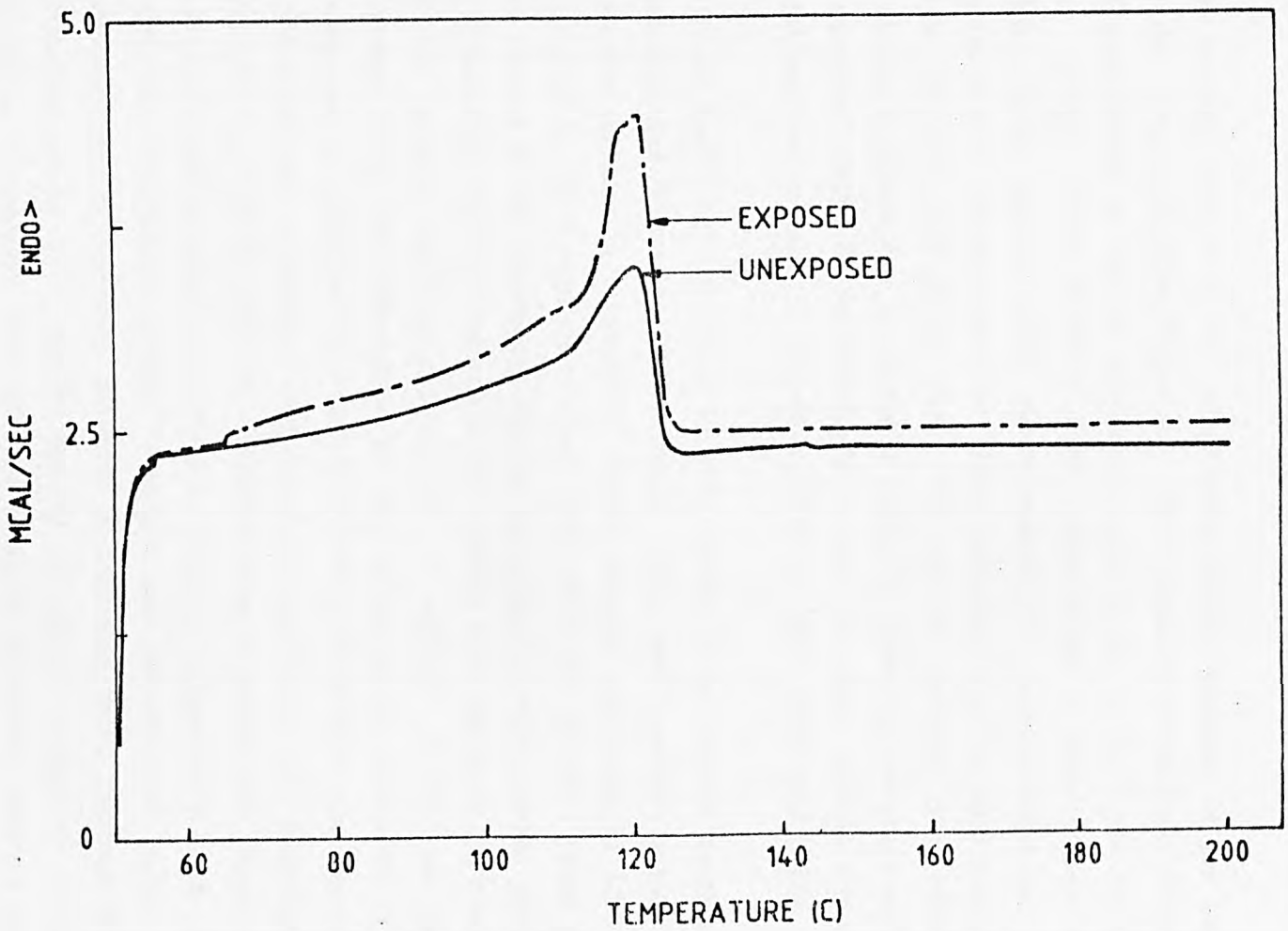

Figure 4.2. DSC thermogram of unexposed and exposed LLDPE sample.

phases are not very different. Near the melting point, however, as a consequence of local melting and recrystallization, major differences occur which may provide useful information about heat content and phase transformation.

The gradual increase in the crystallinity during exposure to the natural weather is apparent from Figure 4.3. The increase in crystallinity from 39% for unweathered to 55% for weathered LLDPE is due to the formation of the new groups, chain breaking, and crosslinking. Polyethylene is a semicrystalline polymer which can be considered to behave like a two-phase system: a well ordered crystalline phase dispersed in a less rigid amorphous phase [Michaels and Bixler, 1961]. The gradual increase in crystallinity, according to Winslow et al., is due to oxidative crystallization and scission of constrained chains in the amorphous region; the chain scission allows the resulting freed segments to crystallize [Winslow et al., 1963b and 1964].

Infrared studies *(Chapter 3)* of LLDPE exposed to the natural weather have indicated the formation of carbonyl, vinyl, and hydroxyl groups. The apparent increase in crystallinity during natural weathering of LLDPE is attributed to the formation of -C=0, -OH, -OOH, etc. groups. These groups are formed in the amorphous regions replacing the $-CH_2$ groups there and thus reducing their concentration. This finding is in line with the discussion on the infrared spectroscopic analysis of exposed polyethylene samples [Luongo, 1963]. The replacement of CH_2 groups by the formation of polar groups can be attributed to chemcrystallization which also causes increase in crystallinity due to increased mobility of polymer chains after degradation. It was observed that the rate of -C=0 formation is considerably suppressed in a more crystalline polyethylene sample, owing to a higher ratio of the oxygen impervious crystalline region, whereas the polyethylene sample with relatively low crystallinity exhibited a relatively rapid increase in -C=O formation owing to a greater amount of oxygen susceptible amorphous regions in the sample. This infrared evidence, therefore, supports the fact that oxygen attack occurs principally in the amorphous regions of the polyethylene in the solid state.

Heat of fusion H_f (per unit mass of specimen) reveals a similar pattern as that of crystallinity. These effects are attributed to the scission of tie

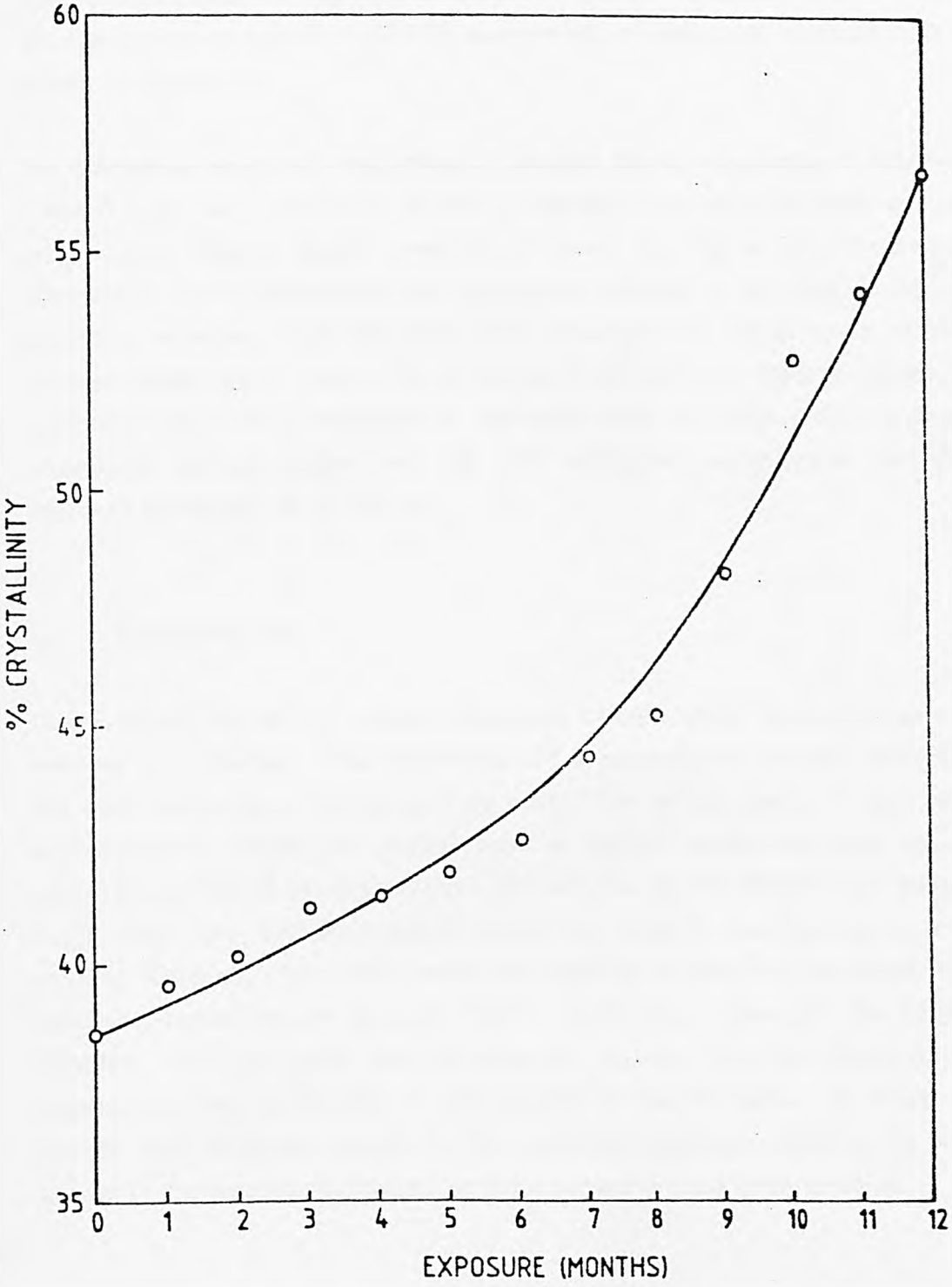

Figure 4.3. Changes in % crystallinity as a function of weathering time.

molecules followed by a growth in the perfection of the crystal lamellae. The change in heat of fusion of LLDPE samples as a function of exposure time is shown in Figure 4.4.

An interesting aspect of morphological changes due to weathering is observed when the percent crystallinity gradually increases and the crystalline melting temperature remains almost constant as shown in Figure 4.5. The results shown lead to the conclusion that prolonged exposure to weather conditions promotes secondary crystallization. It is suspected that the creation of new intermolecular polar bonds (due to carbonyl groups) may lead to secondary crystallization. Similar behavior of increased peak area and almost constant crystalline melting temperature for UV weathered polyethylene was also observed by Mathur et al. [1981].

4.4 CONCLUSION

In this work, the thermal characteristics of LLDPE when exposed to natural weather are reported. The morphology of a polyethylene greatly influences the shape and position of the melting peak. The melting peaks of unexposed and naturally weathered LLDPE have a similar shape, implying similar melting behavior of the crystallites. The maxima of the endothermic melting (T_m) peak does not shift much during the LLDPE samples exposure to natural weather. The area under the melting endotherm increased with exposure, indicating an increase in the crystalline content of the LLDPE samples. It is concluded that the apparent increase in crystallinity during exposure to natural weather is attributable to the formation of functional groups. This formation occurs in the amorphous regions, replacing the $-CH_2$ groups in the amorphous region, and thus reducing their concentration.

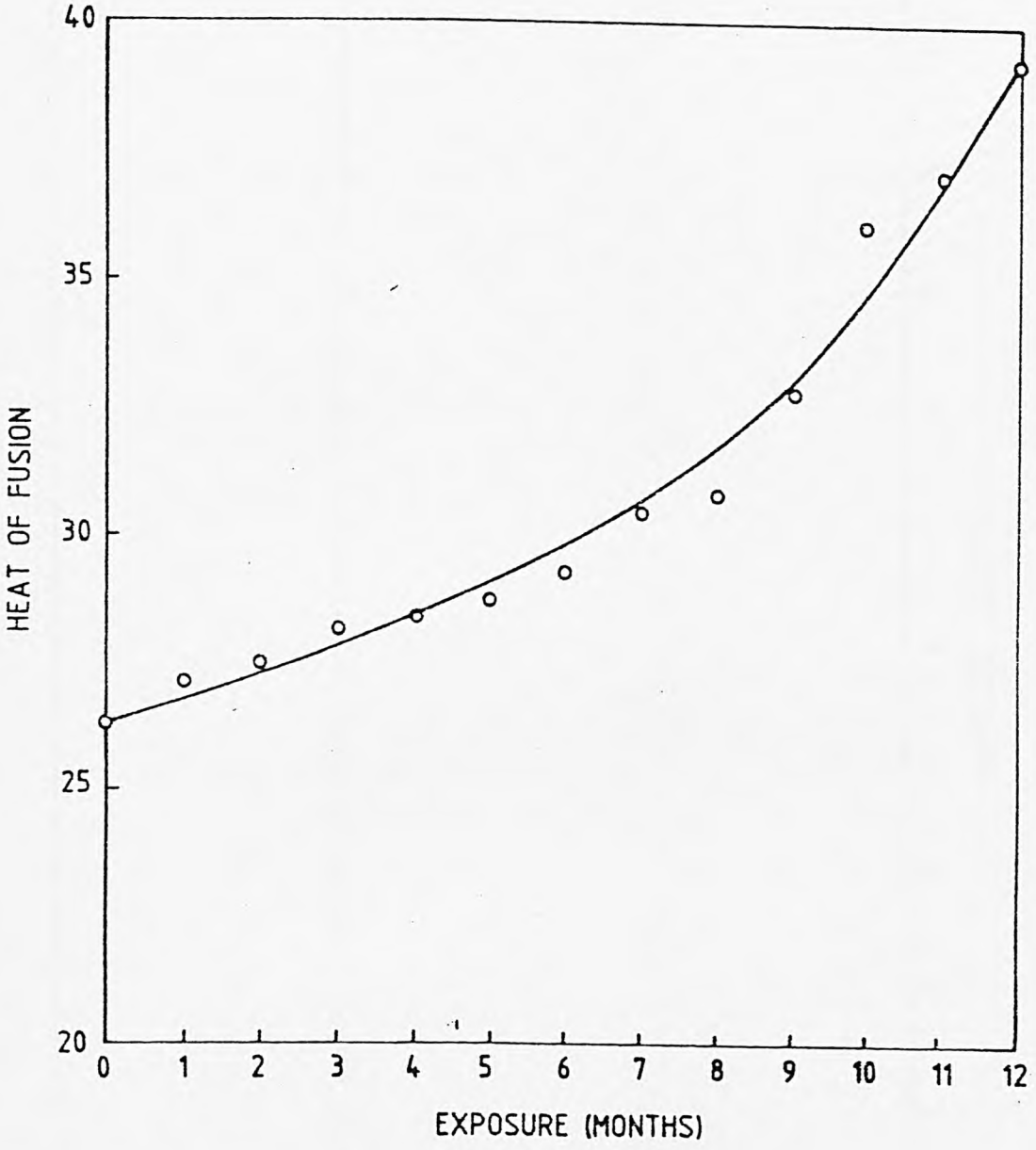

Figure 4.4. Changes in heat of fusion as a function of weathering time.

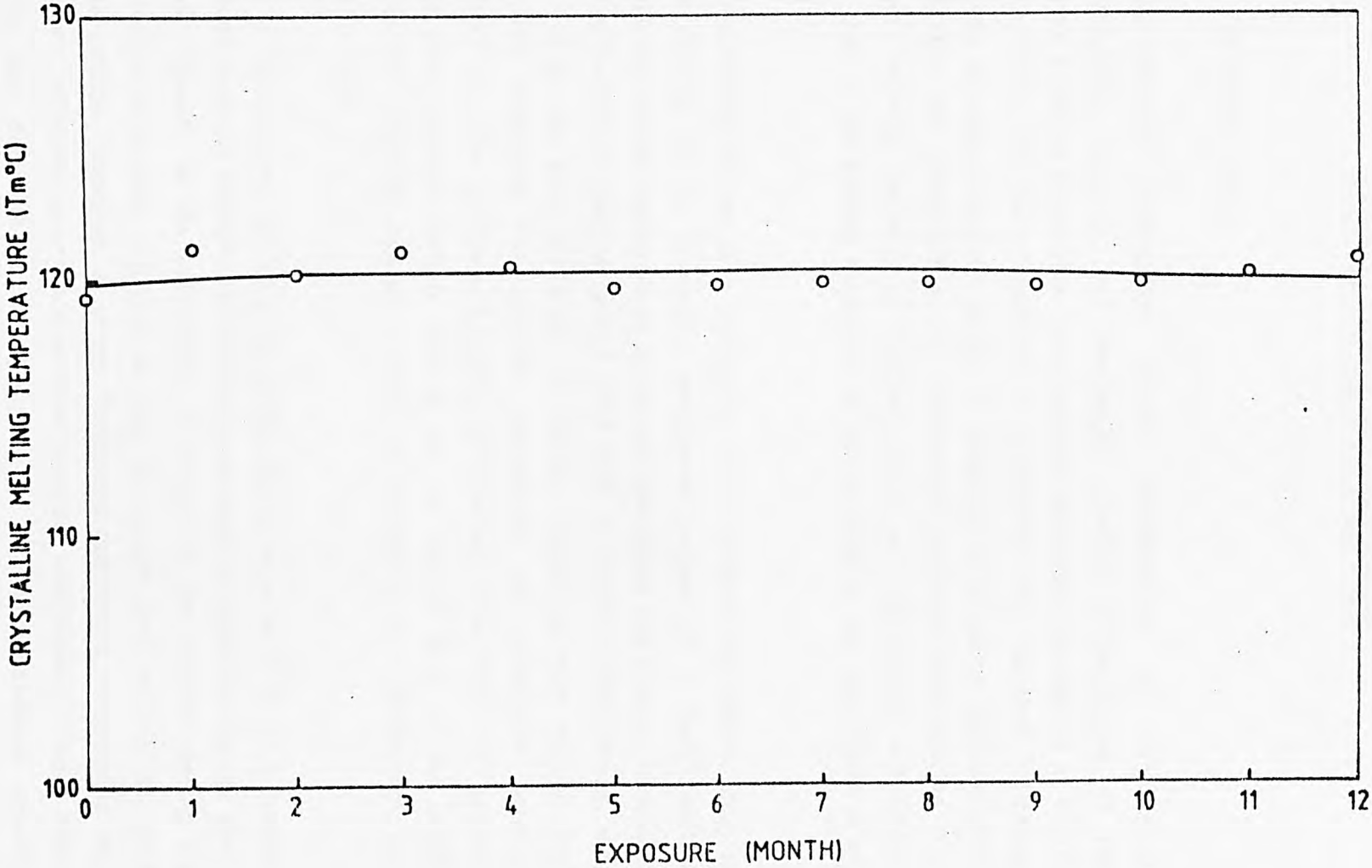

Figure 4.5. Changes in crystalline melting temperature as a function of weathering time.

Chapter 5

MECHANICAL PROPERTIES

5.1 INTRODUCTION

Weather-induced degradation causes deterioration of mechanical characteristics, cracking, and eventually complete disintegration of the material. Ultimate mechanical characteristics (especially elongation at break) of polyolefins are more sensitive to irradiation than methods reflecting chemical changes. Although, series of processes involved in photochemical degradation are precursors of the mechanical properties deterioration. The ultimate behavior responds to localized structural irregularities and defects more than to the average properties of the material in the bulk [Raab et al., 1982]

The mechanical failure of a polyolefin occurs because degradation leads to chain scission in the accessible, amorphous regions of a semicrystalline morphology. Whilst measurement of oxygen absorption and product formation by spectroscopic techniques give a good deal of chemical information, they may not be the good predictors of failure. Depending upon sample type, oxidation conditions and polymer morphology the correlation between chemical induction periods and mechanical lifetimes varies from very good to rather poor. Common failure criteria are the loss of 50 % of the initial mechanical properties (tensile strength, % elongation, etc.) [Billingham and Calvert, 1983].

Some of the reactions taking place during degradation result in cross linking and some in chain scission. The relative occurrence of cross-linking and chain scission depends on the availability of oxygen in the polymer during the photooxidation process, and thus on both the oxygen pressure and the speed of the process. Therefore, at severe irradiation conditions, crosslinking may occur to a relatively greater extent than at milder conditions. Although cross-linking may dominate in the beginning of the photooxidation process, generally chain scission reactions predominate ultimately resulting in a reduction in molecular weight of the polymer, and consequently in a

deterioration of the mechanical properties, such as tensile strength, and percent elongation [Raab et al., 1987].

In this chapter change in significant mechanical properties will be studied for LLDPE samples exposed to the severe natural weather of Dhahran, Saudi Arabia.

5.2 EXPERIMENTAL

5.2.1 Test Specimens and conditions

The test specimens were prepared according to the recommendations made in ASTM Standard [ASTM Standard, D-638M-84, 1984]. Machining operation was used to form the specimens which were free of visible flaws, scratches, or imperfections. Test conditions were maintained according to the standard laboratory atmosphere of 23+2oC and 50+5% relative humidity.

5.2.2 Material Testing System (MTS)

The 25 Kilonewtonn material testing system (MTS) model 812 was used to determine the tensile properties of unexposed and exposed LLDPE samples. The system uses servohydraulic technology which allows precise control of load, displacement, and strain and provides the capabilities for performing diverse static and dynamic test procedure. Through the use of closed loop servohydraulic control, the test system has extensive flexibility and is able to operate over a broad force range with precise displacements and strain rates. The block diagram shown in Figure 5.1 illustrates the principle of closed-loop control used in the system. During a test, the force, strain, or displacement applied to a specimen is measured by a transducer and continuously compared to the signal from the manual command control. Any difference between the measured (feedback) value and command value results immediately in a corrective signal from the controller to the servovalve. Correspondingly, the servovalve causes the actuator to be moved to the desired or command position to minimize and correct the difference. The system automatically maintains the piston at the command valve throughout a test to provide precise control under static or dynamic conditions. The

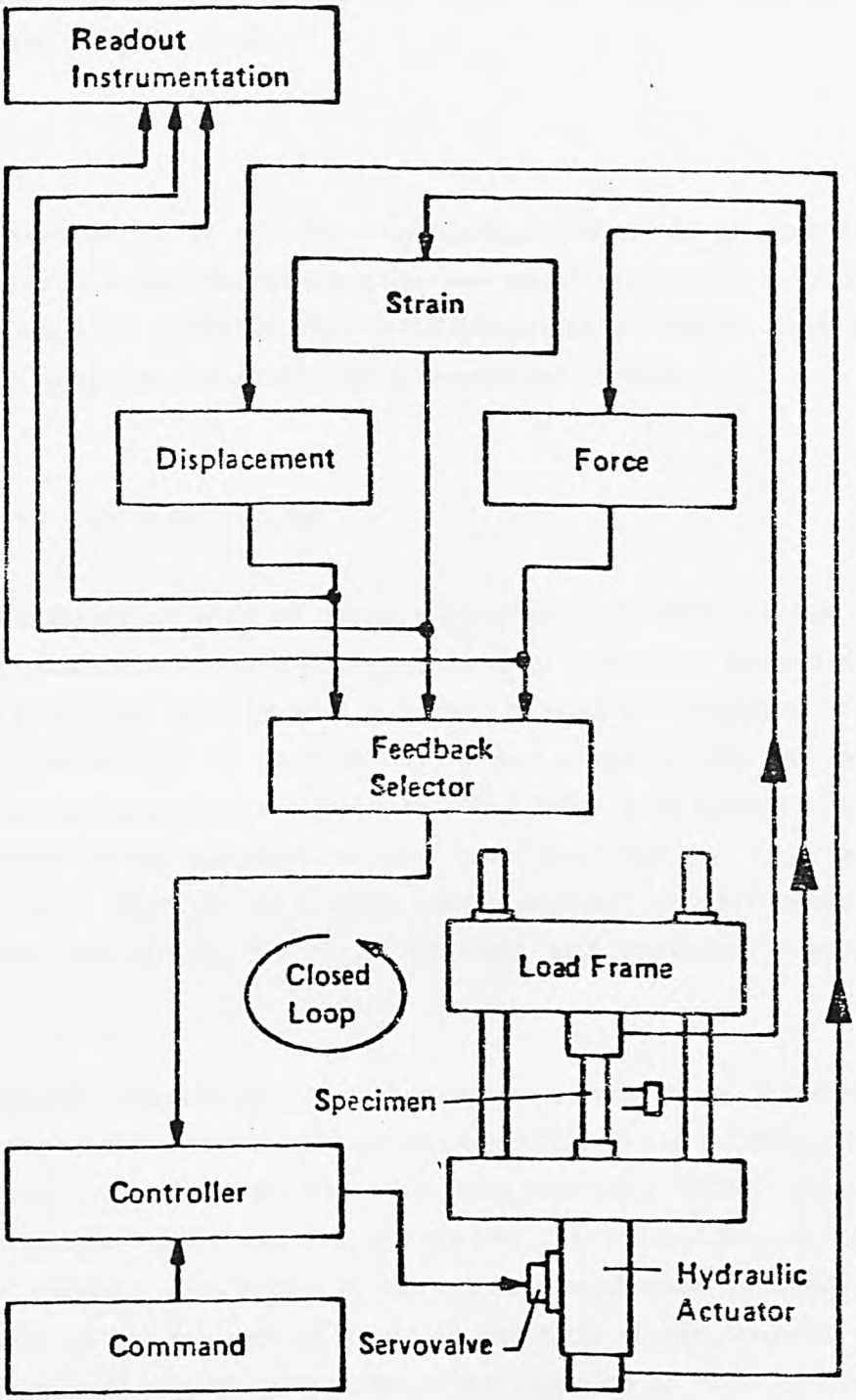

Figure 5.1. Block diagram of MTS system.

feedback selector allows the operator to select the control (command) parameter for the test [MTS, 1982]

5.2.3 Procedure

The samples were drawn at periodic predetermined intervals of time for mechanical behavior study. The testing speed was maintained at 100 mm/min. and in accordance with ASTM Standard [ASTM Standard D-638M-84, 1984] an average of five specimens was considered a representative value.

5.3 RESULTS AND DISCUSSION

The load vs elongation curve of an unexposed sample of LLDPE is shown in Figure 5.2. It shows a very sharp force maximum at low strain. Beyond this point there is a decrease in force with a further increase in elongation. The curve then flattens out and the force remains almost constant. The load then increases before the rupture of the specimen. This behavior is typical of low molecular weight linear polymers as has been described by Popli and Mandelkern [1987]. However an LLDPE sample exposed for 4500 hours to natural weather lost almost all of its ductility and exhibited a brittle fracture.

The photochemical degradation of polyethylene results from competing reactions of cross linking and chain scission that occur in the material. The crosslinking may predominate the chain breaking [Hawkins, 1964]. Ultimate mechanical properties of the material are used to characterize the degraded specimens. A characteristic feature of the ultimate mechanical properties is their sensitivity to the presence of flaws in the bulk of the material. It facilitates the use of ultimate properties in the detection of those processes which occur localized in certain sites. The stress strain tests are a simple but very sensitive detection method and react to photooxidative degradation much earlier and a more pronounced way [Akay et al., 1980b] than in the usual physicochemical analytical methods . The sensitivity of the ultimate properties in photooxidative degradation is mainly due to the key role of defects or cracks in the fracture behavior of materials and the heterogeneous character of the degradation process. It is observed that the photodegradation

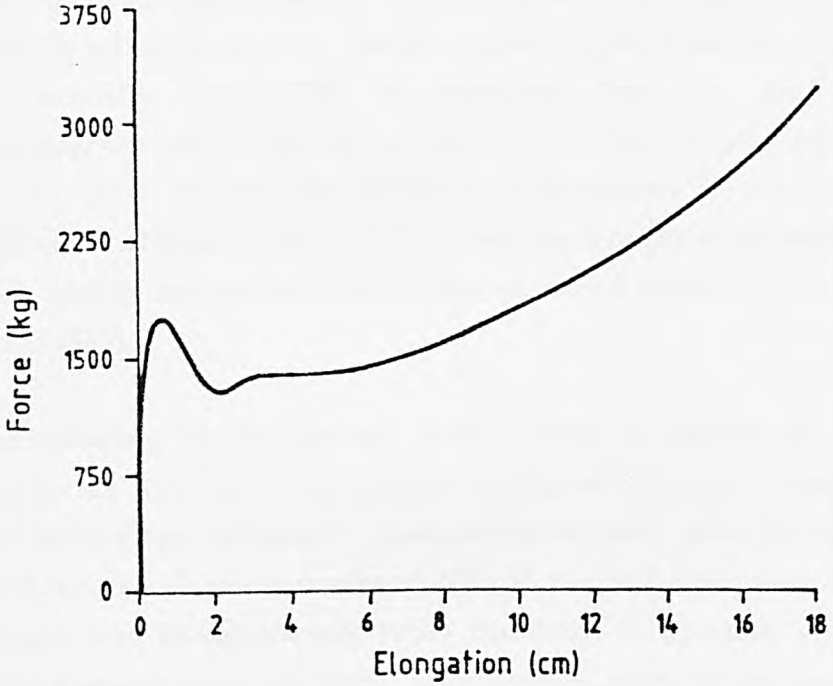

Figure 5.2. The force elongation diagram of unexposed LLDPE.

proceeds preferentially in a comparatively localized region near the initiation site which can be either photosensitive impurity, a structural element, etc. The localization of the degradation process is a consequence of the low molecular mobility both of the polymer and of the photoactive site in the solid state. Chemical reasons are also involved which include zip mechanism of degradation along the polymer chain. The probability of the occurrence of these degradation sites is higher in the surface layer of the sample but such sites may also lie inside the bulk of material [Vink, 1979]. While the ultimate behavior is governed by a single extreme defect, spectral analytical methods yield integral characteristics of the material in bulk. Therefore, chemical methods reflect structural changes caused by photooxidative degradation in a less sensitive way. This is especially true for the first stage of photodegradation, where the process is still localized only in a finite number of very small regions. The schematic diagrams in Figure 1.15 illustrates the subsequent effects of UV radiation and mechanical stress on the formation of week centers and microcracks in sites of initial chemical heterogeneties [Raab et al., 1982].

Dimensionless tensile strength and percent elongation of LLDPE against weathering time have been plotted in Figures 5.3 and 5.4 respectively. There is a sudden loss in both of these properties soon after the exposure. Within three months of exposure almost 50% of the properties were lost. The tensile strength and elongation and break continued to decrease with time, then the curve flattened and continued monotonously with the exposure time. At this stage the specimens had lost all of their elongation and became so brittle and weak that they would break during handling. The data shows that Dhahran's weather is highly aggressive to the plastic. Unstabilized LLDPE film 5 mils thick has been shown to retain its 50% elongation for almost four months of outdoor exposure in Florida, USA [Pouncy, 1985]. As the degradation rate has an inverse relationship with the thickness of the sample, thick plaque samples exposed at Dhahran should show a slower degradation rate compared to films exposed at Florida but the failure criterion of 50% loss of elongation reaches in less then three months at Dhahran site.

The Fourier Transform Infrared (FTIR) spectroscopy results for the natural exposure of LLDPE film at Dhahran, Saudi Arabia have been reported in Chapter 3. Significant changes in the carbonyl, vinyl, hydroxyl, and

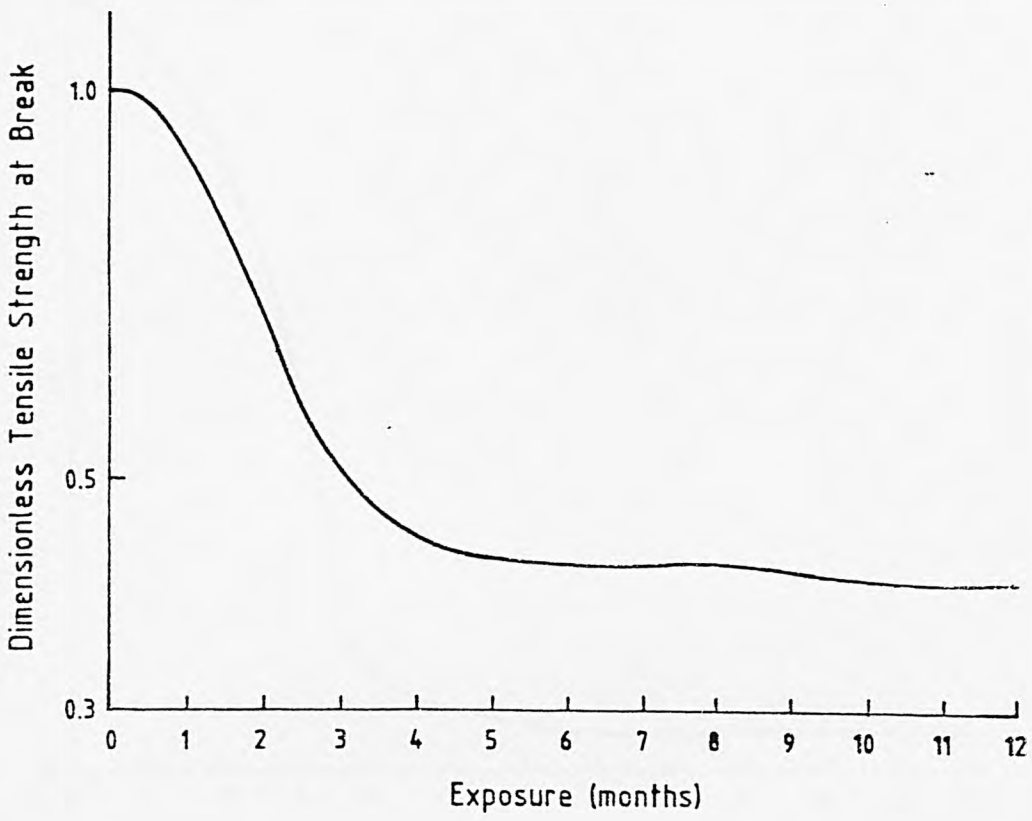

Figure 5.3. Dimensionless tensile strength as a function of weathering time.

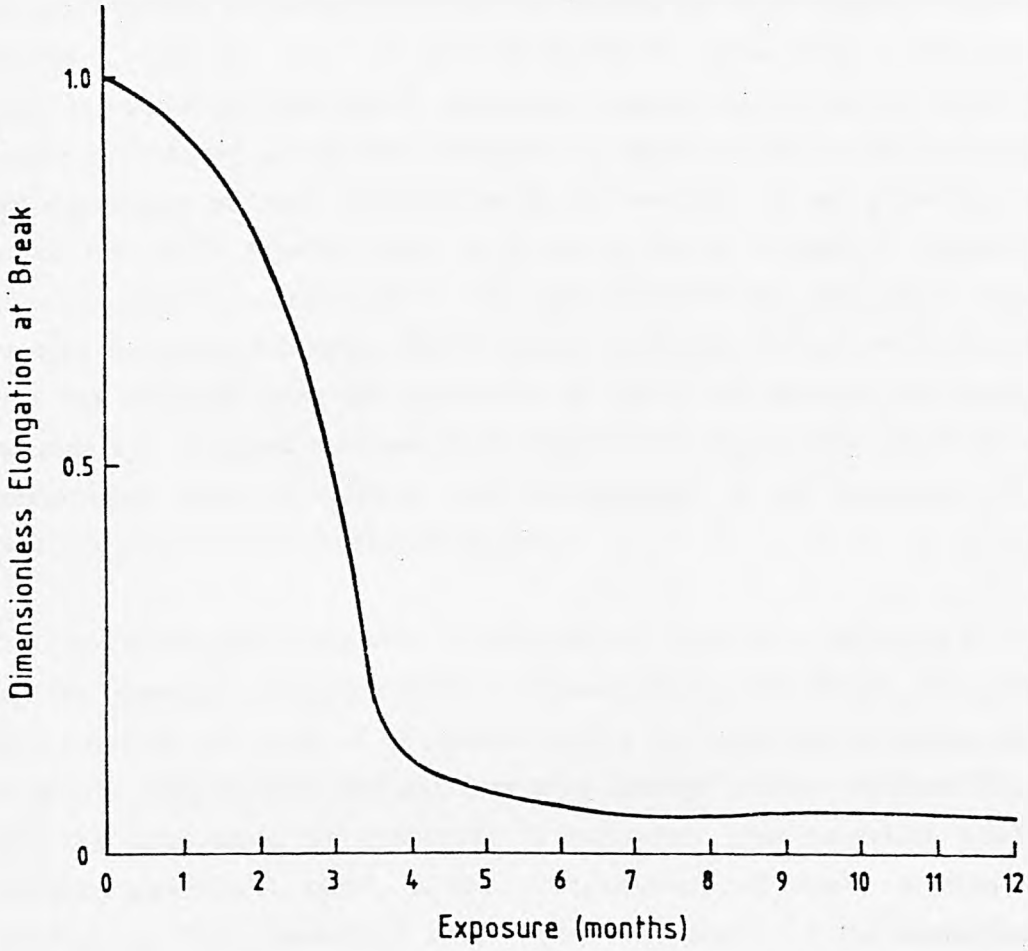

Figure 5.4. Dimensionless % elongation as a function of weathering time.

vinylidene functional groups had been observed. The macromolecules of LLDPE undergo simultaneous process of cross linking and chain scission which results in the decay of significant properties of the material. The loss in elongation and tensile strength at break of the material is supplemented by the rapid growth in carbonyl groups even during the early stages of exposure. Figures 5.5 and 5.6 show the plot of growth in carbonyl as a function of decay in tensile strength and % elongation respectively. It clearly shows that growth in carbonyl groups concentration is a direct indication of the physical and mechanical property degradation of the material. It has generally been agreed that chain scission leads to a loss in tensile strength in contrast to network structure development through cross-linking, in which tensile strength normally increases. The decrease in tensile strength with exposure time was expected from the broadening of the FTIR spectra. This supports the generally accepted mechanism of polyethylene degradation which involve beta-scission. The beta-scission leads subsequently to the formation of the C=O group rather than to the OH group.

The photooxidation mechanism of polyethylene have been discussed in detail and the important points are well established [Ranby and Rabek, 1975]. These points include the need of photosensitization by impurities or chromophoric structural irregularities, the importance of peroxy radicals as chain carriers, and the importance of carbonyls in secondary photooxidation products. Another significant point is the predominance of chain scission over crosslinking. The crosslinking can become important on a thermomechanical level only when the polymer is rich in double bonds. As indicated by Figure 3.7 in Chapter 3, unexposed LLDPE samples contained unsaturation (vinylidene groups). These groups crosslink at the beginning of exposure and once the initially present vinylidene have disappeared, this crosslinking process rapidly becomes negligible in comparison with the chain scission. This fact is clearly indicated by the disappearance of vinylidene peak in the FTIR difference spectra of exposed specimen (Figure 3.6). The determination of carbonyl groups by infrared shows that the concentration of oxidation products decreases very rapidly from the surface toward the interior of specimen [Cunliffe and Davis, 1982, and Blais et al., 1972]. Such a degradation gradient would appear to generate stresses which can initiate cracks.

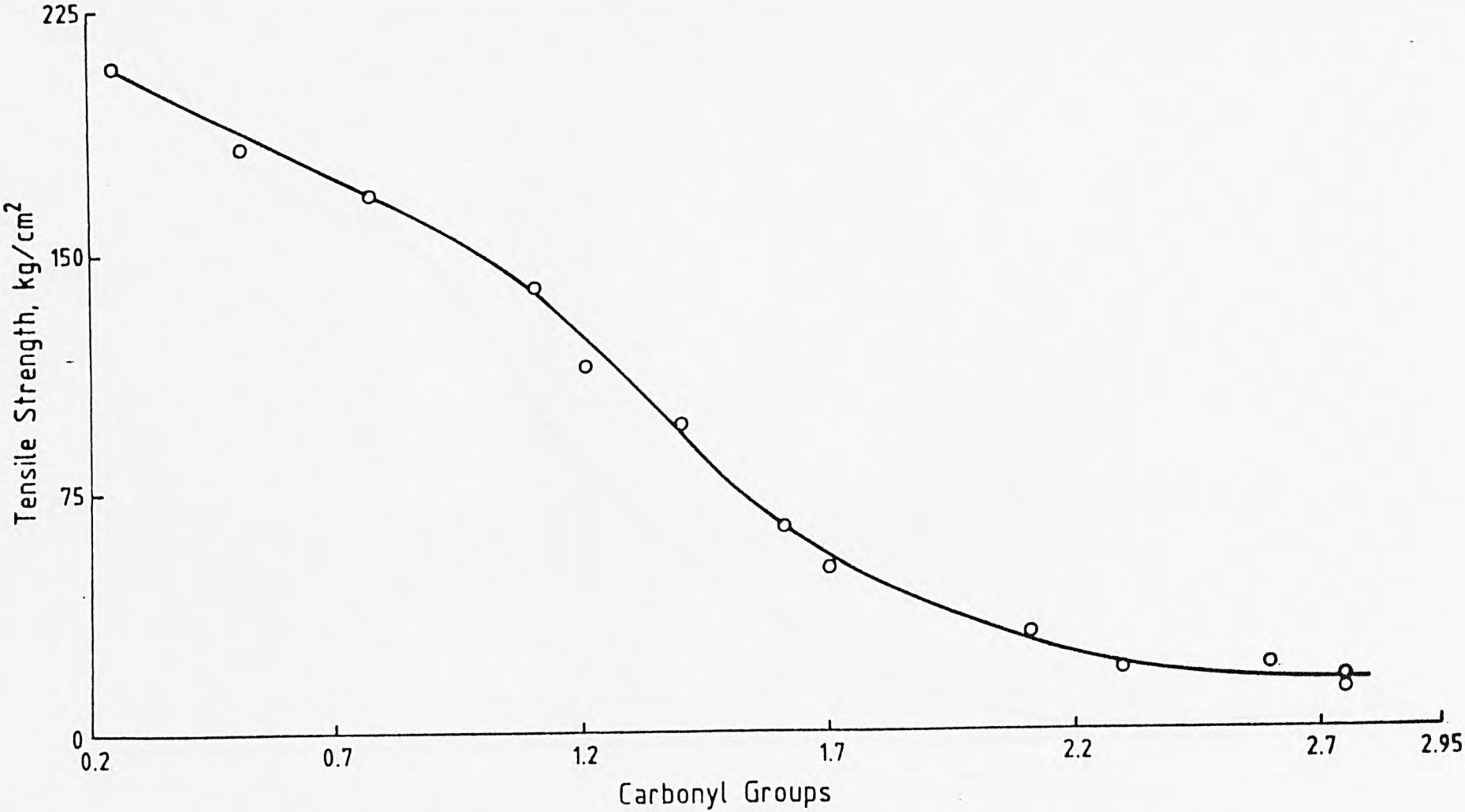

Figure 5.5. Growth in carbonyl groups as a function of loss in tensile strength.

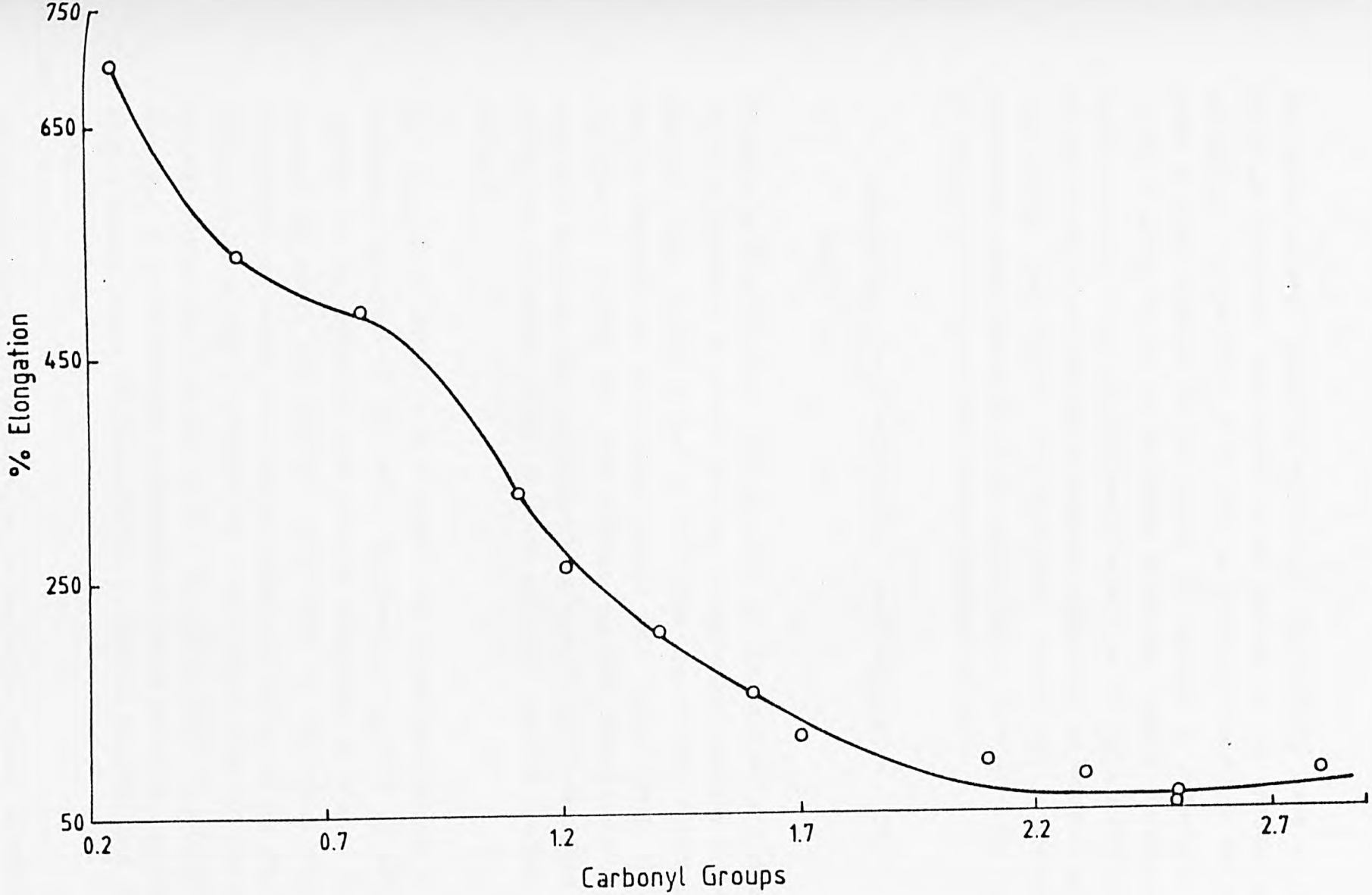

Figure 5.6. Growth in carbonyl groups as a function of loss in % elongation.

The shorter polymer chains formed by the chain-scission reactions can reorganize themselves, this results in an increase in the density and consequently in crystallinity of the polymer during photooxidation and can result in crack formation in the surface. The increase in crystallinity is already observed during the discussion of thermal analysis (Chapter 4). Figure 5.7 and 5.8 present the relationship between the change in crystallinity and loss in tensile strength and % elongation respectively. As indicated, some cross-linking accompanies weather-induced degradation (increasing crystallinity), chain scission at alkoxy radicals appears to be the main cause of embrittlement in hydrocarbon polymers [Winslow, 1977a]:

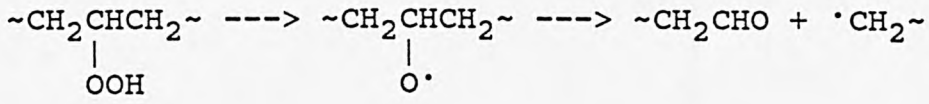

Crosslinking of polyethylene, which generally contain vinylidene groups, may also be supplemented by that of additional crystallization especially at longer exposure times. Secondary chemocrystallization due to UV radiation is already discussed for polyethylene [Pabiot and Verdu, 1981]. This is explained by assuming that chain segments resulting from photooxidative scission of the chains which originally were present in amorphous regions can additionally crystallize owing to their sufficient mobility during the exposure.

The macroalkoxy radical plays a central role in the deterioration of the mechanical properties of polyolefins. Extensive entanglement of polymer segments in the amorphous zone between crystallites is believed to be essential for tough and extensible films. Only the amorphous zone of polyethylene are readily penetrable by oxygen, so that all of the observed photooxidation damage is concentrated in this region. Thus the backbone cleavage which occurs from upto 50 % of the alkoxy radical in polyethylene must lead to the catastrophic deterioration in tensile properties that results after a critical degree of photooxidation is achieved [Carlsson and Wiles, 1976]

As previously known, the measuring of the elongation to break of polymeric materials in weathering tests often proves to be a more reliable method than

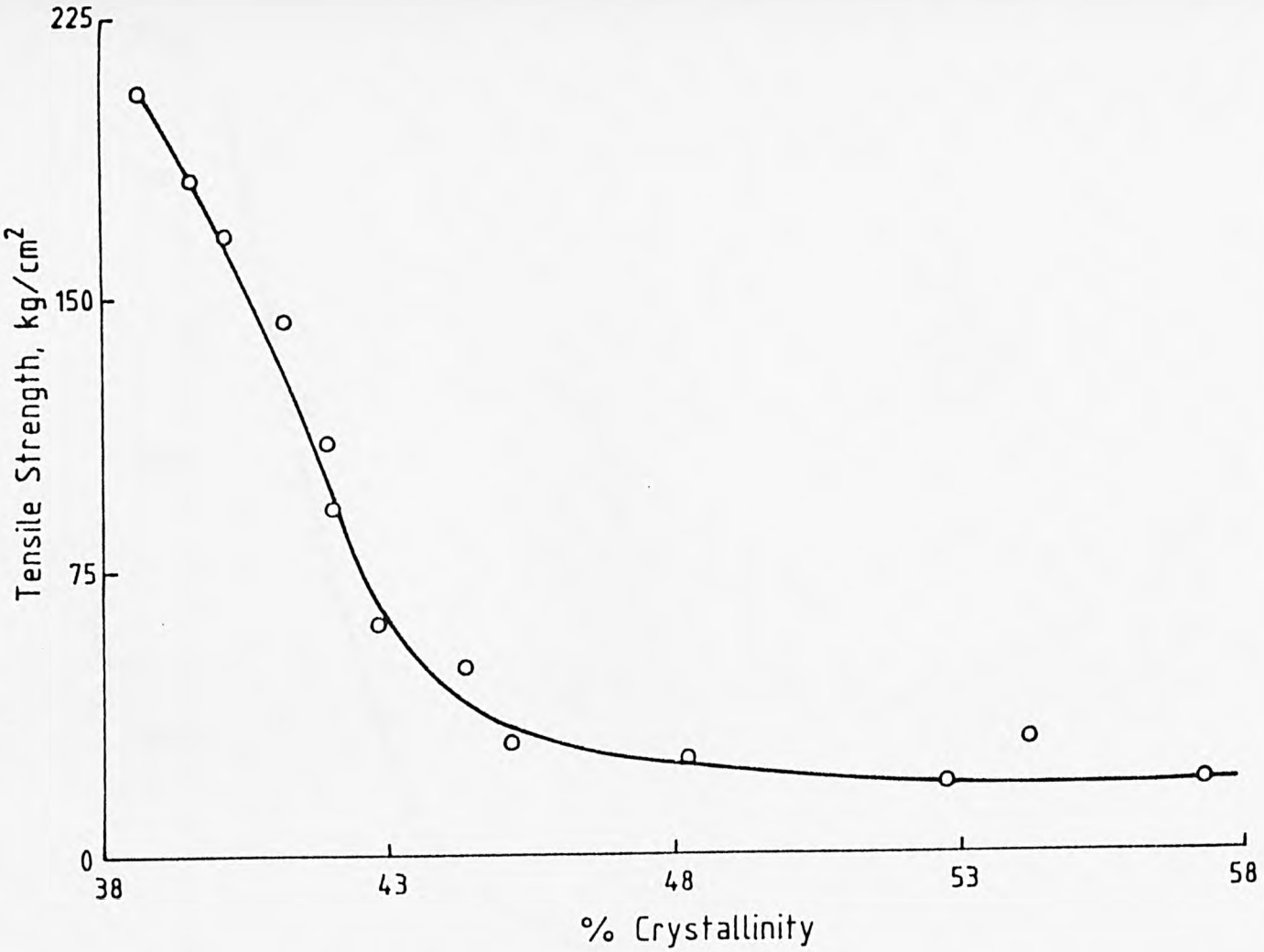

Figure 5.7. Change in crystallinity as a function of loss in tensile strength.

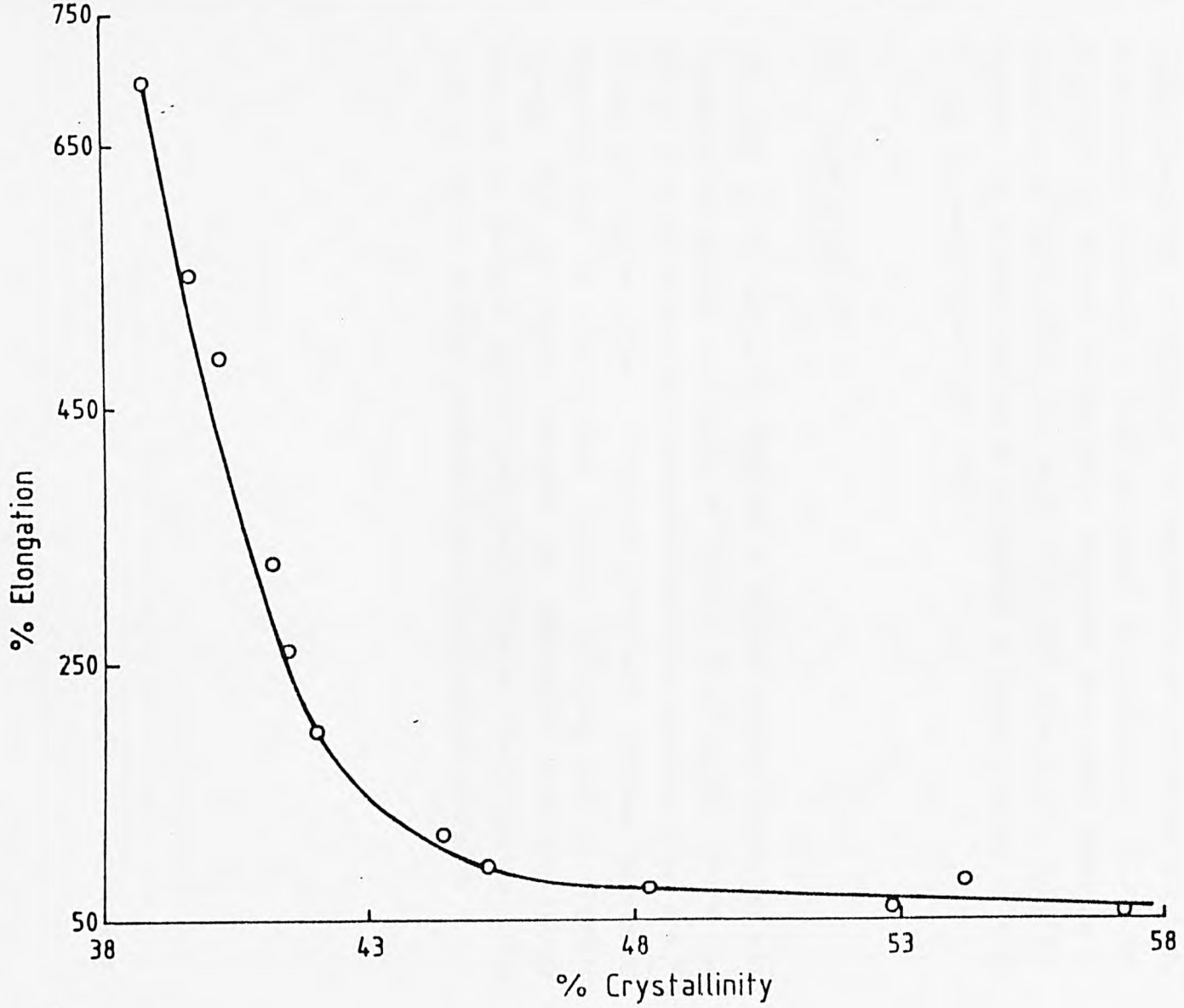

Figure 5.8. Change in crystallinity as a function of loss in % elongation.

the determination of breaking strength. With polyethylene, this fact is ascribed to the well-established process of cross-linking of polymer chains. Such cross-linking rends it more difficult for one chain to slip past another when mechanical stress is applied in tensile testing apparatus. The chain scission process also occurs, but at low exposures its intensity is not sufficient to be reliably monitored by breaking strength determinations. The percent elongation loss showed a slight initial elongation gain which according to Gottfried and Dutzer [1961], may be due to the early presence of crosslinking reactions and to slight increase of crystallinity of polymer caused by mild thermal treatment [Mlinac et al., 1976]

5.4 CONCLUSIONS

The study of the mechanical behavior of LLDPE samples unexposed and exposed in the natural environment of Dhahran, Saudi Arabia, reveals that the rate of decay in significant mechanical properties (tensile strength and % elongation) is higher. Increase in carbonyl groups with decreasing mechanical properties does not show a linear behavior indicating that the chemical changes does not directly influence the mechanical properties. Similar behavior of increased %crystallinity with decaying mechanical properties indicates that the process of secondary chemcrystallization takes place.

Chapter 6

MATHEMATICAL MODELING

6.1 INTRODUCTION

Models are representative of objects, processes, or systems that are to be described or whose patterns of behavior is to be analyzed. These models are mathematical if the representations are mathematical relationships. The mathematical model solution in many cases requires a computational/simulation approach. It is now widely acknowledged that, along with the traditional and theoretical methodologies, advanced work in various areas of science and engineering has come to rely critically on the computational/simulation approach [Al-Rabeh, 1988].

The weathering of plastics is dependent on almost all parameters of environment. The weather is so variable from time to time and from place to place that even comparison among outdoor tests obtained at different seasons, years, or locations have been inadequate. Mathematical approach in describing the weather-induced degradation of plastics is considered for the purpose of experimental data presentation, prediction, and understanding of this complex phenomena [Lindgren and McElrath, 1971].

The previous discussion on this subject has already elaborated that the weathering of plastic is inherently related to weather variables. Regression analysis is a statistical technique for modeling and investigating the relationship between the dependent and independent variables. Its broad appeal results from the conceptually simple process of using an equation to express the relationship between a set of variables. In the field of plastic weathering regression analysis can be used to build a model that expresses degradation in significant property of plastic as a function of weather parameters.

In this chapter statistical techniques will be used to determine the significant weather parameters influencing the decay in significant plastic properties.

Based on these parameters three different mathematical model will be developed representing the degradation in mechanical property (tensile strength), chemical property (carbonyl groups), and thermal property (percent crystallinity). Selection of weather parameter significant for specific model will be accomplished using the stepwise regression analysis technique [Hines and Montgomery, 1972]. Finally, mathematical models will be developed using multiple linear regression and residual analysis will also be presented to evaluate the goodness of fit. In the present analysis computation has been carried out using statistical analysis system (SAS) software package on mainframe IBM 3033 computer.

6.2 VARIABLE DESCRIPTION

The independent variables considered are the significant weather parameters. Mathematically:

$$\text{Degradation (DG)} = F\,(AT,AH,UV,CU,RD,CR) \qquad (1)$$

Where:
DG = Degradation of significant plastic property, AT = Average monthly temperature (^{o}C), AH = Average monthly relative humidity (%), UV = Average monthly UV Radiation dose (Langleys), CU = Cumulative monthly UV radiation (Langleys), RD = Average total solar radiation (Langleys), CR = Cumulative total solar radiation (Langleys).

The descriptive statistical analysis of weather data was carried out with the purpose of viewing the frequency distribution and determining some potential outliers which can misinterpret the total behavior [Beckman and Cook, 1983]. Frequency distribution and histograms of weather parameters are presented in Figures 6.1 to 6.6 for AT, AH, UV, CU, RD, and CR, respectively.

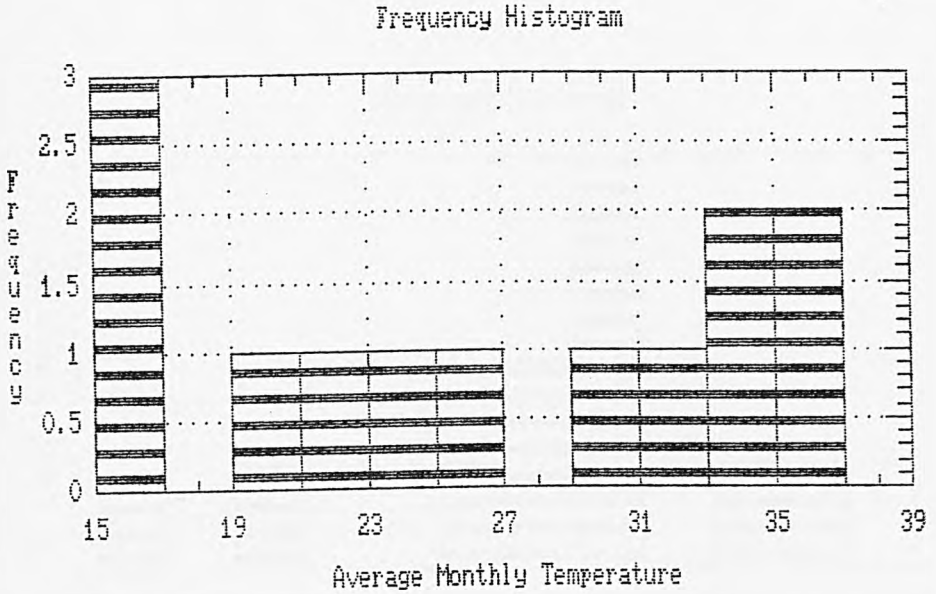

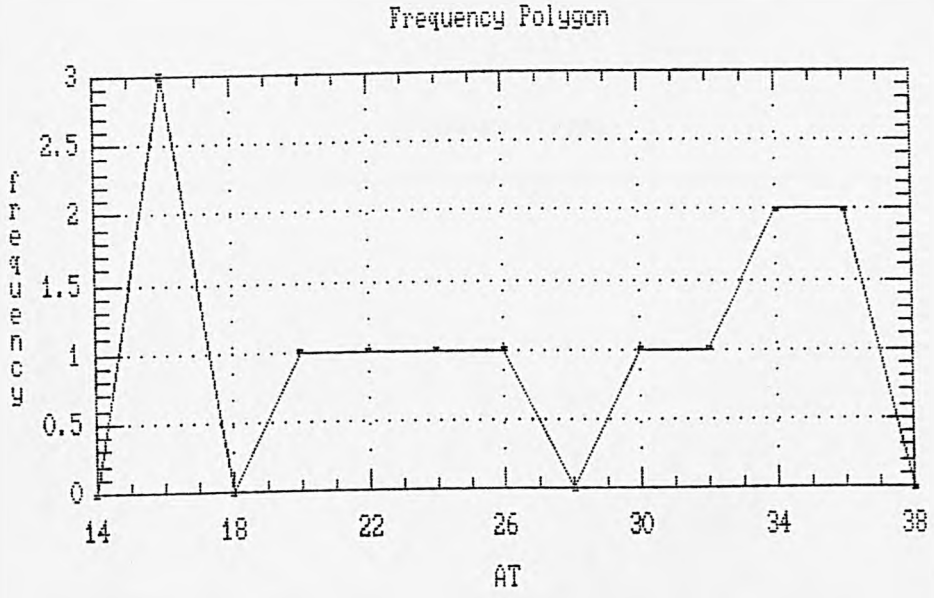

Figure 6.1. Frequency histogram and polygon of average monthly temperature (AT).

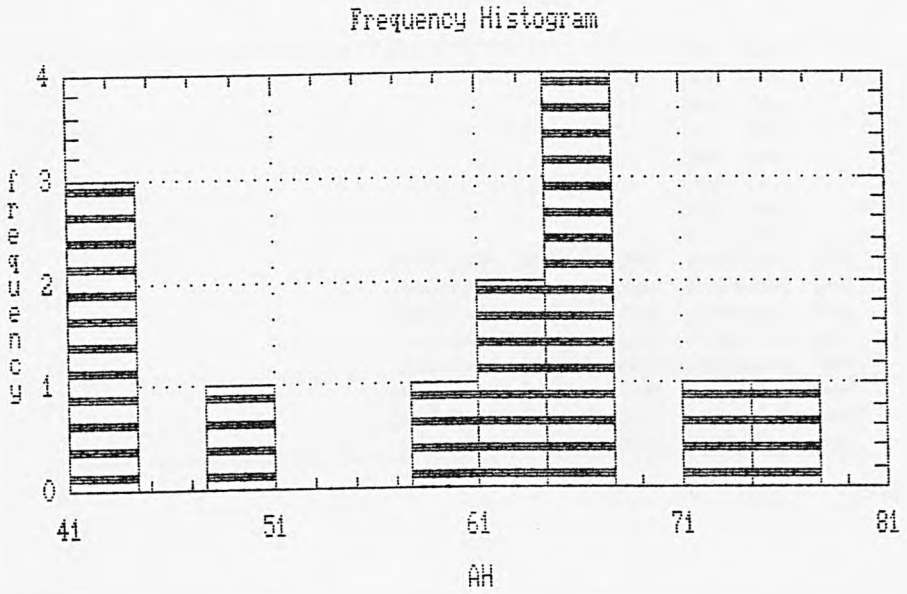

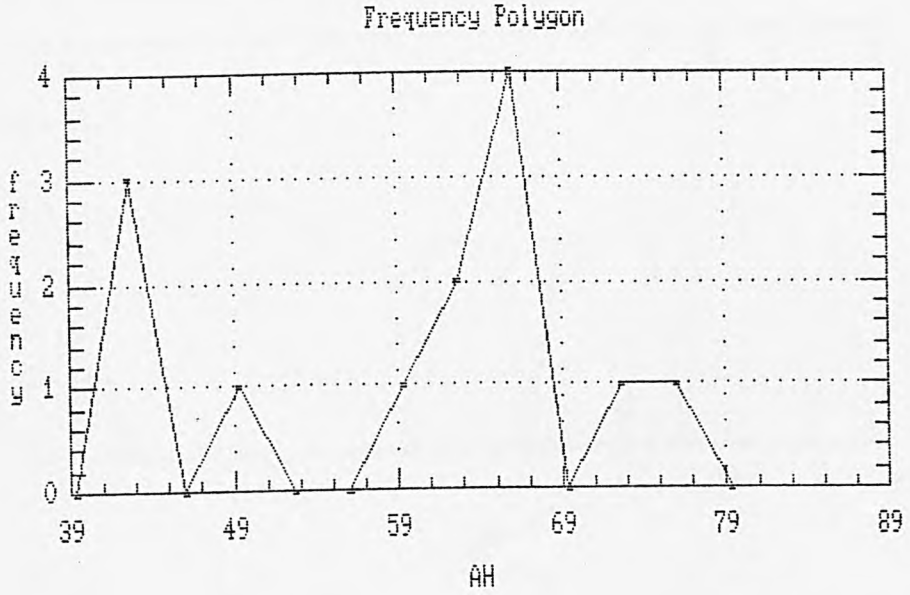

Figure 6.2. Frequency histogram and polygon of average monthly humidity (AH).

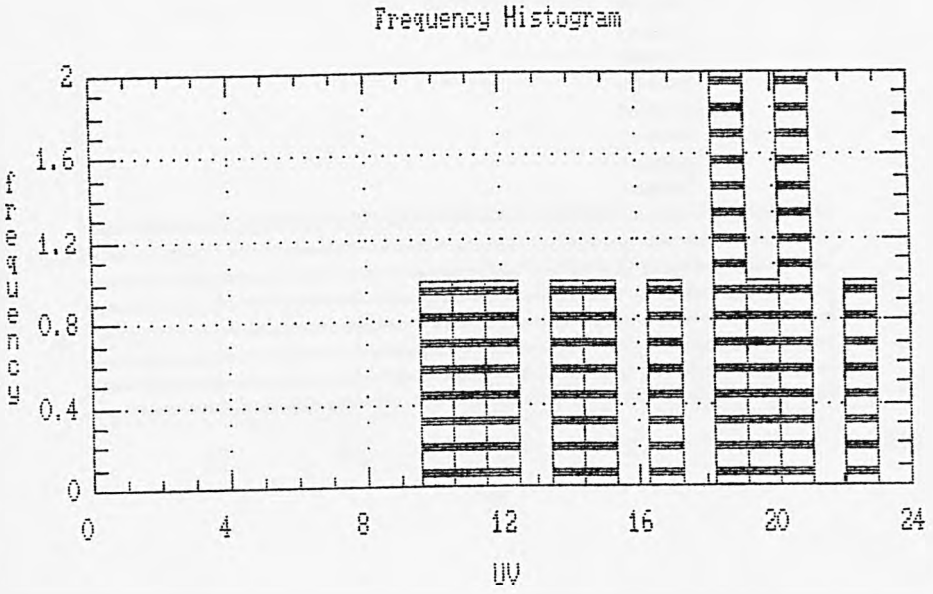

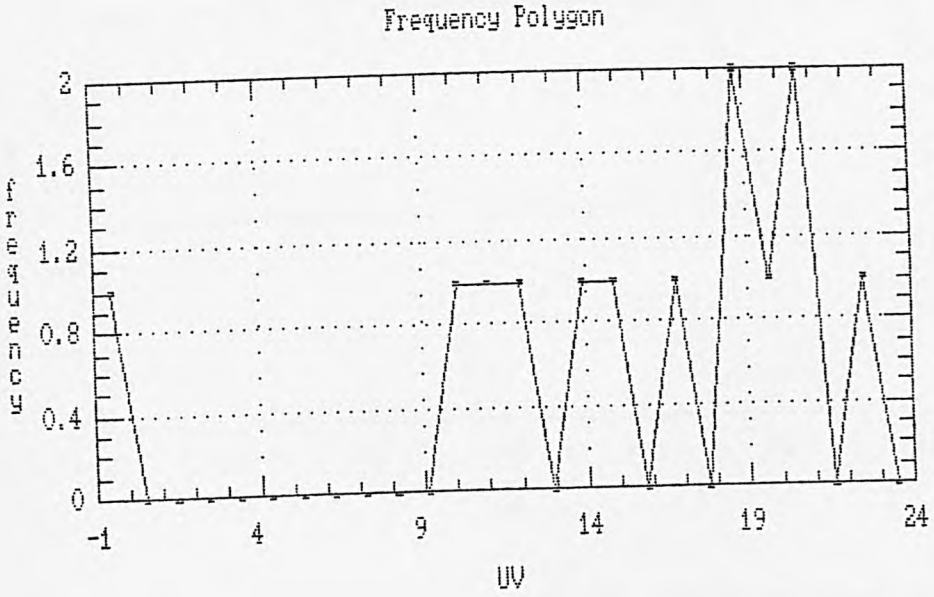

Figure 6.3. Frequency histogram and polygon of average monthly UV radiation (UV).

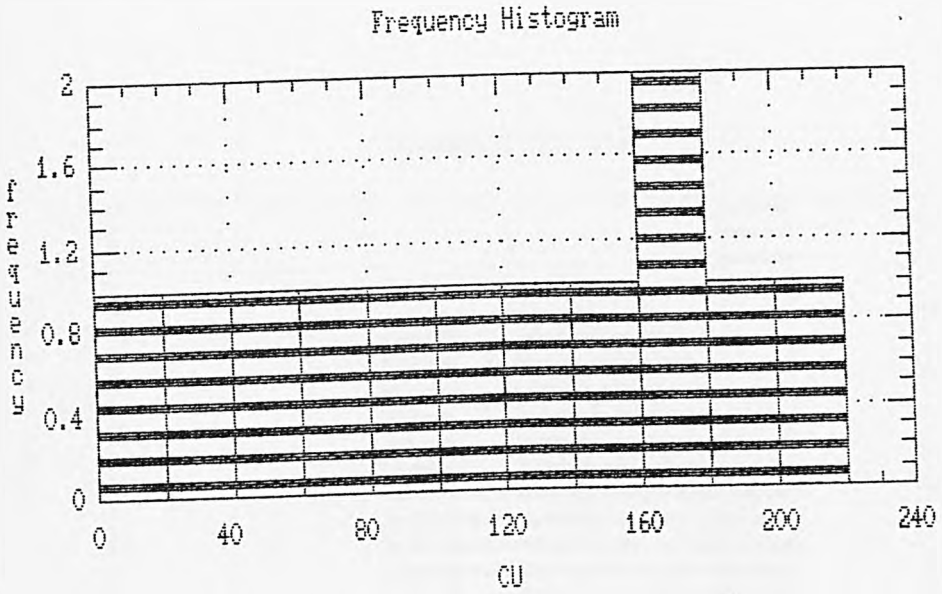

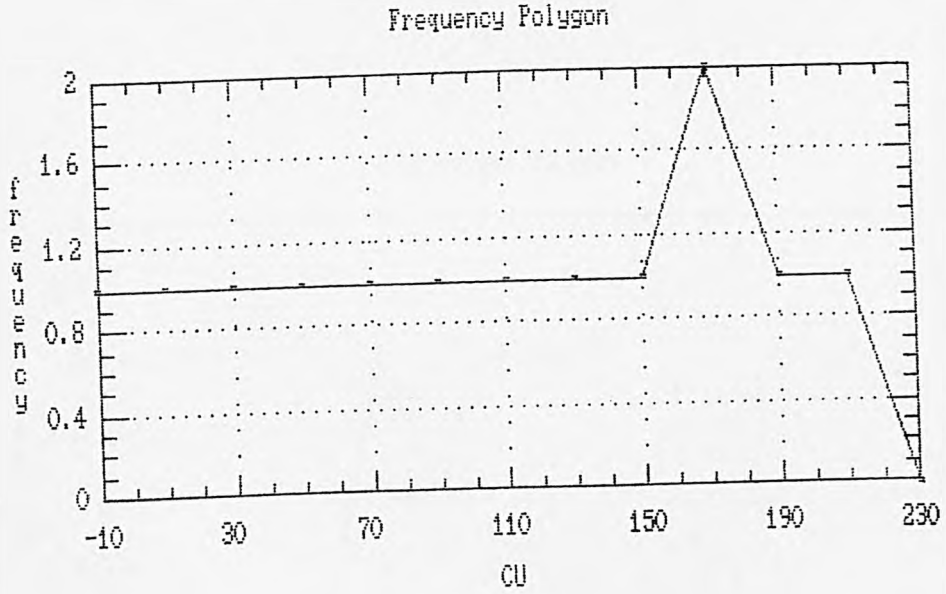

Figure 6.4. Frequency histogram and polygon of cumulative UV radiation (CU).

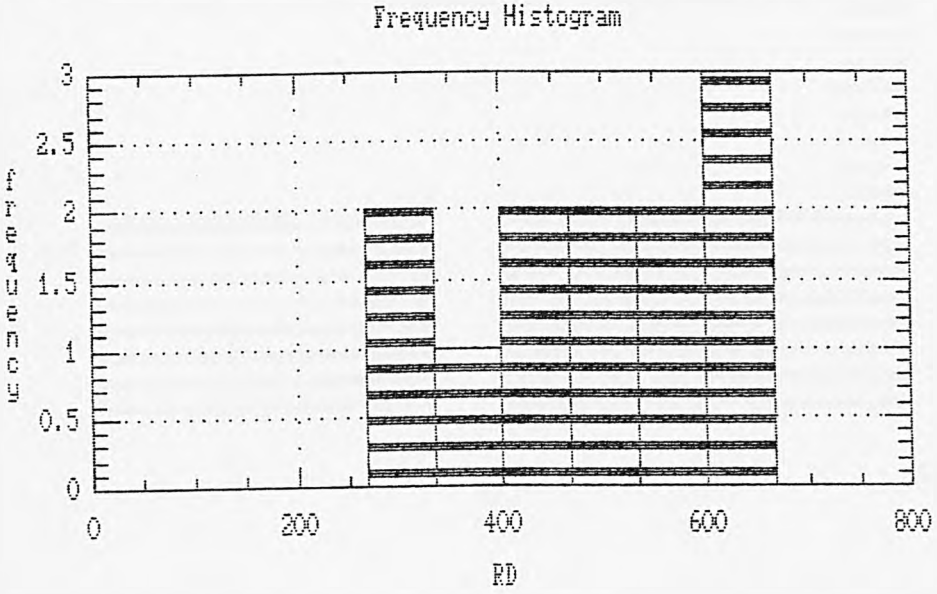

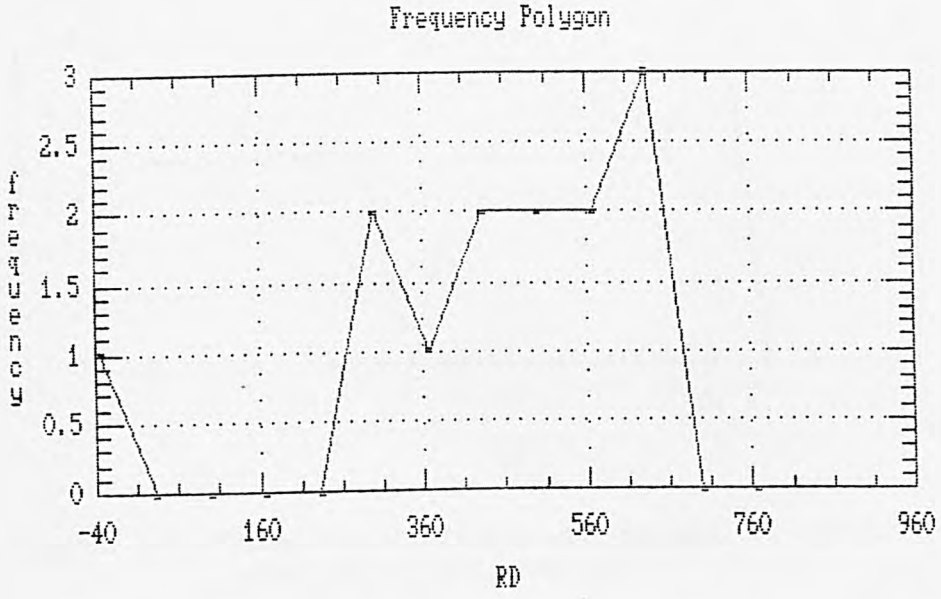

Figure 6.5. Frequency histogram and polygon of average monthly total solar radiation (RD).

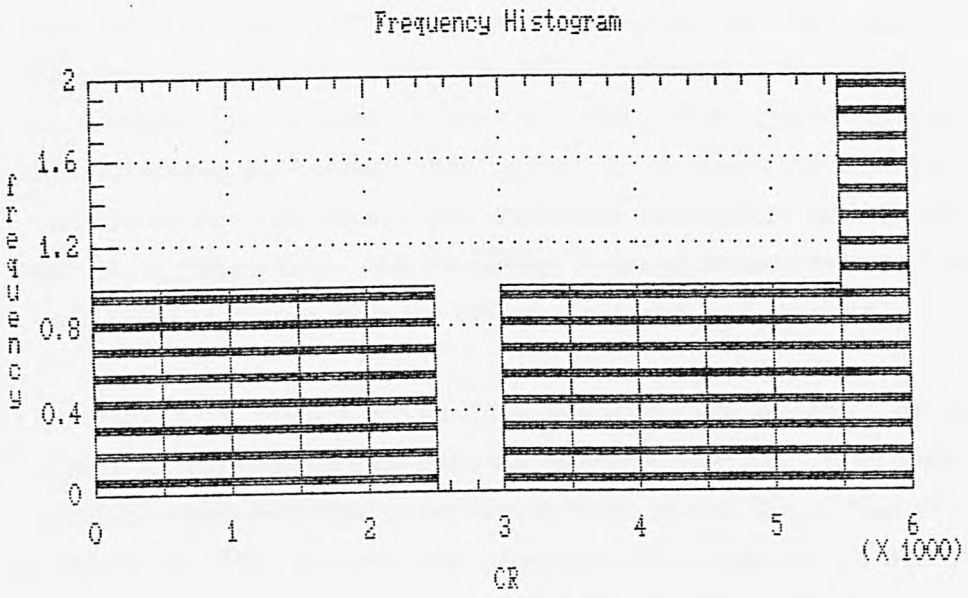

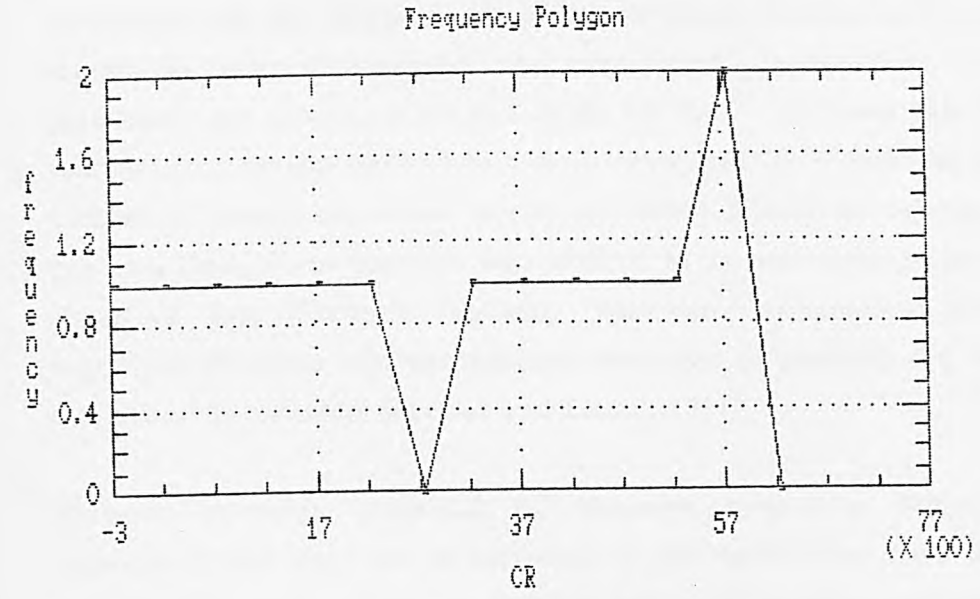

Figure 6.6. Frequency histogram and polygon of cumulative total solar radiation (cr).

6.3 VARIABLES SELECTION

The theoretical background of weather-induced degradation of polyethylene developed in the previous chapters indicate that the regressor variables (weather parameters) included are influential. Some of the weather parameters are deleted from the discussion either because of their insignificance or because their effect is incorporated in other parameters considered for this study. The discarded parameters include maximum and minimum temperature and humidity. Average temperature and humidity are considered to incorporate the effect of minima and maxima.

Building a regression model that includes only a subset of the available regressors involves two conflicting objectives. Firstly, it is desirable to have a model which includes as many regressors as possible so that the information content in these factors can influence the predicted values of dependent variable. Secondly, it is recommended to include as few regressors as possible because the variance of the prediction variable increases as the number of regressors increases. In this work effort is made to find a model that is a compromise between these two objectives.

The selection of variables considered significant for the mathematical model was based on the stepwise regression methods. Evaluation of all possible regressions for determining the significant independent variables is practically not possible [Cox and Snell, 1974]. To overcome this burdensome computation, various method have been developed for evaluating only a small number of subset regression models by either adding or deleting regressors one at a time. These methods are referred to as stepwise-type procedure and classified into forward selection, backward elimination and stepwise regression. Stepwise uses the selection strategies in choosing the variables for the models it considers [Freund and Littell, 1981].

Forward selection technique of stepwise procedure begins with the assumption that there are no regressors in the model other than the intercept. An effort is made to find an optimal subset by inserting regressors into the model one at a time. The first regressor selected for entry into the equation is the one that has the largest simple correlation with the response variable. The chosen regressor will produce the largest value of the F-statistics for testing

significance of regression. This regressor is entered if the F-statistics exceeds a preselected F-value, say F_{IN} (or F-to-enter). The second regressor chosen for entry is the one that now has the largest correlation with response variable after adjusting for the effect of the first regressor entered in the model. These correlation are referred as partial correlation. In general at each step the regressor having the highest partial correlation with response variable is added to the model if its partial F-statistics exceeds the preselected entry level F_{IN}. The procedure terminates either when the partial F-statistics at a particular step does not exceed F_{IN}, or when the last candidate regressor is added to the model [Montgomery and Peck, 1982].

Forward selections begin with no regressors in the model and attempts to insert variables until a suitable model is obtained. Backward elimination attempts to find a good model by working in the opposite direction. It begins with calculating statistics for a model including all of the independent variables. Then the partial F-statistics is computed for each regressor as if it were the last variable to enter the model. The smallest of these partial F-statistics is compared with a pre selected value, F_{OUT} (or F-to-remove), for example, and if the smallest partial F-value is less than F_{OUT} that regressor is removed from the model. Now a regression model with one less independent variable is fit, the partial F-statistics for this new model calculated, and the procedure repeated. The program terminates when the smallest partial F-value is not less than the preselected cutoff value F_{OUT}. Stepwise regression is a modification of forward selection in which at each step all regressors entered into the model previously are reassessed via their partial F-statistics. A regressor added at an early step may now be redundant because of the relationships between it and regressors now in equation. If the partial F-statistics for a variable is less than F_{OUT}, that variable is dropped from the model. Stepwise regression requires two cutoff values, F_{IN} and F_{OUT} [Montgomery and Peck, 1982].

The coefficient of multiple determination (R^2) has been widely used as a measure of the adequacy of a regression model. Generally it is not straight forward to use R^2 as a criterion for choosing the number of regressors to include in the model. However, for fixed number of variables, R^2 can be used to compare the generated models. Mallows has proposed a criterion that is related to the mean square error of fitted and is called Mallow's C_p

statistics [Mallows, 1973]. Generally small values of C_p are desirable, C_p value less than number of independent variables represent a model with lower total errors [Mallows, 1973]. The RSQUARE procedure of SAS was used to determine R^2 and Mallow's C_p statistics for each model. The program evaluates each combination of a dependent variable with the independent variables. If K independent variables are specified, the program evaluates each of the 2^{K-1} linear models: K of the models include one independent variable, K(K-1)/2 of the model include two independent variables, and so on. For each model evaluated, the program prints the unadjusted R^2 value and Mallow's C_p statistics [SAS, 1982].

6.4 MODEL I

Mechanical properties of plastics are an important ultimate indicators of plastic behavior when exposed to weather. Mathematically:

Degradation rate $\propto$ drop in mechanical properties

Therefore the dependence of mechanical property (tensile strength - TS) on weather parameters is presented in a functional relationship of the form:

TS = F(AT, AH, UV, CU, RD, CR).

6.4.1 Variable Selection

SAS stepwise regression algorithm was used and the results of forward selection procedure are presented in Figure 6.7. In this program cutoff value F_{IN} is specified by choosing a type I error rate α. Therefore, the regressor with highest partial correlation with dependent variable is added to the model if its partial F-statistics exceeds $F_{\alpha,1,n-p}$. In this work $\alpha = .05$ to determine F_{IN}. In Figure 6.7 it is shown in step 1 that the regressor most highly correlated with tensile strength of plastic is cumulative UV (CU). The F-statistics associated with the model using CU is $F = 178.29 > F_{.05,1,11} = 4.48$, CU is added to the equation. At step 2 the regressor having the largest partial correlation with TS (or the largest partial F statistic given that CU is

```
FORWARD SELECTION PROCEDURE FOR DEPENDENT VARIABLE TS

STEP 1    VARIABLE CU ENTERED          R SQUARE = 0.94188759
                                       C(P) =    236.76583913
                DF    SUM OF SQUARES  MEAN SQUARE        F   PROB>F
REGRESSION       1    51459.37660039  51459.37660   178.29   0.0001
ERROR           11     3174.93109192    288.63010
TOTAL           12    54634.30769231
                B VALUE    STD ERROR   TYPE II SS        F   PROB>F
INTERCEPT   180.2620773
CU           -0.9187786   0.06880966  51459.37660   178.29   0.0001
BOUNDS ON CONDITION NUMBER:             1,            1
-----------------------------------------------------------------
STEP 2    VARIABLE UV ENTERED          R SQUARE = 0.99635160
                                       C(P) =      8.42960718
                DF    SUM OF SQUARES  MEAN SQUARE        F   PROB>F
REGRESSION       2    54434.97999182  27217.49000  1365.46   0.0001
ERROR           10      199.32770049     19.93277
TOTAL           12    54634.30769231
                B VALUE    STD ERROR   TYPE II SS        F   PROB>F
INTERCEPT   214.5621089
UV           -2.6135216   0.21390572   2975.60339   149.28   0.0001
CU           -0.8574241   0.01876697  41607.39820  2087.39   0.0001
BOUNDS ON CONDITION NUMBER:     1.077119,     4.308475
-----------------------------------------------------------------
STEP 3    VARIABLE AT ENTERED          R SQUARE = 0.99843059
                                       C(P) =      1.63727803
                DF    SUM OF SQUARES  MEAN SQUARE        F   PROB>F
REGRESSION       3    54548.56387834  18182.85463  1908.54   0.0001
ERROR            9       85.74381397      9.52709
TOTAL           12    54634.30769231
                B VALUE    STD ERROR   TYPE II SS        F   PROB>F
INTERCEPT   220.5149542
AT           -0.5800969   0.16800505    113.58389    11.92   0.0072
UV           -2.1178201   0.20610607   1005.90465   105.58   0.0001
CU           -0.8425488   0.01367105  36186.53117  3798.28   0.0001
BOUNDS ON CONDITION NUMBER:     2.319667,     16.82329
-----------------------------------------------------------------
NO OTHER VARIABLES MET THE 0.0500 SIGNIFICANCE LEVEL FOR ENTRY
SUMMARY OF FORWARD SELECTION PROCEDURE FOR DEPENDENT VARIABLE TS
      VARIABLE  NUMBER     PARTIAL      MODEL
STEP  ENTERED       IN       R**2       R**2         C(P)
   1  CU               1     0.9419     0.9419      236.766
   2  UV               2     0.0545     0.9964        8.430
   3  AT               3     0.0021     0.9984        1.637
      VARIABLE
STEP  ENTERED          F     PROB>F   LABEL
   1  CU         178.2883     0.0001   CUMULATIVE UV RADIATION
   2  UV         149.2820     0.0001   UV RADIATION
   3  AT          11.9222     0.0072   MONTHLY AVERAGE TEMPERATURE
-----------------------------------------------------------------
```

Figure 6.7 Computer output (SAS) of stepwise forward selection procedure applied to LLDPE tensile strength data.

in the model) is UV, and since the partial F-statistics is F = 149.28 which exceeds $F_{IN} = F_{.05,1,10} = 4.96$, UV is added to the model. In the third step, AT exhibits the highest partial correlation with TS. The partial F statistic is 11.92 which is larger than $F_{IN} = F_{.05,1,9} = 5.12$, and so AT is added to the model. At this point the remaining candidate regressors are AH, RD, and CR, and for which the partial F-statistics does not exceed $F_{.05,1,8} = 5.32$, so the forward selection procedure terminates with

$$TS = 220.51 - 0.58\ AT - 2.12\ UV - 0.84\ CU$$

as the final model.

Backward elimination algorithm of SAS was also used and the results are presented in Figure 6.8. In this run, cutoff value F_{OUT} is chosen as $\alpha = .05$. Thus a regressor is dropped if its partial F-statistics is less than $F_{.05,\ 1,\ n-p}$. Step 0 shows the results of fitting the full model. The smallest partial F-value is F = 0.00 and it is associated with CR. Thus since $F = 0.00 < F_{OUT} = F_{.05,1,6} = 5.99$, CR is removed from the model. At step 1 the results of fitting five-variable model involving (AT, AH, RD, UV, CU) are presented. The smallest partial F-value in this model , F = 0.07, is associated with AH. Since $F = 0.07 < F_{OUT} = F_{.05,\ 1,\ 7} = 5.59$, AH is removed from the model. Similarly in step 2 RD is removed. At step 3 the results of fitting the three-variable model involving (AT, UV, CU) is shown. The smallest partial F-statistics in this model is F = 11.92, associated with AT, and since this exceeds $F_{.05,\ 1,\ 9} = 5.12$, no further regressor can be removed from the model. Therefore, backward elimination terminates, yielding the final model

$$TS = 220.51 - .58\ AT - 2.12\ UV - .84\ CU.$$

Figure 6.9 presents the results of using SAS stepwise regression algorithm. The α level for either adding or removing a regressor is specified as 0.05. At step 1, the procedure begins with no variables in the model and tries to add CU. Since the partial F-statistics at this step exceeds $F_{IN} = F_{.05,\ 1,\ 11} = 4.48$, CU is added to the model. At step 2 UV is added to the model and at step 3 AT is incorporated in the model. At this point the remaining candidate regressors are (RD, AH, CR), which cannot be added because its partial F-values does not exceed preset limits. Therefore stepwise regression terminates

```
BACKWARD ELIMINATION PROCEDURE FOR DEPENDENT VARIABLE TS

STEP 0    ALL VARIABLES ENTERED          R SQUARE = 0.99858127
                                         C(P) =      7.00000000
                DF     SUM OF SQUARES    MEAN SQUARE          F     PROB>F
REGRESSION       6     54556.79656782  9092.7994280     703.86     0.0001
ERROR            6        77.51112449    12.9185207
TOTAL           12     54634.30769231
                 B VALUE     STD ERROR    TYPE II SS          F     PROB>F
INTERCEPT  223.71602893
AT          -0.66596961    0.29662351    65.11941108       5.04     0.0659
AH          -0.03576751    0.21996207     0.34158168       0.03     0.8762
RD           0.06228173    0.14520012     2.37684146       0.18     0.6829
UV          -3.86652610    4.24373749    10.72402102       0.83     0.3974
CR          -0.00306899    0.19224686     0.00329220       0.00     0.9878
CU          -0.75164105    5.57965056     0.23443355       0.02     0.8972
BOUNDS ON CONDITION NUMBER:      147326.3,      1773238
-----------------------------------------------------------------------
STEP 1    VARIABLE CR REMOVED            R SQUARE = 0.99858121
                                         C(P) =      5.00025484
                DF     SUM OF SQUARES    MEAN SQUARE          F     PROB>F
REGRESSION       5     54556.79327562  10911.358655     985.36     0.0001
ERROR            7        77.51441669    11.073488
TOTAL           12     54634.30769231
                 B VALUE     STD ERROR    TYPE II SS          F     PROB>F
INTERCEPT  223.81007022
AT          -0.66446342    0.26036275     72.122188       6.51     0.0380
AH          -0.03818386    0.14776395      0.739447       0.07     0.8035
RD           0.06036701    0.07576728      7.029435       0.63     0.4518
UV          -3.80979869    2.14785921     34.839898       3.15     0.1194
CU          -0.84071275    0.02210916  16011.618821    1445.94     0.0001
BOUNDS ON CONDITION NUMBER:      203.4466,      2047.439
-----------------------------------------------------------------------
STEP 2    VARIABLE AH REMOVED            R SQUARE = 0.99856768
                                         C(P) =      3.05749415
                DF     SUM OF SQUARES    MEAN SQUARE          F     PROB>F
REGRESSION       4     54556.05382844  13639.013457    1394.34     0.0001
ERROR            8        78.25386387     9.781733
TOTAL           12     54634.30769231
                 B VALUE     STD ERROR    TYPE II SS          F     PROB>F
INTERCEPT  220.82661930
AT          -0.61758948    0.17554466    121.071055      12.38     0.0079
RD           0.06207538    0.07093946      7.489950       0.77     0.4071
UV          -3.86575104    2.00841490     36.239041       3.70     0.0904
CU          -0.84490637    0.01411211  35062.998573    3584.54     0.0001
BOUNDS ON CONDITION NUMBER:      201.8977,      1596.415
-----------------------------------------------------------------------
```

Figure 6.8. Computer output (SAS) of stepwise backward elimination procedure applied to LLDPE tensile strength data.

```
STEP 3    VARIABLE RD REMOVED          R SQUARE = 0.99843059
                                       C(P) =     1.63727803

                DF     SUM OF SQUARES   MEAN SQUARE         F     PROB>F
REGRESSION       3     54548.56387834  18182.854626   1908.54     0.0001
ERROR            9        85.74381397     9.527090
TOTAL           12     54634.30769231

                 B VALUE     STD ERROR     TYPE II SS         F     PROB>F
INTERCEPT  220.51495418
AT          -0.58009691    0.16800505     113.583887     11.92     0.0072
UV          -2.11782006    0.20610607    1005.904655    105.58     0.0001
CU          -0.84254882    0.01367105   36186.531173   3798.28     0.0001
BOUNDS ON CONDITION NUMBER:      2.319667,      16.82329
-----------------------------------------------------------------------
ALL VARIABLES IN THE MODEL ARE SIGNIFICANT AT THE 0.0500 LEVEL.
SUMMARY OF BACKWARD ELIMINATION PROCEDURE FOR DEPENDENT VARIABLE TS
        VARIABLE   NUMBER     PARTIAL      MODEL
STEP    REMOVED         IN       R**2       R**2         C(P)
   1    CR               5     0.0000     0.9986      5.00025
   2    AH               4     0.0000     0.9986      3.05749
   3    RD               3     0.0001     0.9984      1.63728
        VARIABLE
STEP    REMOVED            F       PROB>F    LABEL
   1    CR            0.0003       0.9878    CUMULATIVE RADIATION
   2    AH            0.0668       0.8035    MONTHLY AVERAGE HUMIDITY
   3    RD            0.7657       0.4071    TOTAL SOLAR RADIATION
-----------------------------------------------------------------------
```

Figure 6.8. (...Contd.)

Computer output (SAS) of stepwise backward elimination procedure applied to LLDPE tensile strength data.

```
STEPWISE REGRESSION PROCEDURE FOR DEPENDENT VARIABLE TS

STEP 1    VARIABLE CU ENTERED          R SQUARE = 0.94188759
                                       C(P) =    236.76583913
                DF  SUM OF SQUARES  MEAN SQUARE        F   PROB>F
REGRESSION       1  51459.37660039  51459.37660   178.29   0.0001
ERROR           11   3174.93109192    288.63010
TOTAL           12  54634.30769231
              B VALUE   STD ERROR   TYPE II SS        F   PROB>F
INTERCEPT  180.262077
CU          -0.918779  0.06880966  51459.37660   178.29   0.0001
BOUNDS ON CONDITION NUMBER:            1,            1
-----------------------------------------------------------------
STEP 2    VARIABLE UV ENTERED          R SQUARE = 0.99635160
                                       C(P) =     8.42960718
                DF  SUM OF SQUARES  MEAN SQUARE        F   PROB>F
REGRESSION       2  54434.97999182  27217.49000  1365.46   0.0001
ERROR           10    199.32770049     19.93277
TOTAL           12  54634.30769231
              B VALUE   STD ERROR   TYPE II SS        F   PROB>F
INTERCEPT  214.562109
UV          -2.613522  0.21390572   2975.60339   149.28   0.0001
CU          -0.857424  0.01876697  41607.39820  2087.39   0.0001
BOUNDS ON CONDITION NUMBER:     1.077119,     4.308475
-----------------------------------------------------------------
STEP 3    VARIABLE AT ENTERED          R SQUARE = 0.99843059
                                       C(P) =     1.63727803
                DF  SUM OF SQUARES  MEAN SQUARE        F   PROB>F
REGRESSION       3  54548.56387834  18182.85463  1908.54   0.0001
ERROR            9     85.74381397      9.52709
TOTAL           12  54634.30769231
              B VALUE   STD ERROR   TYPE II SS        F   PROB>F
INTERCEPT  220.514954
AT          -0.580097  0.16800505    113.58389    11.92   0.0072
UV          -2.117820  0.20610607   1005.90465   105.58   0.0001
CU          -0.842549  0.01367105  36186.53117  3798.28   0.0001

BOUNDS ON CONDITION NUMBER:     2.319667,     16.82329
-----------------------------------------------------------------
NO OTHER VARIABLES MET THE 0.0500 SIGNIFICANCE LEVEL FOR ENTRY
SUMMARY OF
STEPWISE REGRESSION PROCEDURE FOR DEPENDENT VARIABLE TS
          VARIABLE        NUMBER    PARTIAL     MODEL
STEP  ENTERED   REMOVED       IN      R**2      R**2        C(P)
   1  CU                      1    0.9419    0.9419     236.766
   2  UV                      2    0.0545    0.9964       8.430
   3  AT                      3    0.0021    0.9984       1.637
          VARIABLE
STEP  ENTERED   REMOVED          F            PROB>F
   1  CU                  178.2883            0.0001
   2  UV                  149.2820            0.0001
   3  AT                   11.9222            0.0072
-----------------------------------------------------------------
```

Figure 6.9 Computer output (SAS) of stepwise regression procedure applied to LLDPE tensile strength data.

with the model:

$$TS = 220.51 - .58\ AT - 2.12\ UV - .84\ CU.$$

It is noticed that the model developed by forward selection, backward elimination, and stepwise regression techniques have resulted in the same intercept, independent variables, and the coefficients of independent variables.

R^2 and Mallow's Cp values were determined using RSQUARE Procedure of SAS software package and the results are shown in Figure 6.10. It is obvious from the table that the best combination of R^2 and Mallow's Cp is for three variable model with AT, CU, UV as independent variables. The value of R^2 is .998 which is extremely good. The Cp value is 1.64 which is minimum of all combinations evaluated and also less than independent variables considered.

6.4.2 Regression Analysis

A multiple regression model was developed using SAS algorithm for the best subset regressor variables. The model incorporates these independent variables which are statistically selected in the previous section (UV, AT and CU) and the TS as dependent variable. The results are presented in Figure 6.11. This figure shows that the regression model is very significant and has a coefficient of variance (CV) of 3.6 and root mean square error of 3.09. The developed model is same as the one proposed by the different variable selection techniques:

$$TS = 220.52 - 0.58\ AT - 0.84\ CU - 2.12\ UV.$$

6.4.3 Residual Analysis

The functional form of the model presented earlier was used to predict the tensile strength (TS) and the results were compared to find the residuals. Residuals are defined as:

N=13 REGRESSION MODELS FOR DEPENDENT VARIABLE: TS
MODEL: MODEL1

NUMBER IN MODEL	R-SQUARE	C(P)	VARIABLES IN MODEL
1	0.04273724	4039.404	AH
1	0.23478987	3227.185	UV
1	0.25087678	3159.151	RD
1	0.32497833	2845.765	AT
1	0.93928701	247.764	CR
1	0.94188759	236.766	CU
2	0.28997257	2995.810	UV RD
2	0.33608978	2800.773	AT UV
2	0.33939210	2786.807	AT RD
2	0.39532613	2550.254	UV AH
2	0.41834753	2452.893	AH RD
2	0.69210519	1295.132	AT AH
2	0.96022382	161.219	AH CR
2	0.96137511	156.350	CU AH
2	0.97145251	113.731	CU CR
2	0.97956231	79.433970	AT CR
2	0.98001899	77.502590	AT CU
2	0.99561044	11.564077	RD CR
2	0.99603117	9.784754	CU RD
2	0.99603223	9.780297	UV CR
2	0.99635160	8.429607	CU UV
3	0.35679148	2715.223	AT UV RD
3	0.46363196	2263.379	UV AH RD
3	0.69647921	1278.634	AT UV AH
3	0.69785458	1272.817	AT AH RD
3	0.97199261	113.447	CU AH CR
3	0.98002991	79.456421	AT AH CR
3	0.98054565	77.275273	AT CU AH
3	0.98215082	70.486789	AT CU CR
3	0.99603963	11.748981	UV RD CR
3	0.99635165	10.429392	CU UV RD
3	0.99646937	9.931535	AH RD CR
3	0.99671527	8.891603	CU AH RD
3	0.99708236	7.339136	UV AH CR
3	0.99711775	7.189460	CU UV CR
3	0.99720840	6.806094	CU UV AH
3	0.99734192	6.241402	CU RD CR
3	0.99772904	4.604229	AT RD CR
3	0.99790438	3.862695	AT CU RD
3	0.99835219	1.968823	AT UV CR
3	0.99843059	1.637278	AT CU UV

Figure 6.10 Computer output (SAS) of RSQUARE and Mallow's Cp procedure applied to LLDPE tensile strength data.

4	0.70551227	1242.432	AT UV AH RD
4	0.98394298	64.907482	AT CU AH CR
4	0.99719686	8.854882	UV AH RD CR
4	0.99726112	8.583107	CU UV AH RD
4	0.99734420	8.231779	CU UV RD CR
4	0.99736602	8.139497	CU UV AH CR
4	0.99737298	8.110047	CU AH RD CR
4	0.99774982	6.516351	AT AH RD CR
4	0.99794352	5.697150	AT CU AH RD
4	0.99818515	4.675249	AT CU RD CR
4	0.99836034	3.934375	AT UV AH CR
4	0.99845255	3.544391	AT CU UV AH
4	0.99847154	3.464060	AT CU UV CR
4	0.99856768	3.057494	AT CU UV RD
4	0.99857478	3.027456	AT UV RD CR
5	0.99738936	10.040779	CU UV AH RD CR
5	0.99838499	5.830128	AT CU AH RD CR
5	0.99853777	5.183987	AT CU UV AH CR
5	0.99857502	5.026441	AT CU UV RD CR
5	0.99857698	5.018147	AT UV AH RD CR
5	0.99858121	5.000255	AT CU UV AH RD
6	0.99858127	7.000000	AT CU UV AH RD CR

Figure 6.10 (...contd.)

Computer output (SAS) of RSQUARE and Mallow's Cp procedure applied to LLDPE tensile strength data.

TENSILE STRENGTH MATHEMATICAL MODEL

GENERAL LINEAR MODELS PROCEDURE

DEPENDENT VARIABLE: TS TENSILE STRENGTH

SOURCE	DF	SUM OF SQUARES	MEAN SQUARE
MODEL	3	54548.56387834	18182.85462611
ERROR	9	85.74381397	9.52709044
CORRECTED TOTAL	12	54634.30769231	

MODEL F = 1908.54 PR > F = 0.0001

R-SQUARE	C.V.	ROOT MSE	TS MEAN
0.998431	3.5987	3.08659852	85.76923077

SOURCE	DF	TYPE I SS	F VALUE	PR > F
AT	1	17754.96599332	1863.63	0.0001
CU	1	35787.69323041	3756.41	0.0001
UV	1	1005.90465461	105.58	0.0001

SOURCE	DF	TYPE III SS	F VALUE	PR > F
AT	1	113.58388652	11.92	0.0072
CU	1	36186.53117283	3798.28	0.0001
UV	1	1005.90465461	105.58	0.0001

PARAMETER	ESTIMATE	T FOR H0: PARAMETER=0	PR > |T|	STD ERROR OF ESTIMATE
INTERCEPT	220.51495418	73.00	0.0001	3.02076942
AT	-0.58009691	-3.45	0.0072	0.16800505
CU	-0.84254882	-61.63	0.0001	0.01367105
UV	-2.11782006	-10.28	0.0001	0.20610607

Figure 6.11 Computer output (SAS) of general linear regression model procedure applied to LLDPE tensile strength data.

$$e_i = y_i - y_i', \qquad i = 1, 2 \ldots n$$

where y_i is an observation and y_i' is the corresponding fitted value. Since a residual may be viewed as the duration between the data and the fit it is a measure of the variability not explained by the model.

The adequacy of the model can be viewed from the plot of residual against predicted values of TS (Figure 6.12). This plot indicates that the residuals can be contained in a horizontal band. The scatter indicates no trend inequality of variance and, therefore, there is no obvious model defect.

Although small departures from normality do not affect the model greatly, gross nonnormality is potentially more serious. A very simple method of checking the normality assumption is to plot the residual on normal probability paper. Figure also shows the normal probability plot of residuals and cumulative percent which shows a reasonable straight line. Slight deviation from the straight line can be attributed to small number of observations (Daniel and Wood, 1980).

6.5 MODEL II

Growth in carbonyl group is an important indication of extent of degradation in polymers. In this section a linear multiple regression model will be developed with carbonyl growth as dependent variable and weather parameters as independent variables.

6.5.1 Variable Selection

Same procedures as used earlier for model I will be used. Figure 6.13 shows the results obtained when a SAS forward selection algorithm was applied to the data. In this program Cutoff value $\alpha = .05$ is specified. It is indicated in the results that most highly correlated regressor with carbonyl growth is CU, and since the statistics associated with the model using CU is F = 524.8 > which is greater than $F_{.05,\ 1,\ 11} = 4.48$, CU is added to the equation. At step 2 the regressor having the largest partial correlation with carbonyl growth is UV, and since the partial F-statistics for this regressor is 6.79 which exceeds

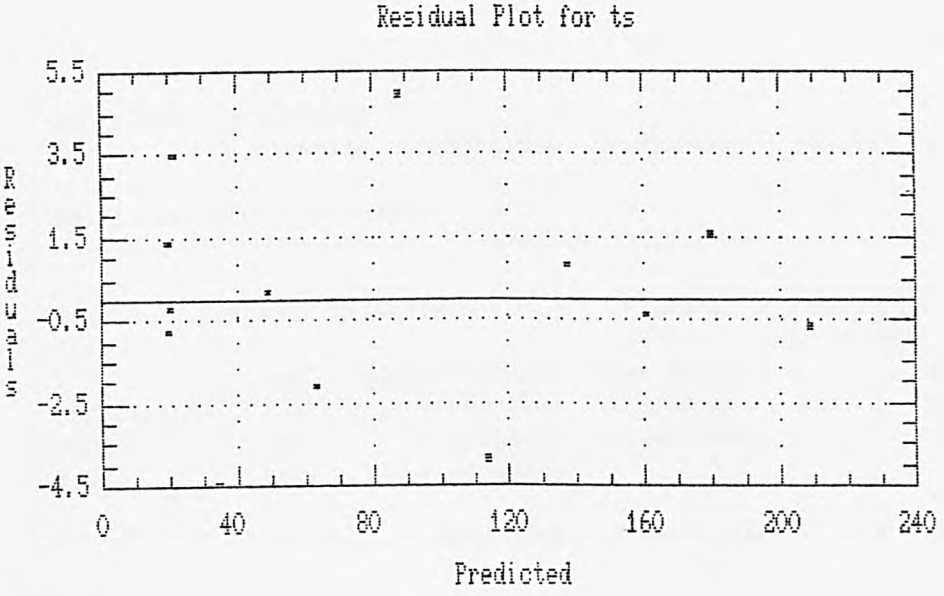

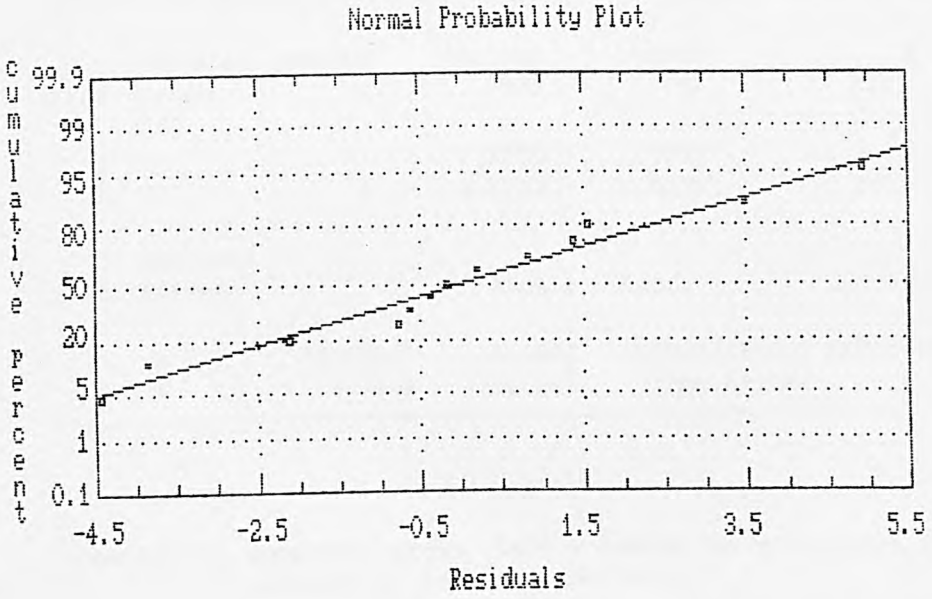

Figure 6.12. Residual and normal probability plot of LLDPE tensile strength model.

```
FORWARD SELECTION PROCEDURE FOR DEPENDENT VARIABLE CA

STEP 1    VARIABLE CU ENTERED          R SQUARE = 0.97945921
                                       C(P) =     11.80734240
                DF    SUM OF SQUARES  MEAN SQUARE        F   PROB>F
REGRESSION       1        7.23124189  7.23124189   524.52   0.0001
ERROR           11        0.15165042  0.01378640
TOTAL           12        7.38289231

                B VALUE    STD ERROR   TYPE II SS        F   PROB>F

INTERCEPT    0.44908868
CU           0.01089143   0.00047556   7.23124189   524.52   0.0001

BOUNDS ON CONDITION NUMBER:            1,            1
-----------------------------------------------------------------

STEP 2    VARIABLE UV ENTERED          R SQUARE = 0.98776628
                                       C(P) =      5.39247629
                DF    SUM OF SQUARES  MEAN SQUARE        F   PROB>F
REGRESSION       2        7.29257207  3.64628603   403.71   0.0001
ERROR           10        0.09032024  0.00903202
TOTAL           12        7.38289231

                B VALUE    STD ERROR   TYPE II SS        F   PROB>F

INTERCEPT    0.29336879
UV           0.01186522   0.00455335   0.06133017     6.79   0.0262
CU           0.01061289   0.00039949   6.37450356   705.77   0.0001

BOUNDS ON CONDITION NUMBER:     1.077119,     4.308475
-----------------------------------------------------------------

NO OTHER VARIABLES MET THE 0.0500 SIGNIFICANCE LEVEL FOR ENTRY

SUMMARY OF FORWARD SELECTION PROCEDURE FOR DEPENDENT VARIABLE CA

     VARIABLE  NUMBER     PARTIAL      MODEL
STEP ENTERED       IN       R**2        R**2          C(P)

   1 CU             1      0.9795      0.9795       11.8073
   2 UV             2      0.0083      0.9878        5.3925

     VARIABLE
STEP ENTERED          F     PROB>F   LABEL

   1 CU         524.5199     0.0001   CUMULATIVE UV RADIATION
   2 UV           6.7903     0.0262   UV RADIATION
-----------------------------------------------------------------
```

Figure 6.13 Computer output (SAS) stepwise forward selection procedure applied to LLDPE carbonyl data.

$F_{IN} = F_{.05,\ 1,\ 10} = 4.96$, UV is added to the model. At this point the partial F-statistics $F_{IN} = F_{.05,\ 1,\ 9} = 5.12$ exceeds F-value of all regressor so the forward selection terminates with

$$CA = 0.29 + .012\ UV + .01\ CU$$

as the final model.

The results of backward elimination procedure for dependent variable CA are presented in Figure 6.14. Step O shows the results of fitting the full model. The smallest partial F-value is F = 0.18 and it is associated with AH. Thus since $F = 0.18 < F_{OUT} = F_{.05,\ 1,\ 6} = 5.99$, AH is removed from the model. At step 1 the results of fitting the five - variables involving (AT, RD, UV, CR, CU) are shown. The smallest partial F-value in this model, $F = 0.88 < F_{OUT} = F_{.05,\ 1,\ 7} = 5.59$, AT is removed from the model. At step 2, the results of fitting the four-variable model is shown. The smallest partial F-statistics in this model is F = 3.90, associated with CU, and since this is less than $F_{OUT} = F_{.05,\ 1,\ 8} = 5.32$, CU is removed from the model. Similarly RD is also removed and finally backward elimination terminates, yielding the final model

$$CA = 0.287 + .012UV + .0004\ CR$$

SAS stepwise regression algorithm was used for stepwise regression and the results are presented in Figure 6.15. At step 1, the procedure begins with no variables in the model and tries to add CU. Since the partial F-statistics at this step exceeds $F_{IN} = F_{.05,\ 1,\ 11} = 3.23$, CU is added to the model. Similarly UV is also added and for the other candidate regressor F-value were found lower than F_{IN}. Therefore, the regression terminates with the model

$$CA = .29 + .012\ UV + .01\ CU.$$

R^2 and Mallow's C_p was determined for each combination of independent variable using SAS algorithm. The results are presented in Figure 6.16. Analyzing the results indicates that the R^2 value is within reasonable limits. Mallow's C_p is less than the number of parameters is only at one point when the number of parameters is 4 (CU, UV, RD, CR), CP = 3.95 and $R^2 = 0.993$.

```
BACKWARD ELIMINATION PROCEDURE FOR DEPENDENT VARIABLE CA

STEP 0    ALL VARIABLES ENTERED          R SQUARE = 0.99407686
                                         C(P) =      7.00000000
                DF   SUM OF SQUARES  MEAN SQUARE        F   PROB>F
REGRESSION       6      7.33916243   1.22319374   167.83   0.0001
ERROR            6      0.04372988   0.00728831
TOTAL           12      7.38289231

                B VALUE   STD ERROR   TYPE II SS        F   PROB>F
INTERCEPT -0.00504506
AT         0.00676125  0.00704551   0.00671206     0.92   0.3743
AH         0.00221525  0.00522462   0.00131028     0.18   0.6863
RD        -0.00495549  0.00344885   0.01504707     2.06   0.2008
UV         0.15926972  0.10079886   0.01819626     2.50   0.1652
CR         0.00540511  0.00456632   0.01021182     1.40   0.2813
CU        -0.14677233  0.13252997   0.00893896     1.23   0.3105

BOUNDS ON CONDITION NUMBER:     147326.3,      1773238
-----------------------------------------------------------------
STEP 1    VARIABLE AH REMOVED            R SQUARE = 0.99389939
                                         C(P) =      5.17977833
                DF   SUM OF SQUARES  MEAN SQUARE        F   PROB>F
REGRESSION       5      7.33785215   1.46757043   228.09   0.0001
ERROR            7      0.04504016   0.00643431
TOTAL           12      7.38289231

                B VALUE   STD ERROR   TYPE II SS        F   PROB>F
INTERCEPT  0.12690454
AT         0.00598345  0.00639156   0.00563887     0.88   0.3804
RD        -0.00583890  0.00258235   0.03289531     5.11   0.0582
UV         0.18560547  0.07459217   0.03983795     6.19   0.0417
CR         0.00673744  0.00311307   0.03013796     4.68   0.0672
CU        -0.18531251  0.09062080   0.02690640     4.18   0.0801

BOUNDS ON CONDITION NUMBER:     77803.07,      780913.6
-----------------------------------------------------------------
STEP 2    VARIABLE AT REMOVED            R SQUARE = 0.99313561
                                         C(P) =      3.95346438
                DF   SUM OF SQUARES  MEAN SQUARE        F   PROB>F
REGRESSION       4      7.33221329   1.83305332   289.36   0.0001
ERROR            8      0.05067902   0.00633488
TOTAL           12      7.38289231

                B VALUE   STD ERROR   TYPE II SS        F   PROB>F
INTERCEPT  0.22089466
RD        -0.00432837  0.00200054   0.02965469     4.68   0.0624
UV         0.14389686  0.05936060   0.03722583     5.88   0.0416
CR         0.00466888  0.00217586   0.02916771     4.60   0.0642
CU        -0.12503730  0.06327470   0.02473758     3.90   0.0836
BOUNDS ON CONDITION NUMBER:     38526.95,      310085.9
-----------------------------------------------------------------
```

Figure 6.14 Computer output (SAS) of stepwise backward elimination procedure applied to LLDPE carbonyl data.

```
STEP 3    VARIABLE CU REMOVED          R SQUARE = 0.98978495
                                       C(P) =     5.34760840
                DF  SUM OF SQUARES  MEAN SQUARE        F   PROB>F
REGRESSION       3      7.30747570   2.43582523   290.68   0.0001
ERROR            9      0.07541660   0.00837962
TOTAL           12      7.38289231
              B VALUE   STD ERROR   TYPE II SS        F   PROB>F
INTERCEPT  0.28988999
RD        -0.00242046  0.00201517   0.01208924     1.44   0.2604
UV         0.08188589  0.05795221   0.01673025     2.00   0.1913
CR         0.00036922  0.00001374   6.05102943   722.11   0.0001

BOUNDS ON CONDITION NUMBER:     190.1819,     1138.214
-----------------------------------------------------------------
STEP 4    VARIABLE RD REMOVED          R SQUARE = 0.98814748
                                       C(P) =     5.00632471
                DF  SUM OF SQUARES  MEAN SQUARE        F   PROB>F
REGRESSION       2      7.29538646   3.64769323   416.85   0.0001
ERROR           10      0.08750585   0.00875058
TOTAL           12      7.38289231
              B VALUE   STD ERROR   TYPE II SS        F   PROB>F
INTERCEPT  0.28718989
UV         0.01247726  0.00447577   0.06800499     7.77   0.0192
CR         0.00036473  0.00001351   6.37731796   728.79   0.0001

BOUNDS ON CONDITION NUMBER:     1.074197,     4.296789
-----------------------------------------------------------------
ALL VARIABLES IN THE MODEL ARE SIGNIFICANT AT THE 0.0500 LEVEL.

SUMMARY OF
BACKWARD ELIMINATION PROCEDURE FOR DEPENDENT VARIABLE CA

      VARIABLE  NUMBER      PARTIAL      MODEL
STEP  REMOVED       IN        R**2        R**2         C(P)
   1  AH               5      0.0002      0.9939      5.17978
   2  AT               4      0.0008      0.9931      3.95346
   3  CU               3      0.0034      0.9898      5.34761
   4  RD               2      0.0016      0.9881      5.00632
      VARIABLE
STEP  REMOVED          F    PROB>F  LABEL
   1  AH          0.1798    0.6863  MONTHLY AVERAGE HUMIDITY
   2  AT          0.8764    0.3804  MONTHLY AVERAGE TEMPERATURE
   3  CU          3.9050    0.0836  CUMULATIVE UV RADIATION
   4  RD          1.4427    0.2604  TOTAL SOLAR RADIATION
-----------------------------------------------------------------
```

Figure 6.14 (...contd)
Computer output (SAS) of stepwise backward elimination procedure applied to LLDPE carbonyl data.

```
STEPWISE REGRESSION PROCEDURE FOR DEPENDENT VARIABLE CA

STEP 1    VARIABLE CU ENTERED          R SQUARE = 0.97945921
                                       C(P) =     11.80734240
                DF  SUM OF SQUARES  MEAN SQUARE        F   PROB>F
REGRESSION       1      7.23124189   7.23124189   524.52   0.0001
ERROR           11      0.15165042   0.01378640
TOTAL           12      7.38289231

              B VALUE   STD ERROR   TYPE II SS        F   PROB>F
INTERCEPT  0.44908868
CU         0.01089143  0.00047556   7.23124189   524.52   0.0001

BOUNDS ON CONDITION NUMBER:            1,            1
----------------------------------------------------------------

STEP 2    VARIABLE UV ENTERED          R SQUARE = 0.98776628
                                       C(P) =      5.39247629
                DF  SUM OF SQUARES  MEAN SQUARE        F   PROB>F
REGRESSION       2      7.29257207   3.64628603   403.71   0.0001
ERROR           10      0.09032024   0.00903202
TOTAL           12      7.38289231

              B VALUE   STD ERROR   TYPE II SS        F   PROB>F
INTERCEPT  0.29336879
UV         0.01186522  0.00455335   0.06133017     6.79   0.0262
CU         0.01061289  0.00039949   6.37450356   705.77   0.0001

BOUNDS ON CONDITION NUMBER:     1.077119,     4.308475
----------------------------------------------------------------

NO OTHER VARIABLES MET THE 0.0500 SIGNIFICANCE LEVEL FOR ENTRY

SUMMARY OF
STEPWISE REGRESSION PROCEDURE FOR DEPENDENT VARIABLE CA

          VARIABLE        NUMBER   PARTIAL    MODEL
STEP  ENTERED   REMOVED       IN     R**2      R**2        C(P)
   1  CU                      1    0.9795    0.9795     11.8073
   2  UV                      2    0.0083    0.9878      5.3925

          VARIABLE
STEP  ENTERED   REMOVED          F          PROB>F
   1  CU                 524.5199          0.0001
   2  UV                   6.7903          0.0262

          VARIABLE
STEP  ENTERED   REMOVED   LABEL
   1  CU                 CUMULATIVE UV RADIATION
   2  UV                 UV RADIATION
```

Figure 6.15 Computer output (SAS) of stepwise regression procedure applied to LLDPE carbonyl data.

N=13 REGRESSION MODELS FOR DEPENDENT VARIABLE: CA
MODEL: MODEL1

NUMBER IN MODEL	R-SQUARE	C(P)	VARIABLES IN MODEL
1	0.12435079	878.012	UV
1	0.12548598	876.862	AH
1	0.13525087	866.971	RD
1	0.18936007	812.160	AT
1	0.97893633	12.337015	CR
1	0.97945921	11.807342	CU
2	0.17018348	833.585	UV RD
2	0.19244490	811.035	AT UV
2	0.19427626	809.180	AT RD
2	0.38343679	617.564	UV AH
2	0.40230088	598.455	AH RD
2	0.67246416	324.786	AT AH
2	0.97896469	14.308279	AH CR
2	0.97957215	13.692939	CU AH
2	0.98041009	12.844124	CU CR
2	0.98094481	12.302463	AT CR
2	0.98101096	12.235461	AT CU
2	0.98720821	5.957790	CU RD
2	0.98751887	5.643099	RD CR
2	0.98776628	5.392476	CU UV
2	0.98814748	5.006325	UV CR
3	0.21219935	793.024	AT UV RD
3	0.44469444	557.512	UV AH RD
3	0.67257128	326.678	AT UV AH
3	0.67283251	326.413	AT AH RD
3	0.98102544	14.220796	AT CU CR
3	0.98262385	12.601638	CU AH CR
3	0.98528621	9.904726	AT AH CR
3	0.98557321	9.614007	AT CU AH
3	0.98809344	7.061071	CU RD CR
3	0.98826054	6.891804	AT CU RD
3	0.98839248	6.758148	AT RD CR
3	0.98889384	6.250283	AT CU UV
3	0.98910196	6.039460	AT UV CR
3	0.98911894	6.022265	CU UV CR
3	0.98918490	5.955448	CU UV RD
3	0.98978495	5.347608	UV RD CR
3	0.99112755	3.987586	AH RD CR
3	0.99123967	3.874009	CU AH RD
3	0.99173196	3.375336	UV AH CR
3	0.99176567	3.341189	CU UV AH

Figure 6.16 Computer output (SAS) of RSQUARE and Mallow's Cp procedure applied LLDPE carbonyl data.

4	0.67964305	321.514	AT UV AH RD
4	0.98647559	10.699915	AT CU AH CR
4	0.98850341	8.645783	AT CU RD CR
4	0.98944378	7.693211	AT CU UV CR
4	0.98981725	7.314887	AT CU UV RD
4	0.99025496	6.871496	AT UV RD CR
4	0.99134695	5.765336	CU AH RD CR
4	0.99146015	5.650669	AT AH RD CR
4	0.99154803	5.561649	AT CU AH RD
4	0.99176875	5.338070	CU UV AH CR
4	0.99201954	5.084024	AT UV AH CR
4	0.99203873	5.064580	AT CU UV AH
4	0.99232020	4.779458	CU UV AH RD
4	0.99246396	4.633832	UV AH RD CR
4	0.99313561	3.953464	CU UV RD CR
5	0.99161221	7.496636	AT CU AH RD CR
5	0.99203876	7.064547	AT CU UV AH CR
5	0.99269369	6.401123	AT CU UV AH RD
5	0.99286610	6.226479	AT UV AH RD CR
5	0.99316773	5.920934	CU UV AH RD CR
5	0.99389939	5.179778	AT CU UV RD CR
6	0.99407686	7.000000	AT CU UV AH RD CR

Figure 6.16 (...contd.)

Computer output (SAS) of RSQUARE and Mallow's Cp procedure applied LLDPE carbonyl data.

The results indicated by forward backward and stepwise do not show a common selection trend. R^2 and Mallow's CP results are also different which is not unusual [Berk, 1978]. In order to have the model which include all those independent variable which are suggested by different methods, all the variable selected were incorporated in the final model. These independent variables are , CU, UV, RD, CR.

6.5.2 Regression Analysis

Based on weather parameters selected in the previous section, a regression model was developed for growth in carbonyl peaks as a function of these variables. The results of general linear models procedure of SAS are shown in Figure 6.17. The figure indicates a coefficient of variance (CV) = 5.07 and root mean square error of .08. Both of these values indicates that the developed model is reliable. The developed model is:

$$CA = 0.22 - 0.125\ CU + 0.144\ UV - 0.004\ RD + 0.005\ CR.$$

6.5.3 Residual Analysis

The adequacy of the model is very well exhibited by the plot of residuals against predicted values (Figure 6.18). The scatter indicates no trends or curvature and inequality of variance also indicates a reasonably good straight line. A slight deviation from straight line can be attributed to small number of observations. This implies that there are no obvious defects in the developed model.

6.6 MODEL III

The percent crystallinity (CY) of polyethylene is observed to increase with the exposure of polymer to the natural environment. In this section a regression model will be developed to present the correlation between crystallinity and weather parameters.

CARBONYL GROUP MATHEMATICAL MODEL

GENERAL LINEAR MODELS PROCEDURE

DEPENDENT VARIABLE: CA CARBONYL GROWTH

SOURCE	DF	SUM OF SQUARES	MEAN SQUARE
MODEL	4	7.33221329	1.83305332
ERROR	8	0.05067902	0.00633488
CORRECTED TOTAL	12	7.38289231	

MODEL F = 289.36 PR > F = 0.0001

R-SQUARE	C.V.	ROOT MSE	CA MEAN
0.993136	5.0720	0.07959195	1.56923077

SOURCE	DF	TYPE I SS	F VALUE	PR > F
CU	1	7.23124189	1141.50	0.0001
UV	1	0.06133017	9.68	0.0144
RD	1	0.01047351	1.65	0.2345
CR	1	0.02916771	4.60	0.0642

SOURCE	DF	TYPE III SS	F VALUE	PR > F
CU	1	0.02473758	3.90	0.0836
UV	1	0.03722583	5.88	0.0416
RD	1	0.02965469	4.68	0.0624
CR	1	0.02916771	4.60	0.0642

PARAMETER	ESTIMATE	T FOR H0: PARAMETER=0	PR > |T|	STD ERROR OF ESTIMATE
INTERCEPT	0.22089466	3.03	0.0164	0.07294617
CU	-0.12503730	-1.98	0.0836	0.06327470
UV	0.14389686	2.42	0.0416	0.05936060
RD	-0.00432837	-2.16	0.0624	0.00200054
CR	0.00466888	2.15	0.0642	0.00217586

Figure 6.17 Computer output (SAS) of general linear model procedure applied to LLDPE carbonyl data.

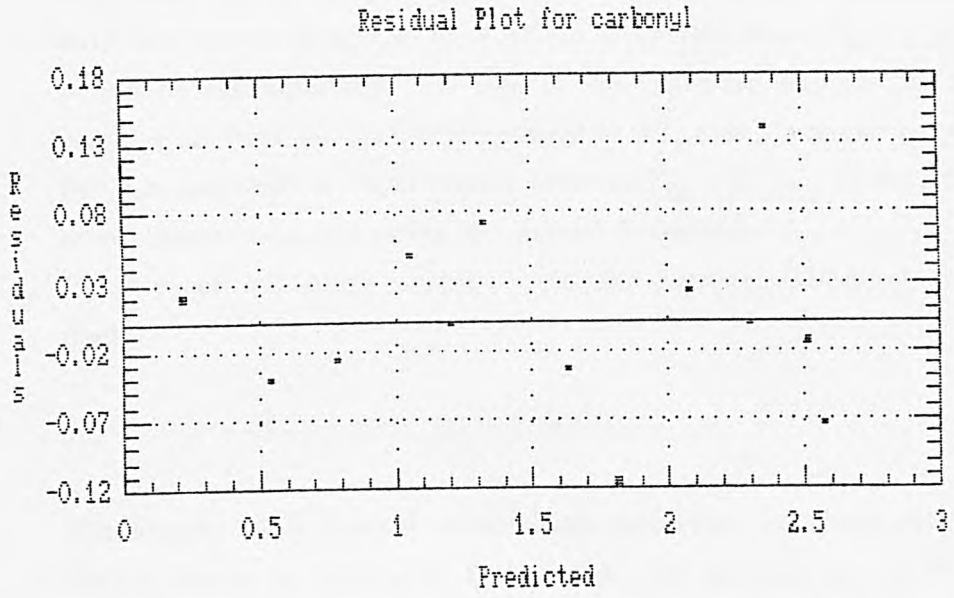

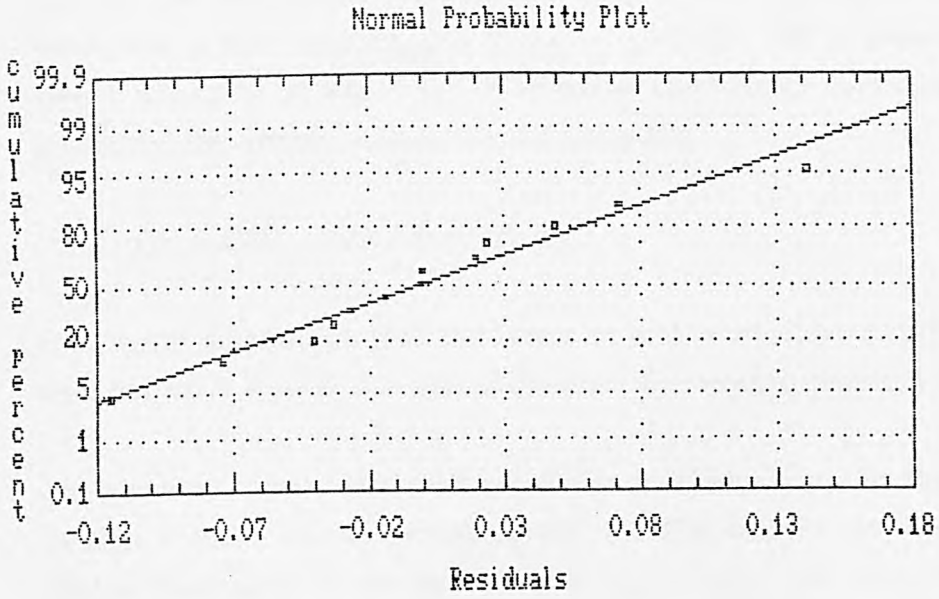

Figure 6.18. Residual and normal probability plot of LLDPE carbonyl model.

6.6.1 Variables Selection

SAS forward selection algorithm was used and results are presented in Figure 6.19. The Cutoff value $\alpha = 0.05$ is preset similar to the earlier two models. The most highly correlated with CY is CR, and since F-statistics associated with the model using CR (F = 68.12) is greater than $F_{.05,\ 1,11} = 4.48$, CR is added to the equation. In step 2 the regressor having the largest partial correlation with percent crystallinity is AT, and since the partial F-statistics for this regressor is 75.14 which exceeds $F_{IN} = F_{.05,1,10} = 4.96$, AT is added to the model. At this point the partial F-statistics $F_{IN} = {}_{.05,1,9} = 5.12$ exceeds F-values of all other regressor, so the forward selection terminates with model.

$$CY = 43.23 - 0.287\ AT + 0.003\ CR.$$

The results of backward elimination procedure is presented in Figure 6.20. Step O shows the fitting of full model. The smallest partial F-value is 0.08 < $F_{OUT} = F_{.05,\ 1,6}$,= 5.99, RD is removed from the model. At step 1, the results of fitting the five variables involving (AT, AH, UV, CR, CU) are shown. The smallest partial F-value in this model is F = 0.02, associated with CR. Since F = 0.02 is less than $F_{OUT} = F_{.05,\ 1,\ 7} = 5.59$, CR is removed from the model. At step 2 the results of fitting the four variable model is shown. The smallest partial F-statistics in this model is 1.07 associated with AH, and since this is less than $F_{OUT} = F_{.05,\ 1,\ 8} = 5.32$, AH is removed from the model. Similarly in step 4 UV is removed and finally backward elimination procedure terminates yielding the final model:

$$CY = 43.31 - 0.29\ AT + .092\ CU.$$

It is worth mentioning that the intercept and coefficient of AT in backward elimination is close to the values obtained by forward selection procedure.

The stepwise regression results are shown in Figure 6.21. As shown in results, in step 1 there are no variables and the CR entered the model, since the partial F-statistics at this step exceeds $F_{IN} = F_{.05,1,11} = 3.23$, CR is added to the model. Similarly in step 2 F-statistics favours the addition of AT in the model. Finally the program is terminated as the F-value of the regressors

```
FORWARD SELECTION PROCEDURE FOR DEPENDENT VARIABLE CY

STEP 1    VARIABLE CR ENTERED          R SQUARE = 0.86096430
                                       C(P) =    71.54071626
               DF    SUM OF SQUARES  MEAN SQUARE        F.  PROB>F

REGRESSION      1      379.86804532  379.8680453    68.12   0.0001
ERROR          11       61.34426237    5.5767511
TOTAL          12      441.21230769

               B VALUE    STD ERROR   TYPE II SS        F   PROB>F

INTERCEPT  37.05077773
CR          0.00271600   0.00032908  379.8680453    68.12   0.0001

BOUNDS ON CONDITION NUMBER:            1,            1
-----------------------------------------------------------------
STEP 2    VARIABLE AT ENTERED          R SQUARE = 0.98366920
                                       C(P) =     2.46011789
               DF    SUM OF SQUARES  MEAN SQUARE        F   PROB>F

REGRESSION      2      434.00695889  217.0034794   301.17   0.0001
ERROR          10        7.20534881    0.7205349
TOTAL          12      441.21230769

               B VALUE    STD ERROR   TYPE II SS        F   PROB>F

INTERCEPT  43.22679719
AT         -0.28667276   0.03307190   54.1389136    75.14   0.0001
CR          0.00316118   0.00012896  432.9807235   600.92   0.0001

BOUNDS ON CONDITION NUMBER:     1.188515,     4.754059
-----------------------------------------------------------------
NO OTHER VARIABLES MET THE 0.0500 SIGNIFICANCE LEVEL FOR ENTRY

SUMMARY OF FORWARD SELECTION PROCEDURE FOR DEPENDENT VARIABLE CY

     VARIABLE  NUMBER     PARTIAL      MODEL
STEP ENTERED       IN       R**2       R**2         C(P)

   1 CR             1      0.8610     0.8610      71.5407
   2 AT             2      0.1227     0.9837       2.4601

     VARIABLE
STEP ENTERED          F     PROB>F   LABEL

   1 CR          68.1164     0.0001  CUMULATIVE RADIATION
   2 AT          75.1371     0.0001  MONTHLY AVERAGE TEMPERATURE
-----------------------------------------------------------------
```

Figure 6.19 Computer output (SAS) of stepwise forward selection procedure applied to LLDPE crystallinity data.

```
BACKWARD ELIMINATION PROCEDURE FOR DEPENDENT VARIABLE CY

STEP 0    ALL VARIABLES ENTERED          R SQUARE = 0.98964233
                                         C(P) =      7.00000000
                DF  SUM OF SQUARES  MEAN SQUARE        F   PROB>F
REGRESSION       6    436.64237597  72.77372933    95.55   0.0001
ERROR            6      4.56993172   0.76165529
TOTAL           12    441.21230769

                B VALUE   STD ERROR   TYPE II SS        F   PROB>F
INTERCEPT   45.6936070
AT          -0.2900256  0.07202419  12.35021328    16.21   0.0069
AH          -0.0236481  0.05340976   0.14931773     0.20   0.6734
RD           0.0099791  0.03525655   0.06101908     0.08   0.7867
UV          -0.3794213  1.03043677   0.10326642     0.14   0.7254
CR          -0.0140199  0.04668013   0.06870414     0.09   0.7741
CU           0.5024750  1.35481451   0.10476778     0.14   0.7235

BOUNDS ON CONDITION NUMBER:     147326.3,      1773238
-----------------------------------------------------------------
STEP 1    VARIABLE RD REMOVED            R SQUARE = 0.98950403
                                         C(P) =      5.08011377
                DF  SUM OF SQUARES  MEAN SQUARE        F   PROB>F
REGRESSION       5    436.58135689  87.31627138   131.98   0.0001
ERROR            7      4.63095080   0.66156440
TOTAL           12    441.21230769

                B VALUE   STD ERROR   TYPE II SS        F   PROB>F
INTERCEPT   46.0543931
AT          -0.2834314  0.06351644  13.17333736    19.91   0.0029
AH          -0.0327807  0.03966712   0.45180114     0.68   0.4358
UV          -0.0883142  0.05903898   1.48032110     2.24   0.1783
CR          -0.0031058  0.02451985   0.01061410     0.02   0.9028
CU           0.1858933  0.71252425   0.04502982     0.07   0.8017
BOUNDS ON CONDITION NUMBER:     46799.17,     467955.9
-----------------------------------------------------------------
STEP 2    VARIABLE CR REMOVED            R SQUARE = 0.98947997
                                         C(P) =      3.09404934
                DF  SUM OF SQUARES  MEAN SQUARE        F   PROB>F
REGRESSION       4    436.57074279  109.1426857   188.11   0.0001
ERROR            8      4.64156490    0.5801956
TOTAL           12    441.21230769

                B VALUE   STD ERROR   TYPE II SS        F   PROB>F
INTERCEPT   46.1334537
AT          -0.2826638  0.05921088  13.2224465     22.79   0.0014
AH          -0.0348963  0.03369411   0.6223367      1.07   0.3306
UV          -0.0855359  0.05133178   1.6110132      2.78   0.1342
CU           0.0956441  0.00496542 215.2676887    371.03   0.0001

BOUNDS ON CONDITION NUMBER:     4.731185,      50.00516
-----------------------------------------------------------------
```

Figure 6.20 Computer output (SAS) of stepwise backward elimination procedure applied to LLDPE crystallinity data.

```
STEP 3    VARIABLE AH REMOVED          R SQUARE = 0.98806946
                                       C(P) =     1.91113375
                DF  SUM OF SQUARES  MEAN SQUARE        F   PROB>F
REGRESSION       3    435.94840613  145.3161354   248.46   0.0001
ERROR            9      5.26390156    0.5848780
TOTAL           12    441.21230769

              B VALUE   STD ERROR   TYPE II SS        F   PROB>F
INTERCEPT  43.3990335
AT         -0.2388827  0.04162697   19.2612688    32.93   0.0003
UV         -0.0927080  0.05106734    1.9275835     3.30   0.1028
CU          0.0918709  0.00338730  430.2416584   735.61   0.0001

BOUNDS ON CONDITION NUMBER:     2.319667,     16.82329
-----------------------------------------------------------------
STEP 4    VARIABLE UV REMOVED          R SQUARE = 0.98370062
                                       C(P) =     2.44191575
                DF  SUM OF SQUARES  MEAN SQUARE        F   PROB>F
REGRESSION       2    434.02082264  217.0104113   301.76   0.0001
ERROR           10      7.19148506    0.7191485
TOTAL           12    441.21230769

              B VALUE   STD ERROR   TYPE II SS        F   PROB>F
INTERCEPT  43.3128103
AT         -0.2915207  0.03311917   55.7184092    77.48   0.0001
CU          0.0921002  0.00375343  432.9945872   602.09   0.0001

BOUNDS ON CONDITION NUMBER:     1.194212,     4.776849
-----------------------------------------------------------------
ALL VARIABLES IN THE MODEL ARE SIGNIFICANT AT THE 0.0500 LEVEL.

SUMMARY OF
BACKWARD ELIMINATION PROCEDURE FOR DEPENDENT VARIABLE CY

     VARIABLE  NUMBER     PARTIAL      MODEL
STEP REMOVED       IN       R**2       R**2         C(P)
   1 RD             5     0.0001     0.9895      5.08011
   2 CR             4     0.0000     0.9895      3.09405
   3 AH             3     0.0014     0.9881      1.91113
   4 UV             2     0.0044     0.9837      2.44192

     VARIABLE
STEP REMOVED          F    PROB>F  LABEL
   1 RD          0.0801    0.7867  TOTAL SOLAR RADIATION
   2 CR          0.0160    0.9028  CUMULATIVE RADIATION
   3 AH          1.0726    0.3306  MONTHLY AVERAGE HUMIDITY
   4 UV          3.2957    0.1028  UV RADIATION
-----------------------------------------------------------------
```

Figure 6.20 (...contd.)

Computer output (SAS) of stepwise backward elimination procedure applied to LLDPE crystallinity data.

```
STEPWISE REGRESSION PROCEDURE FOR DEPENDENT VARIABLE CY

STEP 1    VARIABLE CR ENTERED          R SQUARE = 0.86096430
                                       C(P) =     71.54071626
                DF  SUM OF SQUARES  MEAN SQUARE        F   PROB>F
REGRESSION       1    379.86804532  379.8680453    68.12   0.0001
ERROR           11     61.34426237    5.5767511
TOTAL           12    441.21230769

              B VALUE   STD ERROR   TYPE II SS        F   PROB>F
INTERCEPT  37.0507777
CR          0.0027160  0.00032908  379.8680453    68.12   0.0001

BOUNDS ON CONDITION NUMBER:            1,            1
-----------------------------------------------------------------

STEP 2    VARIABLE AT ENTERED          R SQUARE = 0.98366920
                                       C(P) =      2.46011789
                DF  SUM OF SQUARES  MEAN SQUARE        F   PROB>F
REGRESSION       2    434.00695889  217.0034794   301.17   0.0001
ERROR           10      7.20534881    0.7205349
TOTAL           12    441.21230769

              B VALUE   STD ERROR   TYPE II SS        F   PROB>F
INTERCEPT  43.2267972
AT         -0.2866728  0.03307190   54.1389136    75.14   0.0001
CR          0.0031612  0.00012896  432.9807235   600.92   0.0001

BOUNDS ON CONDITION NUMBER:     1.188515,     4.754059
-----------------------------------------------------------------
NO OTHER VARIABLES MET THE 0.0500 SIGNIFICANCE LEVEL FOR ENTRY

SUMMARY OF
STEPWISE REGRESSION PROCEDURE FOR DEPENDENT VARIABLE CY

          VARIABLE        NUMBER   PARTIAL    MODEL
STEP  ENTERED   REMOVED       IN     R**2      R**2        C(P)
   1  CR                      1   0.8610    0.8610     71.5407
   2  AT                      2   0.1227    0.9837      2.4601

          VARIABLE
STEP  ENTERED   REMOVED          F          PROB>F
   1  CR                  68.1164          0.0001
   2  AT                  75.1371          0.0001

          VARIABLE
STEP  ENTERED   REMOVED   LABEL
   1  CR                 CUMULATIVE RADIATION
   2  AT                 MONTHLY AVERAGE TEMPERATURE
-----------------------------------------------------------------
```

Figure 6.21 Computer output (SAS) of stepwise regression procedure applied to LLDPE crystallinity data.

were lower than F_{IN}, thereby terminating stepwise algorithm with the final model

$$CY = 43.2 - 0.29\ AT + 0.003\ CR.$$

R^2 and Mallow's CP are presented in Figure 6.22. As indicated in the figure there are more than one instances when CP is less then number of parameters. Therefore, those independent variables suggested by stepwise procedures are AT, UV, CU and CR are selected for the model. A preliminary residual analysis was carried out and it was observed that the scatter of residual is indicating a slight trend. In addition to this, normal probability was not exhibiting a straight line behavior. Different combinations were used and it was found that the best fit is obtained by considering AT, CU, and CR as independent variable.

6.6.2 Regression Analysis

Multiple linear regression model was developed for percent crystallinity change with weather parameters with AT, CU, and CR as independent variables. The results of general linear model procedure of SAS are shown in Figure 6.23. The figure indicates a coefficient of variance (CV) = 1.98 and root mean square error of 0.89. Both of these values indicate that the developed model is adequate.

The developed model is

$$CY = 43.31 - 0.29\ AT + 0.08\ CU + 0.00008\ CR$$

6.6.3 Residual Analysis

The results of residual and normal probability plots are shown in Figure 6.24. The plot of residuals does not indicate any serious model inadequacies. The scatter does not have any trend or curvature or inequality of variance. The residuals are also plotted on normal probability paper. Since the residuals fall approximately along a straight line, it is concluded that there is no severe departure from normality. These plots do not indicate any serious model inadequacies.

N=13 REGRESSION MODELS FOR DEPENDENT VARIABLE: CY
MODEL: MODEL1

NUMBER IN MODEL	R-SQUARE	C(P)	VARIABLES IN MODEL
1	0.00039603	570.051	RD
1	0.00132731	569.512	UV
1	0.00232594	568.933	AT
1	0.31110677	390.063	AH
1	0.85741582	73.596281	CU
1	0.86096430	71.540716	CR
2	0.00902399	567.053	AT RD
2	0.01293424	564.788	AT UV
2	0.04885118	543.982	UV RD
2	0.33948825	375.622	UV AH
2	0.34663948	371.479	AH RD
2	0.47960128	294.457	AT AH
2	0.92059458	38.998037	CU AH
2	0.92151646	38.464013	AH CR
2	0.92208489	38.134730	CU CR
2	0.94441413	25.199829	CU UV
2	0.94535850	24.652772	UV CR
2	0.94594643	24.312197	CU RD
2	0.94700637	23.698194	RD CR
2	0.98366920	2.460118	AT CR
2	0.98370062	2.441916	AT CU
3	0.05067191	544.928	AT UV RD
3	0.40508654	339.622	UV AH RD
3	0.49725457	286.231	AT AH RD
3	0.50157951	283.725	AT UV AH
3	0.93185543	34.474843	CU AH CR
3	0.94646894	26.009517	CU UV RD
3	0.94769519	25.299177	UV RD CR
3	0.95137817	23.165693	CU UV CR
3	0.95405094	21.617408	CU RD CR
3	0.95951153	18.454195	CU UV AH
3	0.95959386	18.406504	UV AH CR
3	0.95980429	18.284602	CU AH RD
3	0.96000494	18.168372	AH RD CR
3	0.98370065	4.441902	AT CU CR
3	0.98582864	3.209197	AT CU AH
3	0.98599912	3.110443	AT AH CR
3	0.98774576	2.098645	AT RD CR
3	0.98781682	2.057484	AT UV CR
3	0.98794270	1.984565	AT CU RD
3	0.98806946	1.911134	AT CU UV

Figure 6.22 Computer output (SAS) of RSQUARE and Mallow's Cp applied to LLDPE crystallinity data.

4	0.52048117	274.776	AT UV AH RD
4	0.95964689	20.375782	CU UV AH CR
4	0.95980435	20.284568	CU UV AH RD
4	0.96002108	20.159024	UV AH RD CR
4	0.96039682	19.941363	CU AH RD CR
4	0.96097146	19.608484	CU UV RD CR
4	0.98614891	5.023672	AT CU AH CR
4	0.98782073	4.055219	AT UV RD CR
4	0.98810361	3.891352	AT CU UV RD
4	0.98816026	3.858535	AT CU RD CR
4	0.98848003	3.673297	AT CU UV CR
4	0.98938560	3.148716	AT AH RD CR
4	0.98940197	3.139235	AT UV AH CR
4	0.98940791	3.135795	AT CU AH RD
4	0.98947997	3.094049	AT CU UV AH
5	0.96165079	21.214964	CU UV AH RD CR
5	0.98930390	5.196044	AT CU UV RD CR
5	0.98940488	5.137553	AT UV AH RD CR
5	0.98940828	5.135582	AT CU AH RD CR
5	0.98948661	5.090204	AT CU UV AH RD
5	0.98950403	5.080114	AT CU UV AH CR
6	0.98964233	7.000000	AT CU UV AH RD CR

Figure 6.22 (...contd.)
Computer output (SAS) of RSQUARE and Mallow's
Cp applied to LLDPE crystallinity data.

PERCENT CRYSTALLINITY MATHEMATICAL MODEL

GENERAL LINEAR MODELS PROCEDURE

DEPENDENT VARIABLE: CY % CRYSTALLINITY

SOURCE	DF	SUM OF SQUARES	MEAN SQUARE
MODEL	3	434.02083298	144.67361099
ERROR	9	7.19147471	0.79905275
CORRECTED TOTAL	12	441.21230769	

MODEL F = 181.06 PR > F = 0.0001

R-SQUARE	C.V.	ROOT MSE	CY MEAN
0.983701	1.9797	0.89389750	45.15384615

SOURCE	DF	TYPE I SS	F VALUE	PR > F
CU	1	378.30241340	473.44	0.0001
AT	1	55.71840924	69.73	0.0001
CR	1	0.00001035	0.00	0.9972

SOURCE	DF	TYPE III SS	F VALUE	PR > F
CU	1	0.01387410	0.02	0.8981
AT	1	27.18563138	34.02	0.0002
CR	1	0.00001035	0.00	0.9972

PARAMETER	ESTIMATE	T FOR H0: PARAMETER=0	PR > |T|	STD ERROR OF ESTIMATE
INTERCEPT	43.31052314	40.10	0.0001	1.07994356
CU	0.08965208	0.13	0.8981	0.68037094
AT	-0.29139216	-5.83	0.0002	0.04995695
CR	0.0000840	0.00	0.9972	0.02335293

Figure 6.23 Computer output (SAS) of general linear model procedure applied to LLDPE crystallinity data.

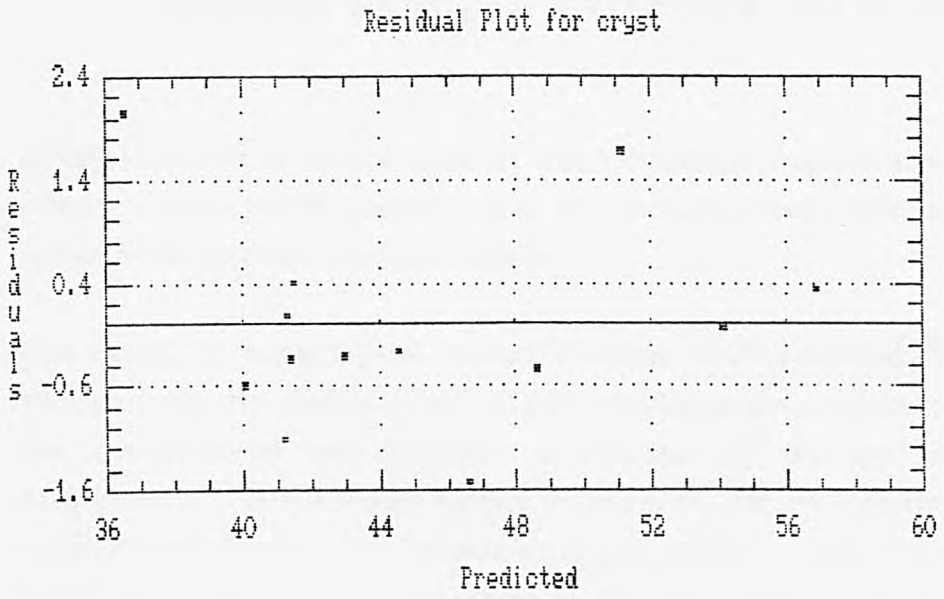

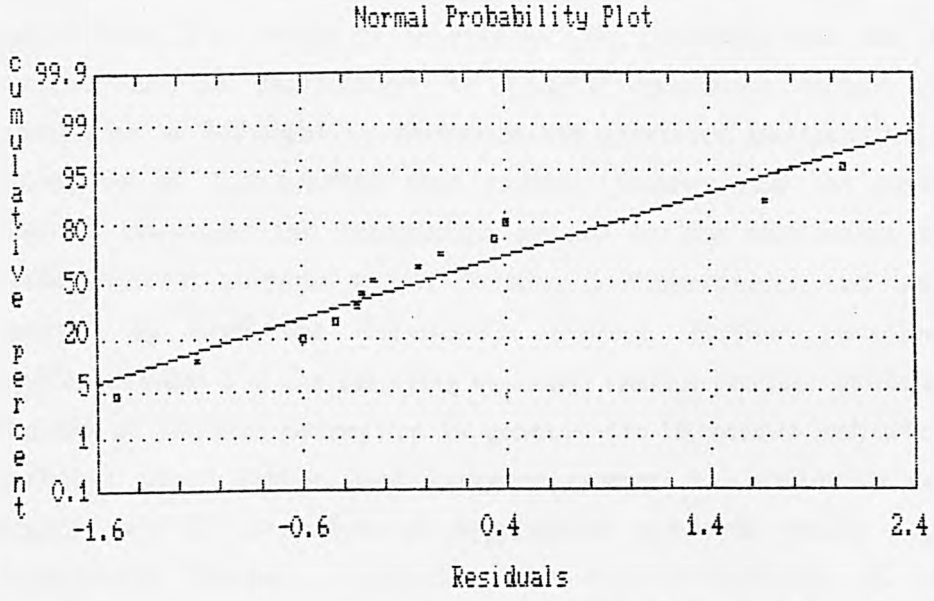

Figure 6.24. Residual and normal probability plot of LLDPE crystallinity model.

Chapter 7

GENERAL RESULTS AND FURTHER WORK

In this thesis we have presented the weather-induced degradation studies of a relatively new type of plastic - linear low density polyethylene, when exposed to one of the extreme climatic regions.

The details of experimental exposure studies were described in Chapter 2 which include the details of the LLDPE specimens preparation, discussion of the meteorological and radiation environment of the test site, and the description of the specimens natural exposure conditions. Despite its nearness to the coast , exposure site (Dhahran, Saudi Arabia) is located in very much desert environment. The high doses of UV and total solar radiation, high levels of temperature and humidity fostered with cold nights and hot days provide a unique weathering laboratory for studying the behavior of plastic properties.

The characterization techniques used to study the degradation are IR spectroscopic studies, differential scanning calorimetric analysis, and mechanical properties determination presented in Chapter 3, 4, and 5, respectively. The results of IR studies have indicated that the initiation of weather-induced degradation in LLDPE specimens occurs due to the absorption of UV-light by chromophores generated photoexcited states. The formation of hydrocarbon free radicals follows and the peroxy radicals formed propagate the degradation process by the abstraction of hydrogen from adjacent polymer chains forming hydroperoxides and more polymer radicals to feed the degradation process. Further photolysis of the hydroperoxides and the resulting carbonyl species produce chain scission and the loss of physical properties. In general, the IR results indicate increase in carbonyl, vinyl, alkene, and hydroxyl groups. An interesting result is the higher rate of formation of degradation products which implies faster degradation. Chapter 3 describes the thermal behavior of the LLDPE specimens exposed to weather. An increase in percent crystallinity is observed with a slight variation in the crystalline melting temperature. The increase in

percent crystallinity can be attributed to the formation of carbonyl and other functional groups. The results of mechanical behavior of LLDPE specimens are presented in Chapter 5. The rapid degradation in mechànical properties (tensile strength and percent elongation) of specimens during natural exposure is observed. The degradation process proceeds with the simultaneous action of chain scission and crosslinking with crosslinking dominating in the beginning.

The results obtained by IR analysis, thermal analysis, and mechanical behavior studies, are linked together. The growth of carbonyl groups and increase in crystallinity can be considered as precursors to drop in ultimate mechanical properties (tensile strength and percent elongation).

Chapter 6 presents the mathematical modelling of the change in mechanical, thermal, and chemical properties of specimens as a function of weather parameters (average temperature, average humidity, UV radiation, cumulative UV radiation, total solar radiation, and cumulative solar radiation). The results indicate that multiple linear relationship exist between weather parameters and the significant polymer properties. One of the most significant results of this work is that different weather parameters play significant role in the degradation of different properties.

We feel that this work presents for the first time extensive studies on the weather-induced degradation of LLDPE. The originality of the work is further established by the fact that the natural environment considered in this work is one of the extreme climates of the world. Very few publications are available on this topic and those available have either considered artificial weatherometer or if natural weather is considered than full characterization, as presented in this work, is not available. It is therefore felt that our work will provide sound basis for carrying out further studies on the weather-induced degradation of LLDPE and LLDPE-based formulations and blends. The experimental data presented in this study provides a baseline for the work in the field of LLDPE formulations for increased useful lifetime in outdoor applications. Outdoor use of LLDPE is limited because of limited number of studies done in this field. Application of LLDPE as an agricultural film (greenhouse, ensilage, mulch, and sacks) is slow because of doubts about the light stability of LLDPE [Turtle, 1986].

In blends LLDPE have been used at relatively low levels (5-15%) in other polymers to gain performance advantage in many applications. Compatibility of LLDPE blends with LDPE, HDPE, and EVA is well published but the performance of these blends in outdoor environment is yet to be explored. Recently there has been great deal of interest in studying the photo-oxidation of LDPE and LLDPE blends [LaMantia, 1985 and LaMantia and Acierno, 1985]. These studies were done in artificial environment and therefore lack the exact behavior of these blends in natural environment.

The effect of comonomer (propene, 1-hexene, 1-octene, and 4-methyl-1-pentene) in the outdoor performance of LLDPE can also be investigated by extending our work which is based on ethylene 1-butene copolymer and so contain ethyl branches. Hexyl branched as well as methyl, butyl, and isobutyl branched copolymers are also being produced and they need to be studied from the weather-induced degradation point of view.

Mathematical modelling work included in this study can also be further extended to include the mathematical relationship between different mechanical, thermal, and chemical properties. In addition to this, our experimental data can be used to develop a mathematical correlation between the results obtained from natural weathering studies and accelerated weathering studies. The developed model can determine the number of artificially accelerated weatherometer hours with natural weathering months.

REFERENCES

ABDELREHMAN, M.A., SAID, S.A.M., SHUAIB, A.N. (1988).
"Comparison Between Atmospheric Turbidity Coefficient of Desert and Temperate Climate," *Solar Energy*, 40(2). (In press.)

ACIERNO, D., CURTO, D., LAMANTIA, F.P., VALENZA, A., and BRANCACCIO, A. (1984).
"Future Trends in Polymer Science and Technology, Polymers:Commodities as Specialities," International Workshop, Capri, Italy, October 8-12, 1984.

ACIERNO, D., BRANCACCIO, A., CURTO, D., LAMANTIA, F.P. and VALENZA, A. (1985).
"Molecular Weight Dependency of Rheological Characteristics of Linear Low Density Polyethylene," *Journal of Rheology*, **29(3)**: 323-334.

ADAMS, J.H. (1970).
"Analysis of Nonvolatile Oxidation Products of A. III Photodegradation," *Journal of Polymer Science: Part A-1*, **8**: 1279-1288.

AKAY, G., TINCER, T., and AYDIN, E. (1980a).
"The Effect of Orientation on the Radiation Induced Degradation of Polymer," *European Polymer Journal*, **16**: 597-600.

AKAY, G., TINCER, T., and ERGOZ, H.E. (1980b).
"A Study of Degradation of Low Density Polyethylene Under Natural Weathering Conditions," *European Polymer Journal*, **16**: 601-605.

AKAY, G. and TINCER, T. (1981).
"The Effect of Orientation on Radiation-Induced Degradation in High Density Polyethylene," *Polymer Engineering and Science*, **21** (1): 8-17.

ALLEN, N.S. (1980).
"Photo-Degradation and Photo-Oxidation of Polyolefins: Importance of Oxygen-Polymer Charge Transfer Complexes," *Polymer Degradation and Stability*, **2**: 155-161.

ALLEN, N.S., PARKINSON, A., LOFFELMAN, F.F., MACDONOLD, P., RAUHUT, M.M., and SUSI, P.V. (1985).
"Photostabilising Action of a P-Hydroxybenzoate Light Stabilizes in Polyolefins: Part IV-Catalyst Effects and Additive Interactions in Linear Low Density Polyethylene," *Polymer Degradation and Stability*, **12**: 363-372.

AL-RABEH, A. H. (1988).
"Modelling and Simulation with Local Flavor," Presented at a Research Institute Technical Seminar, KFUPM/RI, Dhahran, Saudi Arabia, June, 1988.

AMIN, M.U. and SCOTT, G. (1974).
"Photo-initiated Oxidation of Polyethylene, Effect of Photo-Sensitizers," *European Polymer Journal,* **10:** 1019-1028.

AMIN, M.U., SCOTT, G., and TILLEKERATNE, M.K. (1975).
"Mechanism of the Photo-Initiation Process in Polyethylene," *European Polymer Journal,* **11:** 85-89.

ANANI, A., MOBASHER, A., and RASOUL, F.A. (1984).
"Use of Photocoustic Spectroscopy in Studying the Natural Weathering of Polyethylene Films," *Journal of Applied Polymer Science,* **29:** 1491-1497.

ASTM STANDARD D-1435 (1979).
Outdoor Weathering of Plastics, 639-644.

ASTM STANDARD D-1928 (1980).
Preparation of Compression Molded Polyethylene Test Sheets and Test Specimens: 230-237.

ASTM STANDARD D-638M-84 (1984).
Tensile Properties of Plastics (Metric), 225-236.

ASTM STANDARD E-793-81 (1981).
Heat of Fusion and Crystallization by Differential Scanning Calorimetry: 675-679.

ASTM STANDARD E-794-81 (1981).
Melting and Crystallization temperature by Differential Scanning Calorimetry: 680-684.

ASTM STANDARD E-967-83 (1983a).
Temperature Calibration of Differential Scanning Calorimeters and Differential Thermal Analyzers: 782-787.

ASTM STANDARD E-968-83 (1983b).
Heat Flow Calibration of Differential Scanning Calorimeters: 788-794.

BAHEL, V., SRINIVASAN, R., and BAKSH, H. (1986).
"Solar Radiation for Dhahran, Saudi Arabia," *Energy*, **11**, 10: 985-989.

BARRALL.II, E. M. and JOHNSON, J. F. (1970).
"Differential Scanning Calorimetry, Theory and Applications," In: **Techniques and Methods of Polymer Evaluation,** Ed. P. E. Slade, Jr. and T. Jenkins (New York: Marcel Dekker), 1-39.

BARTICK, E.G. (1979).
"The Identification of a Polymer Additive Using Difference Spectroscopy with the Infrared Data Station," *Perkin-Elmer Infrared Bulletin 70.*

BECKMAN, R. J. and COOK, R. D. (1983).
"Outlier....s," *Technometrics,* 25:119-149

BERK, K. N. (1978).
"Comparing Subset Regression Procedures," *Technometrics, 20:1-6*

BILLINGHAM, N.C. and CALVERT, P.D. (1983).
"The Degradation and Stabilization of Polyolefins - An Introduction," In: **Degradation and Stabilisation of Polyolefins,** Ed: N.S. Allen, (London: Applied Science), 1-28.

BILLINGHAM, N.C., PRENTICE, P. and WALKER, T.J. (1976).
"Some Effects of Morphology on Oxidation and Stabilization of Polymer," *Journal.of Polymer Science Symposium*, **No. 57,** 287-297.

BILLMEYER, JR., F.W. (1984).
Textbook of Polymer Science, 3rd Ed. (New York: John Wiley).

BLAGA, A. and YAMASAKI, R.S. (1976).
"Mechanical Behavior of Polyolefins," *Journal of Material Science,* **11:** 1513-1530.

BLAIS, P., CARLSSON, D.J., and WILES, D.M. (1972).
"Surface Changes During A Photo-oxidation: A Study by Infrared Spectroscopy and Electron Microscopy," *Journal of Polymer Science*, Part A-1, **10:** 1077-1092.

BOBALEK, E.G., HENDERSON, J.N., SERAFINI, T.T., and SHELTON, J.R. (1959).
"Oxidation of Polyethylene," *Journal of Applied Polymer Science,* **2:** 47-59.

BORK, S. (1984).
"Linear Low Density Polyethylene (LLDPE) - Properties, Processing, and Application," *Kunstsoffe*, **74**: 474-479.

BRENNAN, W.P. (1977).
"Characterization and Quality Control of Engineering Thermoplastics by Thermal Analysis," In: **Thermal Analysis Application Study 22**, (Connecticut: Perkin-Elmer).

BRENNAN, W.P. (1978).
"Characterization of Polyethylene Films by Differential Scanning Calorimeters," In: **Thermal Analysis Application Study 24**, (Connecticut: Perkin-Elmer).

BRENNAN, W.P. and GRAY, A.P. (1973).
"The Calorimetric Precision and Accuracy of a Scanning Calorimeter," In: **Thermal Analysis Application Study 9**, (Connecticut: Perkin-Elmer).

BRITISH STANDARD (BS) 2782: PART 9: METHOD 901A, (1977).
Compression Moulding Test Specimens of Thermoplastics Materials, British Standard Institution.

BRITISH STANDARD (BS) 2782: PART 5: METHOD 550A, (1981).
Methods of Exposure to Natural Weathering, British Standard Institution (BSI).

BURGESS, A. R. (1952)
"Degradation and Weathering of Plastics," *Chemistry and Industry*, January 26: 78-81.

CADY, L.D. (1987)
"LLDPE Properties Tied to Branch Distribution," *Plastic Engineering*, January: 25-27.

CARLSSON, D.J. and WILES, D.M.(1976).
"The Photooxidative Degradation of A. Part 1: Photooxidation and Photooxidation Processes," *Journal of Macromolecules Science-Review in Molecular Chemistry*, **C14(1)**: 65-106.

CARLSSON, D.J., DOBBIN, C.J.B. and WILES, D.M. (1985).
"Direct Observation of Macroperoxyl Radical Propagation and Termination by Electron Spin Resonance and Infrared Spectroscopies," *Macromolecules*, **18**: 2092-2094.

CERNIA, E., MANCINI, C., and MONTAUDO, G. (1963).
"Contribution to the Investigation of Polyethylene by Infrared Techniques," *Polymer Letter*, **1**: 371-377.

CHAN, M.G. and HAWKINS, W.L. (1968).
"Internal Reflection Spectroscopy in the Prediction of Outdoor Weatherability," Polymer Preprint, *American Chemical Society, Polymer Chemistry Division*, 1638-1643.

CHIRINOS-PADRON, A.J., HERNANDEZ, P.H., CHAVEZ, E., ALLEN, N.S. VASILIOU, C., and DEPOORTERE, M. (1987a).
"Influence of Unsaturation and Metal Impurities on the Oxidative Degradation of High Density Polyethylene," *European Polymer Journal*, **23 (12)**: 935-940.

CHIRINOS-PADRON, A.J., HERNANDEZ, P.H., ALLEN, N.S., VASILION, C., and MARSHALL, G.P. (1987b).
"Synergism of Antioxidants in High Density Polyethylene," *Polymer Degradation and Stability*, **19**: 177-189.

COATES, J.P. and SETTI, L.C. (1983).
"Performance and Applications of the Perkin-Elmer 1500 Series Fourier Transform Spectrophotometers," Perkin Elmer, Conn., USA, Number: L-784.

COULSON, K. L. (1975).
Solar Terrestrial Radiation. (New York: Academic press).

COX, D. R. and SNELL, E. J. (1974).
"The Choice of Variables in Observational Studies," *International Statistical Review*, **23**: 51-59.

CUNLIFFE, A.V. and DAVIS, A. (1982).
"Photo-oxidation of Thick Polymer Samples - Part II: The Influence of Oxygen Diffusion on the Natural and Artificial Weathering of Polyolefins," *Polymer Degradation and Stability*, **4**: 17-37.

DANIEL, C. and WOOD, F. S. (1980).
Fitting Equation to Data. (New York: Wiley).

D'ESPOSITO, L. and KOENIG, J.L. (1978).
"Applications of Fourier Transform Infrared to Synthetic Polymers and Biological Macromolecular," In: **Fourier Transform Infrared Spectroscopy**, Ed. Ferroro, J.R. and Basile, L.J. (New York : Academic), Chapter 2: 61-97.

DAVIS, A. and SIMS, D. (1983).
Weathering of Polymers. (London: Applied Science).

EDWARD, G.H. (1986).
"Crystallinity of Linear Low Density Polyethylene and of Blends with High Density Polyethylene," *British Polymer Journal*, **18(2)**: 88-93.

FANCONI, B.M. (1984).
"Fourier Transform Infrared Spectroscopy of Polymers - Theory and Application," *Journal of Testing and Evaluation*, January 1984: 33-39.

FLESHER, J.R. (1980).
"Polyethylene," In: **Modern Plastic Encyclopedia**, Ed. J. Agranoff,, (New York: McGraw-Hill), 57 (10A): 62-68.

FRANCE, C., HENDRA, P. J., MADDAMS, W. F., and WILLIS, H. A. (1987).
"A Study of Linear Low-Density Polyethylenes: Branch Content, Branch Distribution and Crystallinity," *Polymer*, **28**: 710-712.

FREUND, R. J. and LITTELL, R. C. (1981).
SAS For Linear Models, A Guide to the ANOVA and GLM Procedure. (North Carolina: SAS Institute).

FURNEAUX, G.C., LEDBURY, K.J., and DAVIS, A. (1981).
"Photo-oxidation of Thick Polymer Samples - Part I: The Variation of Photo-oxidation with Depth in Naturally and Artificially Weathered Low Density Polyethylene," *Polymer Degradation and Stability*, **3**: 431-442.

GEETHA, R., TORIKAI, A., NAGAYA, S., and FUEKI, K. (1987).
"Photooxidative Degradation of Polyethylene:Effect of Polymer Characteristics of Chemical Changes and Mechanical Properties. Part 1 - Quenched Polyethylene," *Polymer Degradation and Stability*, **19**: 279-292.

GHANI, R. (1987).
"Processing, Heat and Light Stabilization of Polyolefins," Presented at a Seminar at KFUPM/RI, Dhahran, Saudi Arabia, October 4, 1987.

GILROY, H. M. (1979).
"Long-Term Photo- and Thermal Oxidation of Polyethylene," In: **Durability of Macromolecular Materials**, Ed: R. K. Eby, *Reprint ACS Symposium Series No. 95*, 63-74.

GOTTFRIED, C. and DUTZER, M.J. (1961).
"Status of Investigation for Improving Weatherability of Linear Polyethylene and Copolymer," *Journal of Appllied Polymer Science*, 5(17): 612-619.

GRAY, A.P. (1970).
"Polymer Crystallinity Determination by DSC," *Thermochimica Acta*, 1: 563-579.

GRAY, V.E. and CADOFF, B.C. (1967).
"Survey of Techniques for Evaluating Effect of Weathering on Plastics," *Applied Polymer Symposia*, No. 4, 85-95.

GRIFFITHS, P.R. (1975).
Chemical Infrared Fourier Transform Spectroscopy, (New York: John Wiley), p 15.

HAMEED, Z., RASOUL, F.A. and ANANI, A. (1980).
"Outdoor Weathering of Colored Polyethylene Films," Annual Report, Kuwait Institute for Scientific Research (KISR), Kuwait, 231-2321.

HAWKINS, W.L., MATREYEK, W., and WINSLOW, F.H. (1959).
"The Morphology of Semicrystalline Polymers. Part I. The Effect of Temperature on the Oxidation of Polyolefins," *Journal of Polymer Science*, 41: 1-11.

HAWKINS, W.L. (1964).
"Thermal and Oxidative Degradation of Polymers," *Society of Plastic Engineers (SPE) Transactions*, 4(3): 187-192.

HAWKINS, W.L. (1984).
Polymer Degradation and Stabilization, (Berlin: Springer-Verlag).

HEACOCK, J.F., MALLORY, F.B., and GAY, F.P. (1968).
"Photodegradation of Polyethylene Film," *Journal of Polymer Science:* Part A-1, 6: 2921-2934.

HENDERSON, S. T. (1970).
Ultraviolet Radiation, (New York: John Wiley).

HINES, W. W. and MONTGOMERY, D. C. (1972).
Probability and Statistics in Engineering and Management Science, (New York: John Wiley).

HU, S., KYU, T., and STEIN, R.S. (1987).
"Characterization and Properties of Polyethylene Blends I. Linear Low Density Polyethylene with High Density Polyethylene," *Journal of Polymer Science: Part B: Polymer Physics*, **25**: 71-87.

HUANG, T.A. and GAMPBELL, G.A. (1986).
"Deformation and Temperature History Comparison for LLDPE and LDPE Elements in the Bubble Expansion Region of Blown Films," *Journal of Plastic Film and Sheeting*, **2**: 30-39.

HUTSON, G.V. and SCOTT, G. (1972).
"The Effect of Oxidation During Processing on the Light Stability of Polyolefins," *Chemistry and Industry*, 16 September, 725-726.

INSTRUCTIONS, MODEL DSC 4, (1983).
Connecticut, Perkin-Elmer Corporation.

IRING, M., FOLDES, E., BARABAS, K., KELEN, T., and TUDOS, F. (1986).
"Thermal Oxidation of Linear Low Density Polyethylene," *Polymer Degradation and Stability*, **14**: 319-332.

JAMES, D.E. (1987)
"Unipol Process Polyethylene: Recent Advances with LLDPE," Union Carbide Corporation, Unipol Systems Department, New Jersey, USA.

JELINSKI, L.W., DUMAIS, J.J., LUONGO, J.P. and CHOLLI, A.L. (1984).
"Thermal Oxidation and Its Analysis at Low Levels in Polyethylene," *Macromolecules*, **17**: 650-1655.

KAMAL, M.R. and SAXON, R. (1967).
"Recent Development in the Analysis and Prediction of the Weatherability of Plastics," *Applied Polymer Symposia*, **4**: 1-28.

KAMAL, M.R. (1970).
"Cause and Effect in the Weathering of Plastics," *Polymer Engineering and Science*, **10(2)**: 108-121.

KATO, Y., CARLSSON, D.J., and WILES, D.M. (1969).
"The Photooxidation of A:Some Effect of Molecular Order," *Journal of Applied Polymer Science*, **13**: 1447-1458.

KAY, E., DAVIS, A., and PALMER, G.L. (1976).
"Recommended Procedures for the Effective Study of the Natural Weathering Behavior of Plastics, in the Weathering of Plastics and Rubbers," *PRI Symposium*, C2.1-C2.12.

KLEMCHUK, P.P. (1985).
"Antioxidants," Reprint: *Ullman's Encyclopedia of Industrial Chemistry*, **A3**: 91-111.

KLEMCHUK, P.P. (1986).
"Ultraviolet Degradation and Stabilization of Polymers," In: **Encyclopedia of Material Science and Engineering,** Ed. Bever, M.B., (Oxford: Pergamon), 5200-5208.

KOENIG, J.L. (1975).
"Application of Fourier Transform Infrared Spectroscopy of Chemical System," *Applied Spectroscopy*, **29(4)**: 293-308.

KOENIG, J.L. (1980).
"Applications of Fourier Transform Infrared to Polymers," In: **Analytical Application of FTIR to Molecules and Biological System,** Ed. J.R. Durig, (New York: D. Reidel), 229-240.

KOENIG, J.L. (1984).
"Fourier Transform Infrared Spectroscopy of Polymers," In: **Spectroscopy: NMR, Fluorescence, FTIR with Contributions,** Ed. C.W. Franks (Berlin: Springer-Verlag), Advances in Polymer Science, **54**: 87-154.

KOVACEVIC, V. HAGE, D., BRAVER, M., MUDRI, I., and CEROUECKI, Z. (1986).
"Mechanical and Structural Studies of Aged Adhesive Composites," *Polimeri*, **7(12)**: 351-355.

KRIMM, S. (1960).
"Infrared Spectra of High Polymer," *Advances in Polymer Science*, **2**, 51-172.

KYU, T., HU.,S., and STEIN, R.S. (1987).
"Characterization and Properties of Polyethylene Blend II. Linear Low Density with Conventional Low Density Polyethylene," *Journal of Polymer Science:Part B. Polymer Physics*, **25**: 89-103.

LAMANTIA, F.P. (1984a).
"Natural Weathering of Low Density Polyethylene-I Structural Modification," *Radiation Physics and Chemistry*, **23(6)**: 699-702.

LAMANTIA, F.P. (1984b).
"Natural Weathering of Low Density Polyethylenes-III Mechanical Properties," *European Polymer Journal*, **20(10)**: 993-995.

LAMANTIA, F.P. (1985).
"Photo-Oxidation of Blends of Low Density Polyethylene and Linear Low Density Polyethylene," *Polymer Degradation and Stability*, **13**: 297-304.

LAMANTIA, F.P. and ACIERNO, D. (1985).
"Mechanical Properties of Blends of Low Density with Linear Low Density Polyethylene," *European Polymer Journal*, **21(9)**: 811-813.

LAMANTIA, F.P., VALENZA, A. and ACIERNO, D. (1986).
"Influence of the Structure of Linear Density Polyethylene on the Rheological and Mechanical Properties of Blends with Low Density Polyethylene," *European Polymer Journal*, **22(8)**: 647-652.

LEAVERSUCH, R. (1986).
"Comonomer Versatility Expands Performance Options in LLDPE," *Modern Plastic*, August 1986: 42-45.

LINDGREN, B. W. and MCELRATH, G. W. (1971).
Introduction to Probability and Statistics," (Macmillan: London).

LUONGO, J.P. (1963).
"Effect of Oxidation on Polyethylene Morphology," *Journal of Polymer Science, Polymer Letter*, **1**: 141-43.

MAADHAH, A.G., HAMID, S.H., and AMIN, M.B. (1985).
"Overview of the Petrochemical Industry in Saudi Arabia," *Arabian Journal for Science & Engineering*, **10(4)**: 327-338.

MALLOWS, C. L. (1973).
"Some Comments on Cp," *Technometrics*, 15: 661-675.

MARTINOVICH, R. J. and HIL, G. R. (1967).
"Practical Approach to the Study of Polyolefin Weatherability," *Applied Polymer Symposia No. 4*, 141-154.

MATHUR, A.B., KUMAR, V., and MATHUR, G.N. (1981).
"Thermal Behavior of Photodegraded Low Density Polyethylene," *Proceeding of 2nd European Thermal Analysis Conference*, London, 1981.

MATREYEK, W. and WINSLOW, F.H. (1975).
"Effect of Carbon Black Antioxidants, and Ultraviolet Absorbers in the Photoxidation of Polyethylene," *Polymer Preprints, Division of Polymer Chemistry, ACS*, 16(1): 606-610.

MCNAUGHTON, J.L. and MORTIMER, C.T. (1975).
"Differential Scanning Calorimetry, IRS," *Physical Chemistry Series 2*, Volume 10, Butterworths, London.

MELLOR, D.C., MOIR, A.B., and SCOTT, G. (1973).
"The Effect of Processing Conditions on the UV Stability of Polyolefins," *European Polymer Journal*, 9: 219-225.

MELTZER, T.H. and MORGANO, P.J. (1961).
"Accelerated Weathering of Polyethylene," *ACS Polymer Preprints*, 8(1): 558-566.

MEYER, F.K., (1983).
"Stabilization of Polyolefins for Outdoor Use," Presented at Petchem Plast '83, Al-Khobar, Saudi Arabia, Nov. 1, 1983.

MEYER, F.K. and PEDRAZZETTI, E. (1986).
"Aspect of L-LDPE Stabilization," Presented at LLDPE in Europe - World Perspectives and Developments, Madrid, Nov. 3-5, 1986.

MICHAELS, A.S. and BIXLER, H.J. (1961).
"Solubility of Gases in Polyethylene," *Journal of Polymer Science*, 50: 393-412.

MINOSHIMA, W. and WHITE, J.L. (1986).
"A Comparative Experimental Study of the Isothermal Shear and Uniaxial Elongational Rheological Properties of Low Density, High Density and Linear Low Density Polyethylenes," *Journal of Non-Newtonian Fluid Mechanics,* **19**: 251-274.

MLINAC, M., ROLICH, J., and BRAVER, M. (1976).
"Photodegradation of Colored Polyethylene Films," *Journal of Polymer Science,* Symposium No. 57: 161-169.

MOBASHER, A. and BAHR, S. (1981).
"Weathering and Degradation of Polyethylene Sheets for Agricultural Applications," Annual Report, Kuwait Institute for Scientific Research, Kuwait, 267-269.

MONTGOMERY, D. C. and PECK, E. A. (1982).
Introduction to Linear Regression Analysis. (New York: John Wiley).

MTS (1982).
Material Testing System (MTS) Technical Proposal No. 83962, MTS Corporation, Minnesota.

MUKHERJEE, A.K., DHARA, S.K., and SHARMA, P.K. (1985).
"A New Ethylene Polymer Linear Low Density Polyethylene (LLDPE)," *Popular Plastic,* October 85: 15-20.

NICKERSON, R.F. (1941).
"Degradation of Cellulose," *Industrial Engineering and Chemistry*, **33**: 1022-1026.

NIMMO, B. and SAID, S.A.M. (1981).
"Direct and Total Measurements for Dhahran, Saudi Arabia," *Proceedings Solar World Forum*, Brighton, England, p 6.

ODIAN, G. (1981).
Principles of Polymerization, (New York: Wiley-Interscience), Chapter 1.

PABIOT, J. and VERDU, J. (1981).
"The Change in Mechanical Behavior of Linear Polymer During Photochemical Ageing," *Polymer Engineering and Science,* **21(1)**: 32-38.

PATTACINI, S.C. and ANACREON, R.E. (1980).
"The Application of Computer Difference Spectroscopy to Films and Coating," *Perkin-Elmer Infrared Bulletin 74*, April 1980, IRB-74.

POPLI, R. and MANPELKERN, L. (1987).
"Influence of Structural and Morphological Factors on the Mechanical Properties of the Polyethylenes," *Journal of Polymer Science: Part B, Polymer Physics*, **25**: 441-483.

POUNCY, H.W. (1985).
"How Photostabilizers Compare in LLDPE Film Weatherability," *Modern Plastic*, March 1985: Volume 62, No. 3, 68-72.

PROSS, A.W. and BLACK, R.M. (1950).
"The Photocatalysed Oxidation of Polyethylene," *Journal of Society of Chemical Industries*, **69**: 113-116.

RAAB, M., HNAT, V., SCHMIDT, P., KOTULAK, L., TAIMR, L., and POSPISIL, J. (1987).
"The Action of Anthraquinone Sensitizers in the Photo-oxidative Degradation of Low Density Polyethylene: Mechanical Evidence of Dark Process," *Polymer Degradation and Stability*, **18**: 123-134.

RAAB, M., KOTULAK, L., KOLARIK, J., and POSPISIL, J. (1982).
"The Effect of Ultraviolet Light on the Mechanical Properties of Polyethylene and Polypropylene Films," **Journal of Applied Polymer Science, 27**: 2457-2466.

RAM, A., Meir, T., and MILTZ, J. (1980).
"Durability of Polyethylene Films," *International Journal of Polymeric Materials*, **8**: 323-336.

RANBY, B. and RABEK, J.F. (1975).
Photodegradation, Photo-oxidation and Photostabilization of Polymers. (London: John Wiley).

RASOUL, F.A. and HAMEED, Z. (1980).
"Weathering and Degradation of Commercially Available Polymers." Annual Report, Kuwait Institute for Scientific Research (KISR), Kuwait, 228-229.

REE, M., KYU, T., and STEIN, R.S. (1987).
"Quantitative Small-Angle Light Scattering Studies of the Melting and Crystallization of LLDPE/LDPE Blend," *Journal of Polymer Science:Part B:Polymer Physics*, **25:** 105-126.

RUGG, F.M., SMITH, J.J., and BACON, R.C. (1954).
"Infrared Spectrophotometric Studies on Polyethylene, II, Oxidation," *Journal of Polymer Science*, **13:** 535-547.

RUNT, J. and HARRISON, I.R. (1980).
"Thermal Analysis of Polymers," In: **Methods of Experimental Physics,** Ed. R.A. Fava, (New York: Academic), **16(B):** 287-345.

RYBNIKAR, F. (1976).
"Crystallization and Structure of Degraded Branched Polyethylene," *Journal of Polymer Science, Symposium No.* 57: 101-107.

RYBNIKAR, F. (1978).
"Photo-Oxidative Aging of Branched Polyethylene," Presented at XIIth Annual Conference of Czechoslovak - French Cooperation on "Degradation and Combustion of Polymers," November 9-14, 1978, Novy, Smokovec, Czechoslovakia.

SABIC MARKETING LTD. (1984).
LADENE FH10018, Data Sheet, B-1-84.

SADRMOHEGH, C. and SCOTT, G. (1980).
"The Effect of Reprocessing on Polymer-I Low Density Polyethylene," *European Polymer Journal*, **16:** 1037-1042.

SAS USER'S GUIDE: STATISTICS (1982).
SAS Institute, Statistical Analysis System, North Carolina.

SATO, Y. and YASHIRO, T. (1978).
"The Effect of Polar Groups on the Dielectric Loss of Polyethylene," *Journal of Applied Polymer Science*, **22:** 2141-2153.

SCHNABEL, W. (1981).
Polymer Degradation, Principles and Practical Applications, (Berlin: Hanser).

SCOTT, G. (1984).
"Some Fundamental Aspects of the Photooxidation and Stabilization of Polymers," *British Polymer Journal*, **16:** 271-283.

SCOTT, G. (1976).
"Mechanism of Photodegradation and Stabilization of Polyolefins," *American Chemical Society Symposium Series*, **23:** 340-366.

SEGUELA, R. and RIETSCH, F. (1986).
"Tensile Drawing Behavior of a Linear Low Density Polyethylene: Change in Physical and Mechanical Properties," *Polymer*, **27:** 31-33.

SEVERINI, F., GALLO, R., IPSALE, S. and DELFANTI, N. (1986).
"Environmental Degradation of Stabilized LDPE: Initial Step," *Polymer Degradation and Stability*, **14:** 341-350.

SEVERINI, F., GALLO, R., IPSALE, S., and DELFANTI, N. (1987).
"Environmental Degradation of Stabilized LDPE: Later Stages," Polymer Degradation of Stability, **3:** 5-64.

SHARPLES, A. (1972).
Crystallinity in Polymer Science, Ed: A.D. Jenkins, (Amsterdam: North-Holland), Vol. 1, Chapter 4..

SHORT, J.N. (1981)
"Olefin Polymers," In: **Kirk-Othmer Encyclopedia of Chemical Technology**, Eds: M. Graysen and D. Eckroth, (New York: Wiley), 3rd Ed., 385-401.

SIESLER, H.W. (1979).
"Characterization of Chemical and Physical Changes of Polymer Structure by Rapid-Scanning Fourier Transform IR (FTIR) Spectroscopy," *Proceeding 5th European Symposium on Polymer Spectroscopy*, Cologne, September 1978, Ed: D.O. Hummel (Weinheim: Verlog).

SIESLER, H.W. and HOLLAN-MORITZ, K. (1980).
Infrared and Raman Spectroscopy of Polymers, (New York: Marcel Dekker).

SILVERSTEIN, R. S., BASSLER, G, C., and MORRILL, T. C. (1981).
Spectrometric Identification of Organic Compounds, (New York: John Wiley).

SPEED, C. S. (1982).
"Formulating blends of LLDPE and LDPE to design better film," *Plastic Engineering*, **July:** 39-42.

SPRINGER, H., HENGS, A., HOHNE, J., SCHICH, A., and HINRICHSEN, G. (1981).
"Investigation on Crystallization and Melting Behavior of Linear Low Density Polyethylene (LLDPE)," *Progress in Colloid & Polymer Science*, 72: 101-105.

STIVALA, S.S., KIMURA, J., and GABBAY, S.M. (1983).
"Thermal Degradation and Oxidative Process," In: **Degradation and Stabilization of Polyolefins**, Ed. N.S. Allen (London: Applied Science).

STRETANSKI, J.A. (1986).
"Light Stabilizers," *Society of Plastic Engineers (SPE) Fall Seminar Series*, September 1-5, 1986.

TABB, D.L., SEVCIK, J.J., and KOENIG, J.L. (1975).
"Fourier Transform Infrared Study of the Effect of Irradiation on Polyethylene," *Journal of Polymer Science:Polymer Physics Edition*, 13: 815-824.

THOMPSON, M. L. (1978).
"Selection of Variables in Multiple Regression: Part I, A Review and Evaluation," *International Statistical Review*, 46: 1-19.

TINCER, T., CIMEN, I., and AKAY, G. (1986).
"The Effect of Additives and Drawing Temperature on Gamma- or Ultraviolet Radiation Induced Oxidative Degradation of Drawn High Density Polyethylene," *Polymer Engineering and Science*, 26(7): 479-487.

TROZZOLO, A.M. (1972).
"Photooxidation of Polyolefins," In: **Polymer Stabilization**, Ed: W.L. Hawkins, (New York: Wiley).

TSUJI, K. and NAGATA, H. (1977).
"Photodegradation of Polyethylene - Effect of Addition of Ferric Stearate," Reprint, *Progress of Polymer Physics of Japan*, 20: 563-569.

TURLEY, R.R. (1979).
"LLDPE Films," *Society of Plastic Engineering 37th Annual Technical Conference*, XXV: 499-512, May 1979.

TURTLE, B.L. (1986).
"Progress of LLDPE in Film Application," *Plastic and Rubber International*, 11(6): 24-27.

VAKHLUEVA, V.I., FINKEL, A.G., SVERDLOV, L.M. and ZAITSEVA, L.A. (1968).
"Theoretical and Experimental Investigation of the Absolute Intensities of Bands in the Infrared Spectra of Polyatomic Molecules," *Optical Spectroscopy*, **25**: 160-161.

VINK, P. (1979).
"Photooxidation of A," *Journal of Applied Polymer Science*: Applied Polymer Symposium 35: 265-273.

WATSON, E.S., ONEIL, M.J., JUSTIN, J., and BRENNER, N. (1966).
"Differential Scanning Calorimetric Studies of Polymer," *Analytical Chemistry*, **36**: 1233-1251.

WEBB, J.D., SCHISSEL, P., THOMAS, T.M., PITTS, J.R., and CZANDERNA, A.W. (1983).
"Transform Infrared (FTIR) Reflection Absorbance Studies," Presented at 27th Annual Technical Symposium, Society for Photo-optical Material Processing Engineers, 16th National Exhibition: 85-95.

WEBB, J.D. (1984).
"Effect of Ultraviolet Radiation on Transparent Polymer Films as Determined Using In Situ FTIR-RA Spectroscopy Volume 1: Photodegradation of Transparent Polymer Film," Solar Energy Research Institute (SERI) Report No. SERI/TR-255-2177. Instrumentation Engineers, Diego, California, 22-26 August, 1983: 1-7.

WEINER, L.R. (1971).
"Development of Method of Analysis using Infrared Spectroscopy for Evaluating Photodegradation Resistance of High Density Polyethylene Compositions," *Proceedings 71 Society of Aerospace Material Process Engineering, 16th National Exhibition*, 85-91.

WHITE, J.L. and YAMANE, H. (1987).
"A Collaborative Study of the Stability of Extrusion, Melt Spinning and Tubular Film Extrusion of Some High-Low and Linear Low Density Polyethylene Samples," *Pure & Applied Chemistry*, **59(2)**: 193-216.

WILES, D.M. and CARLSSON, D.J. (1985).
"New Aspects of the Photooxidation and Photostabilization of Polyolefins," In: **New Trends in the Photochemistry of Polymers**, Eds. N.S. Allen and J.F. Rabek, (London: Elsevier).

WILLBOURN, A. H. (1959).
"Polymethylene and the Structure of Polyethylene: Study of Short-Chain Branching, its Nature and Effects," *Journal of Polymer Science, Nottingham Symposium*, 34: 569-597.

WINSLOW, F.H. and MATREYEK, W. (1962).
"Degradation of Polyolefins," ACS Meeting, Washington, D.C., March 1984, Chicago Division of Polymer Chemistry, 5, 552-557.

WINSLOW, F.H., ALOISIO, C.J., HAWKINS, W.L., MATREYEK, W. and MATSUOKA, S. (1963a).
"Effect of Morphology on Oxidative Crystallization of Polyolefins," *ACS Polymer Preprint*, 4(2): 706-716.

WINSLOW, F.H. ALOISIO, C.J., HAWKINS, W.L., MATREYEYK, W., and MATRSUOKA, S. (1963b).
"Oxidative Crystallization of Polyethylene," *Chemical Industries (London)*, 1465-1471.

WINSLOW, F.H. and MATREYEK, W. (1964).
"Thermal Oxidation of Polyolefins," Paper presented at ACS Division of Polymer Chemistry Meeting in Chicago, 552-557.

WINSLOW, F.H. and HAWKINS, W.L. (1967).
"Some Weathering Characteristics of Plastics," *Applied Polymer Symposia*, No.4: 29-39.

WINSLOW, F.H., MATREYEK, W. and TROZZOLO, A.M. (1969).
"Weathering of Polyethylene," *Polymer Preprint*, ACS Division of Polymer Chemistry 10(2): 1271-1280.

WINSLOW, F.H., MATREYEK, W. and TROZZOLO, A.M. (1972).
"Weathering of Polymers," *Society of Plastic Engineers (SPE)*, 18: 766-772.

WINSLOW, F.H. (1977a).
"Environmental Degradation," In: **Treatise on Materials Science and Technology**, Ed. J.M. Schultz, (New York: Academic),Vol. 10, Part B: 741-776.

WINSLOW, F.H. (1977b).
"Photo-oxidation of High Polymer," *Pure and Applied Chemistry*, 49: 495-499.

WMO (1983).
"Guide to Meteorological Instruments and Methods of Observation," *World Meteorological Organization*, No. 8

WUNDERLICH, B. and CROMIER, C.M. (1967).
"Heat of Fusion of Polyethylene," *Journal of Polymer Science*, Part A-2, 5: 987-988.